

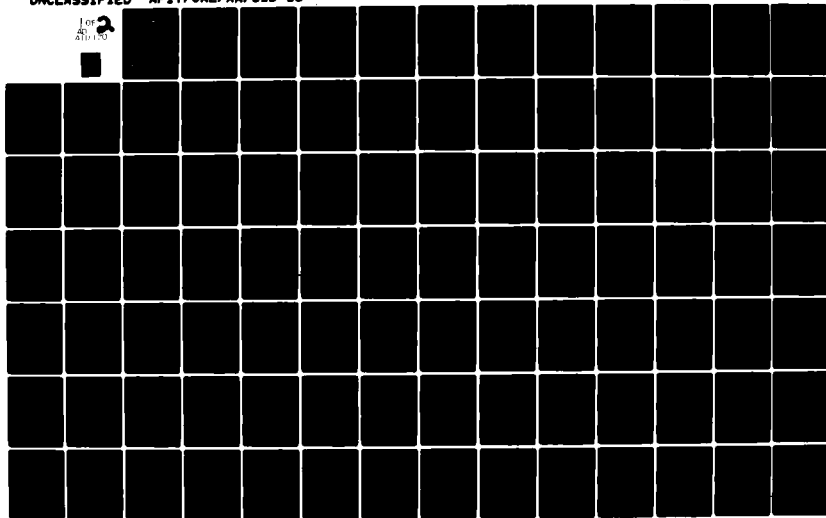
AD-A111 170

AIR FORCE INST OF TECH WRIGHT-PATTERSON AFB OH SCHOOL--ETC F/8 22/2  
DESIGN OF A DIGITAL CONTROLLER FOR A LARGE FLEXIBLE SPACE STRUC--ETC(U)  
DEC 81 D B LEONETT  
AFIT/8AE/AA/81D-18

UNCLASSIFIED

NL

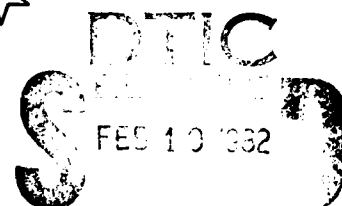
for  
20100



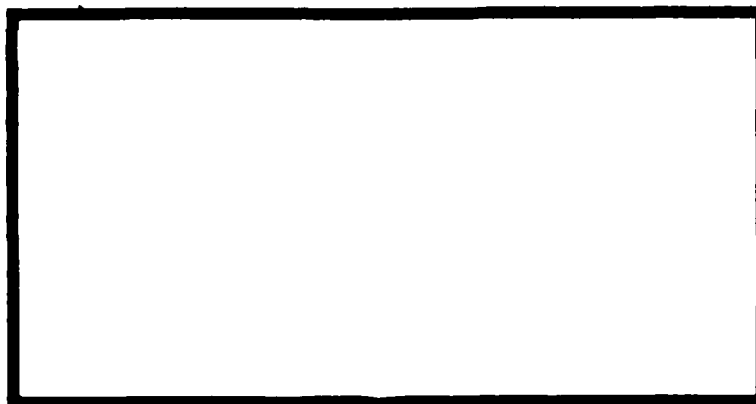
AD A111170

LEVEL II

①



E



DTIC FILE COPY

UNITED STATES AIR FORCE  
AIR UNIVERSITY  
AIR FORCE INSTITUTE OF TECHNOLOGY  
Wright-Patterson Air Force Base, Ohio

This document has been approved  
for public release and sale; its  
distribution is unlimited.

82 02 18 034

AFIT/GAE/AA/81D-18

II

(1)

DESIGN OF A DIGITAL CONTROLLER FOR A  
LARGE FLEXIBLE SPACE STRUCTURE

THESIS

AFIT/GAE/AA/81D-18

David B. Leggett  
2d Lt USAF

Approved for public release; distribution unlimited

DESIGN OF A DIGITAL CONTROLLER  
FOR A LARGE FLEXIBLE SPACE  
STRUCTURE

THESIS

Presented to the Faculty of the School of Engineering  
of the Air Force Institute of Technology

Air University

in Partial Fulfillment of the  
Requirements for the Degree of  
Master of Science

by

David B. Leggett

2d Lt            USAF

Graduate Aerospace Engineering

December 1981

Accession For	
NTIS	★
REF	
Ch	
Dist	
A	

Approved for public release; distribution unlimited.

## Preface

I would like to express my gratitude to my thesis advisor, Captain J. T. Silverthorn, who directed my efforts as this thesis progressed. His help in explaining the concepts and correcting my mistakes is greatly appreciated. In addition, I would like to thank Captain J. Rader whose sequence on optimization techniques was invaluable. I would also like to thank Dr. R. A. Calico who explained to me the system model and its equations of motion. Without the help of all of them, I could not have finished this thesis. Most of all, however, I would like to thank my wife, without whose support and understanding I would not have survived this thesis.

## Contents

	Page
Preface . . . . .	ii
List of Figures . . . . .	v
List of Tables . . . . .	vii
Abstract . . . . .	viii
I Introduction . . . . .	1
II System Model . . . . .	4
General Description . . . . .	4
Equations of Motion . . . . .	8
Equations of Motion - Discrete Time . . . . .	12
III Discrete Optimal Control Theory . . . . .	15
IV Design I . . . . .	20
System Design . . . . .	20
System Performance . . . . .	25
V Design II . . . . .	35
System Performance . . . . .	45
VI Design III . . . . .	55
System Performance . . . . .	63
VII Effects of Sampling Time . . . . .	73
Aliasing . . . . .	73
System Performance . . . . .	75
Effects of Performance Index Approximation . . . . .	76
VIII Conclusions . . . . .	94
Bibliography . . . . .	96
Appendix A: Eigenvector Results of NASTRAN Analysis . . . . .	97

	Page
Appendix B: Matrices $B_c$ , $B_s$ , $B_r$ . . . . .	100
Appendix C: Open-loop Eigenvalues and Time Response . . . . .	102
Vita . . . . .	106

# List of Figures

Figure	Page
1. Cross Sectional View of the System Model . . . . .	5
2. View of System Model Down Y and Z Axes . . . . .	6
3. Z-Plane Plot of Eigenvalues of Design I . . . . .	29
4. LOSX vs TIME, Design I, $Q=Q_{OB}=I$ , $T=.1$ . . . . .	30
5. LOSY vs TIME, Design I, $Q=Q_{OB}=I$ , $T=.1$ . . . . .	31
6. LOSX vs TIME, Design I, $Q=Q_{OB}=10I$ , $T=.1$ . . . . .	33
7. LOSY vs TIME, Design I, $Q=Q_{OB}=10I$ , $T=.1$ . . . . .	34
8. Z-Plane Plot of Eigenvalues of Design II . . . . .	48
9. LOSX vs TIME, Design II, $Q=Q_{OB}=I$ , $T=.1$ . . . . .	49
10. LOSY vs TIME, Design II, $Q=Q_{OB}=I$ , $T=.1$ . . . . .	50
11. LOSX vs TIME, Design II, $Q=Q_{OB}=10I$ , $T=.1$ . . . . .	51
12. LOSY vs TIME, Design II, $Q=Q_{OB}=10I$ , $T=.1$ . . . . .	52
13. LOSX vs TIME, Design II, $Q=Q_{OB}=100I$ , $T=.1$ . . . . .	53
14. LOSY vs TIME, Design II, $Q=Q_{OB}=100I$ , $T=.1$ . . . . .	54
15. Z-Plane Plot of Eigenvalues of Design III . . . . .	66
16. LOSX vs TIME, Design III, $Q=Q_{OB}=I$ , $T=.1$ . . . . .	67
17. LOSY vs TIME, Design III, $Q=Q_{OB}=I$ , $T=.1$ . . . . .	68
18. LOSX vs TIME, Design III, $Q=Q_{OB}=10I$ , $T=.1$ . . . . .	69
19. LOSY vs TIME, Design III, $Q=Q_{OB}=10I$ , $T=.1$ . . . . .	70
20. LOSX vs TIME, Design III, $Q=Q_{OB}=100I$ , $T=.1$ . . . . .	71
21. LOSY vs TIME, Design III, $Q=Q_{OB}=100I$ , $T=.1$ . . . . .	72
22. Eigenvalue Movement as T Increases, Design II . . . . .	78
23. LOSX vs TIME, Design II, $Q=Q_{OB}=100I$ , $T=.3$ . . . . .	79



Figure	Page
24. LOSY vs TIME, Design II, $Q=Q_{OB}=100I$ , $T=.3$ . . .	80
25. LOSX vs TIME, Design II, $Q=Q_{OB}=100I$ , $T=.5$ . . .	81
26. LOSY vs TIME, Design II, $Q=Q_{OB}=100I$ , $T=.5$ . . .	82
27. LOSX vs TIME, Design II, $Q=Q_{OB}=100I$ , $T=.7$ . . .	83
28. LOSY vs TIME, Design II, $Q=Q_{OB}=100I$ , $T=.7$ . . .	84
29. Eigenvalue Movement as T Increases, Design III . . . . .	86
30. LOSX vs TIME, Design III, $Q=Q_{OB}=100I$ , $T=.3$ . . .	87
31. LOSY vs TIME, Design III, $Q=Q_{OB}=100I$ , $T=.3$ . . .	88
32. LOSX vs TIME, Design III, $Q=Q_{OB}=100I$ , $T=.5$ . . .	89
33. LOSY vs TIME, Design III, $Q=Q_{OB}=100I$ , $T=.5$ . . .	90
34. LOSX vs TIME, Design III, $Q=Q_{OB}=100I$ , $T=.7$ . . .	91
35. LOSY vs TIME, Design III, $Q=Q_{OB}=100I$ , $T=.7$ . . .	92

## List of Tables

Table	Page
I. Node Coordinates . . . . .	7
II. Key Results of NASTRAN Eigenvalue Analysis . . . . .	7
III. Initial Conditions for Time History Response . . . . .	8
IV. Eigenvalues of Design I . . . . .	28
V. Eigenvalues of Design I . . . . .	32
VI. Eigenvalues of Design II . . . . .	47
VII. Eigenvalues of Design III . . . . .	65
VIII. Eigenvalues of Design II . . . . .	77
IX. Eigenvalues of Design III . . . . .	85

Abstract

Modern optimal control techniques are used to design a digital controller for a large, flexible space structure. The structure is modeled as a tetrahedron formed by four lumped masses connected by massless truss members. A NASTRAN analysis is used to generate the twelve mode shapes and frequencies of oscillation.

The controller is designed in discrete time using linear optimal regulator theory. The states consist of mode amplitudes and velocities. Because these amplitudes and velocities are not directly available to the controller, an observer is used to estimate the states. The feedback gains for both controller and observer are determined using steady-state optimal regulator theory. The controller is designed based upon only four modes of the system. The four highest frequency modes are truncated from the design to signify system reduction.

Active control is achieved using six collocated sensor-actuator pairs. The effectiveness of the controller is determined using the pointing accuracy as a figure of merit. The controller is judged by its ability to bring the "pointer" back to the nominal line of sight from an initial displacement.

Three controller designs are compared. The first demonstrates the effects of "control" and "observation

spillover". The second uses a singular value decomposition technique to generate a gain matrix to eliminate the spillover terms. The second design also uses a simplified discrete performance index for optimal control. The third design uses the same technique as the second to eliminate the control and observer spillover, but it uses a more accurate performance index.

The first design proved to be inadequate to achieve the desired performance because of the spillover terms. When the gain was increased to achieve the desired performance, the system became unstable. Both designs II and III were able to achieve the desired performance for small sampling times. For increasingly larger sampling times, system performance was degraded though for both designs the system remained stable. In addition, for small sampling times, the simplified performance index proved to provide a very accurate approximation.

DESIGN OF A DIGITAL CONTROLLER  
FOR A LARGE FLEXIBLE SPACE  
STRUCTURE

I Introduction

The promise of a viable space transportation system in the near future has inspired a new breed of satellite designs. These new designs are far larger and structurally more flexible than their predecessors. Flexible structures of this type can present problems to the control designer as they may exhibit hundreds of low-frequency vibrational modes of oscillation. Using classical control methods it is extremely difficult to design a controller to insure the stability of so many modes.

One of the most widely accepted design techniques to counter this problem is the application of modern state space control theory to a reduced order controller. This technique can be applied to a wide variety of flexible structures. It has previously been applied using optimal time-invariant linear regulator theory for active control (Ref 1).

The active control is applied to only a small number of critical modes, called the "controlled modes". The choice of which modes to control is based on desired system

response. Usually the lowest frequency modes are selected; however, this is not always possible nor always desired. While the controller acts on the controlled modes, the control inputs and sensor outputs are affected by the remaining modes. These effects are known as "control spillover" and "observation spillover", respectively (Ref 2). The effects of some of these uncontrolled modes can make the system unstable. Therefore, the effects of such modes must be "suppressed" in the controller design. These modes are known as "suppressed modes". The remaining modes are not modeled in the controller design and are called "residual modes".

In previous work (Ref.1), this design technique has been applied in the continuous-time domain. However, any control system based on a digital computer must be a discrete-time system. Meirovitch (Ref 3) has shown that discretizing a system designed in continuous-time can lead to instabilities as the sample time gets large. To avoid this problem, such a system should be designed in discrete time.

The principle purpose of this thesis is to design a digital controller for a representative space structure. The effects of the suppressed modes and of different sampling times will be examined. Two variations will be made to the design of the controller and a range of sampling times will be used. Since many satellites are used to beam energy or information back to the Earth, the performance of the

different designs will be judged using, as a figure of merit, the deviation of a nominal line of sight.

The first design variation involves the effects of the suppressed modes. The system will first be designed ignoring the suppressed modes. The system will then be designed to eliminate the spillover terms in the state space matrix so as to suppress the modes. The performance of the two designs will then be compared.

The second design variation involves the performance index used to obtain the feedback gains. At first a simplified approximation to the discretized performance index is used. Then a much more accurate performance index is used and the two systems compared.

The first sampling time examined is one whose sampling frequency is well above that of the highest natural frequency of the modeled modes. This sampling time should provide good system response. A range of larger sampling times will then be used to see the effects of sampling time on system stability.

## II System Model

### General Description

Since a mathematical analysis of a continuously distributed space structure is computationally impossible, the structure is modeled as a discretely distributed system. The model used is one developed by the Charles Stark Draper Laboratory (Ref 4). It was developed to act as a standard space structure for controller designs. The model is a tetrahedron composed of lumped masses and interconnected truss members. The truss members are assumed to be massless and exert no bending moments, only axial forces. This model is illustrated in Figures 1 and 2. It consists of ten nodes at the numbered grid points. The node coordinates are given in Table I. The masses are located at nodes one through four. Each mass has three degrees of freedom, which gives the system twelve modes. The nodes at grid points five through ten are fixed. Six collocated sensor/actuator pairs are located on the truss members extending from these nodes and are oriented along the members. The sensors sense position only.

The key results of a NASTRAN eigenvalue analysis of this model are presented in Table II. The eigenvectors associated with these eigenvalues are shown in Appendix A.

For the time response, the nominal line of sight of the tetrahedron shaped "antenna" is along the z-axis from



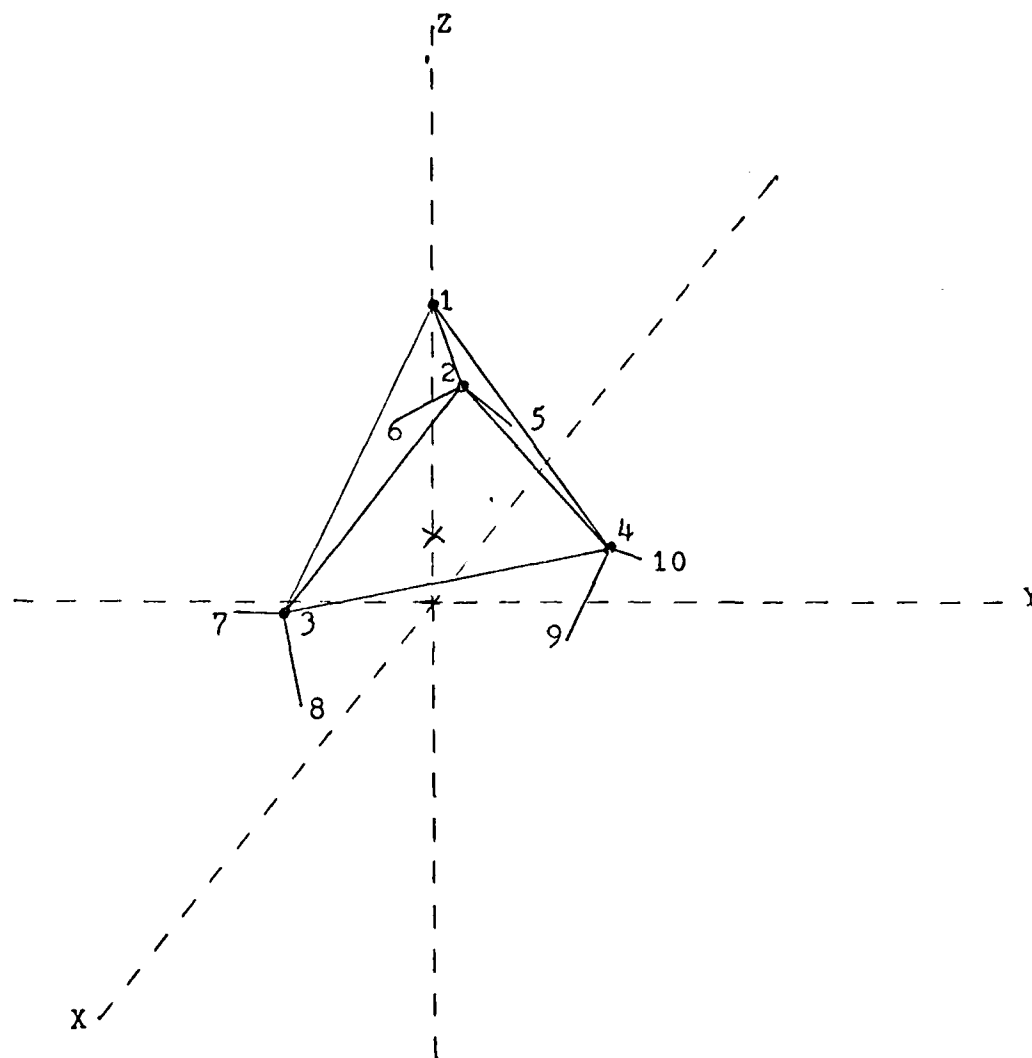


Figure 1. Cross Sectional View of the System Model

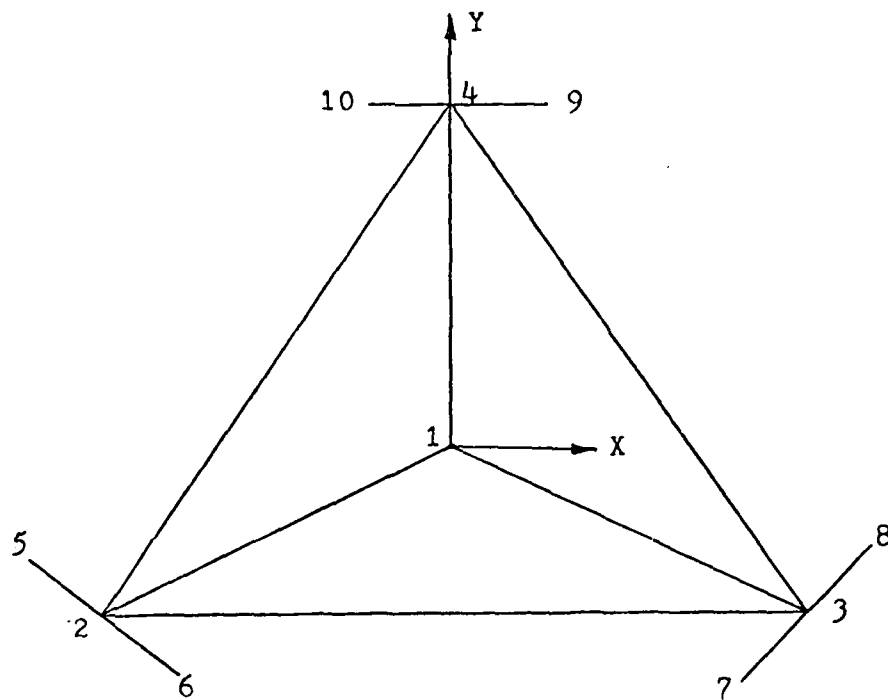
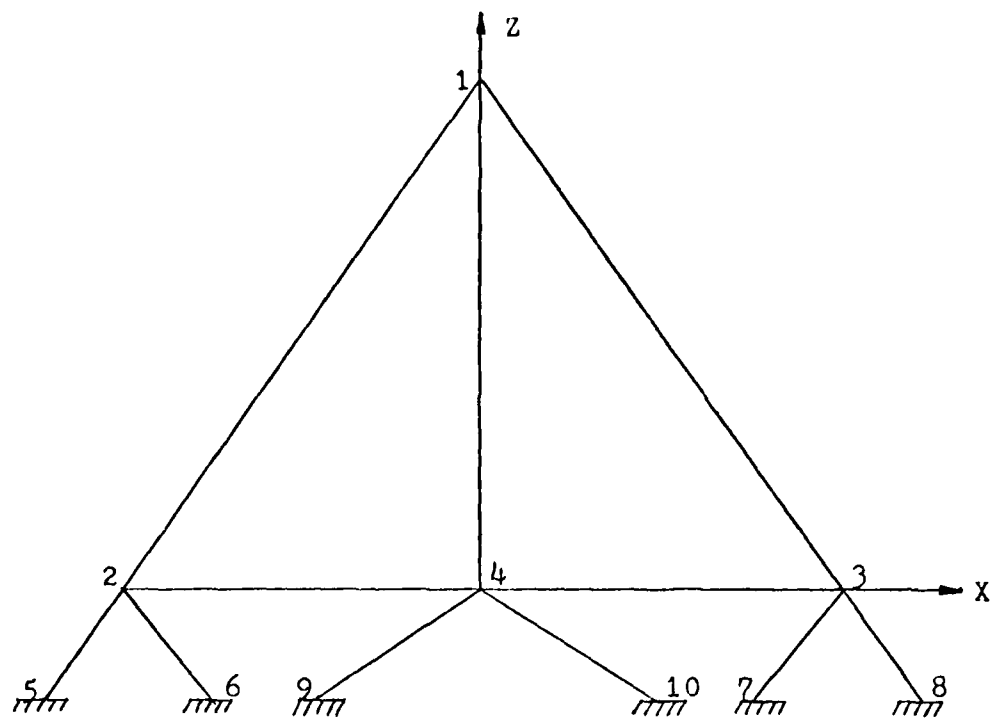


Figure 2. View of System Model Down Y and Z Axes

node 1. Since displacements along the z-axis do not disturb this line of sight, only perturbations in the x- and y-directions are considered. The mode initial conditions are listed in Table III.

Table I  
Node Coordinates

<u>Node</u>	<u>X</u>	<u>Y</u>	<u>Z</u>
1	0.0	0.0	10.165
2	-5.0	-2.887	2.0
3	5.0	-2.887	2.0
4	0.0	5.7735	2.0
5	-6.0	-1.1547	0.0
6	-4.0	-4.6188	0.0
7	4.0	-4.6188	0.0
8	6.0	-1.1547	0.0
9	2.0	5.7735	0.0
10	-2.0	5.7735	0.0

Table II  
Key Results of NASTRAN Eigenvalue Analysis

<u>Mode</u>	<u>Generalized Mass</u>	<u>Generalized Stiffness</u>	<u><math>\omega_n</math> (rad/sec)</u>
1	1.0E+00	1.37E+00	1.17E+00
2	1.0E+00	2.15E+00	1.47E+00
3	1.0E+00	8.79E+00	2.96E+00
4	1.0E+00	1.26E+01	3.56E+00
5	1.0E+00	1.48E+01	3.85E+00
6	1.0E+00	2.65E+01	5.15E+00
7	1.0E+00	3.22E+01	5.67E+00
8	1.0E+00	3.26E+01	5.71E+00
9	1.0E+00	7.99E+01	8.93E+00
10	1.0E+00	1.06E+02	1.03E+00
11	1.0E+00	1.19E+02	1.09E+01
12	1.0E+00	1.95E+02	1.40E+01

Table III

## Initial Conditions for Time History Response

<u>Mode</u>	<u>Displacement (n)</u>	<u>Velocity (<math>\dot{n}</math>)</u>
1	-0.001	-0.003
2	0.006	0.010
3	0.001	0.030
4	-0.009	-0.020
5	0.008	0.020
6	-0.001	-0.020
7	-0.002	-0.003
8	0.002	0.004
9	0.000	0.000
10	0.000	0.000
11	0.000	0.000
12	0.000	0.000

Equations of Motion

The vibrational motion of a large space structure is given by the equation

$$M \ddot{\underline{q}}(t) + E \dot{\underline{q}}(t) + K \underline{q}(t) = D \underline{u}(t) \quad (1)$$

where

$\underline{q}$  = an  $n$ -vector of generalized coordinates

$M$  = an  $n \times n$  symmetric mass matrix

$E$  = an  $n \times n$  symmetric damping matrix

$K$  = an  $n \times n$  symmetric stiffness matrix

$\underline{u}$  = an  $n_{act}$ -vector of inputs

$D$  = an  $n \times n_{act}$  matrix of actuator coefficients

and where the dimensions  $n$  and  $n_{act}$  are the number of modes and the number of actuators, respectively.

Equation (1) can be written in modal coordinates,  $\eta$ , by using the transformation

$$\underline{q}(t) = \phi \underline{\eta}(t) \quad (2)$$

where  $\phi$  is the nxn modal matrix for Eq (1). This modal matrix satisfies the conditions

$$\phi^T M \phi = I \quad (3)$$

$$\phi^T K \phi = \omega^2 \quad (4)$$

$$\phi^T E \phi = 2 \zeta \omega \quad (5)$$

where

$I$  = an nxn identity matrix

$2\zeta\omega$  = an nxn diagonal damping matrix

$\omega^2$  = an nxn diagonal matrix of eigenvalues of Eq (1)

With this transformation, Eq (1) becomes

$$\ddot{\underline{\eta}}(t) + 2\zeta\omega \dot{\underline{\eta}}(t) + \omega^2 \underline{\eta}(t) = \phi^T D \underline{\mu}(t) \quad (6)$$

Equation (6) put into state vector form is

$$\dot{\underline{x}}(t) = A \underline{x}(t) + B \underline{\mu}(t) \quad (7)$$

where

$$\underline{x} = \begin{bmatrix} \underline{\eta} \\ \dot{\underline{\eta}} \end{bmatrix} \quad (8)$$

$$A = \begin{bmatrix} 0 & I \\ -\omega^2 & -2\zeta\omega \end{bmatrix} \quad (9)$$

$$B = \begin{bmatrix} 0 \\ \phi^T D \end{bmatrix} \quad (10)$$

The output equation from the sensors is of the form

$$\underline{y}(t) = C_p \underline{q}(t) \quad (11)$$

where  $C_p$  is an  $n_{sen} \times n$  matrix of sensor coefficients. The dimension  $n_{sen}$  is equal to the number of sensors.

Using the transformation of Eq (2), the output equation becomes

$$\underline{y}(t) = C \underline{x}(t) \quad (12)$$

where

$$C = [C_p \phi \mid 0]$$

Equations (7) and (12) are the equations of motion in the form to be used in the controller design. The state vector,  $\underline{x}$ , is of dimension  $2n$ . As previously discussed, the system modes can be separated into controlled, suppressed, and residual modes. When such a partitioning is made, the corresponding states of the state vector are also partitioned. The controlled states are those states directly controlled to achieve the specified performance. The suppressed states are those uncontrolled states which may still strongly influence the system's performance and should be accounted for in the design of the controller. The residual states correspond to those modes which have such a high natural frequency that they will probably not be excited by the controller and thus may be left out of the controller design.

With this partitioning of states, the state equation becomes

$$\dot{\underline{x}}_c(t) = A_c \underline{x}_c(t) + B_c \underline{u}(t) \quad (14a)$$

$$\dot{\underline{x}}_s(t) = A_s \underline{x}_s(t) + B_s \underline{u}(t) \quad (14b)$$

$$\dot{\underline{x}}_r(t) = A_r \underline{x}_r(t) + B_r \underline{u}(t) \quad (14c)$$

where

$$A_j = \begin{bmatrix} 0 & I \\ -\omega^2 & -2j\omega \end{bmatrix} ; j = c, s, r \quad (15a)$$

$$B_j = \begin{bmatrix} 0 \\ \phi_j^T D \end{bmatrix} ; j = c, s, r \quad (15b)$$

The matrices  $\phi_j^T D$  are those matrices whose elements are linear combinations of the mode shapes,  $\phi$ . The matrices  $B_c$ ,  $B_s$ ,  $B_r$  are shown in Appendix B.

With partitioning the output equation, Eq (12) becomes

$$\underline{y}(t) = C_c \underline{x}_c(t) + C_s \underline{x}_s(t) + C_r \underline{x}_r(t) \quad (19)$$

where

$$C_j = \begin{bmatrix} C_p \phi_j & 0 \end{bmatrix} ; j = c, s, r \quad (20)$$

The matrices  $C_p \phi_j$  are also matrices whose elements are linear combinations of the mode shapes. For the special case

where the position sensors and point actuators are collocated and aligned, the  $B_j$  and  $C_j$  matrices are related by

$$C_c = B_c^T \quad (22a)$$

$$C_s = B_s^T \quad (22b)$$

$$C_r = B_r^T \quad (22c)$$

In order to design a digital controller in discrete time, these equations must be discretized.

#### Equations of Motion - Discrete Time

In a sampled-data control system the control inputs,  $\underline{u}_d$ , instead of changing continuously in time, are incremented only at discrete time instances. Between those instances, the input is held constant. Thus, the discrete control input,  $\underline{u}_d$ , is

$$\underline{u}_d(t) = \underline{u}(kT) \quad \text{for } kT \leq t < (k+1)T \quad (23)$$

where  $k = 0, 1, 2, \dots$ , and  $T$  is the sampling time.

It can be shown that the state space representation of the system in discrete time is then

$$\underline{x}[(k+1)T] = \underline{\Phi}(T) \underline{x}(kT) + \underline{\Gamma}(T) \underline{u}(kT) \quad (24)$$



The matrix  $\Phi(T)$  is related to the continuous-time  $A$  matrix by

$$\Phi(T) = e^{AT} \quad (25)$$

$\Gamma(T)$  is related to the continuous-time  $B$  matrix by

$$\Gamma(T) = \int_0^T e^{A\tau} d\tau B \quad (26)$$

$\Phi(T)$  and  $\Gamma(T)$  are not functions of time but are functions of the system sampling time. This sampling time is usually a constant in the system as it will be in this analysis. Therefore,  $\Phi(T)$  and  $\Gamma(T)$  are constants and for convenience will be written as  $\Phi$  and  $\Gamma$ .

As in the continuous-time domain, the state equation, Eq (24), can be partitioned into

$$\underline{x}_c[(k+1)T] = \Phi_c \underline{x}_c(kT) + \Gamma_c \underline{u}(kT) \quad (27a)$$

$$\underline{x}_s[(k+1)T] = \Phi_s \underline{x}_s(kT) + \Gamma_s \underline{u}(kT) \quad (27b)$$

$$\underline{x}_r[(k+1)T] = \Phi_r \underline{x}_r(kT) + \Gamma_r \underline{u}(kT) \quad (27c)$$

where

$$\Phi_c = e^{A_c T} \quad (28a)$$

$$\Gamma_c = \int_0^T e^{A_c \tau} d\tau B_c \quad (28b)$$

$$\Phi_s = e^{A_s T} \quad (29a)$$

$$\Gamma_s = \int_0^T e^{A_s \tau} d\tau B_s \quad (29b)$$

$$\Phi_r = e^{A_r T} \quad (30a)$$

$$\Gamma_r = \int_0^T e^{A_r \tau} d\tau B_r \quad (30b)$$

The continuous-time output equation, Eq (19), becomes

$$\underline{y}(kT) = C_c \underline{x}_c(kT) + C_s \underline{x}_s(kT) + C_r \underline{x}_r(kT) \quad (31)$$

Equations (27) and (31) are the equations to which the controller design will be applied.

### III Discrete Optimal Control Theory

In all of the following designs, the feedback gains for the controller and the observer are designed using optimal control theory. There are some differences between the performance index for a discrete-time system and that for a continuous-time system. In this chapter, discrete optimal control theory is reviewed to demonstrate these differences.

In the continuous-time case, the performance index frequently used for systems described by

$$\dot{\underline{x}}(t) = A \underline{x}(t) + B \underline{u}(t) \quad (32)$$

is given by

$$J = \frac{1}{2} \int_0^{\infty} \underline{x}^T(t) Q \underline{x}(t) + \underline{u}^T(t) R \underline{u}(t) dt \quad (33)$$

where  $Q$  is a  $2n \times 2n$  positive semi-definite state weighting matrix and  $R$  is an  $n_{act} \times n_{act}$  positive definite control weighting matrix. The solution to this problem is known to be

$$\underline{u}^*(t) = F \underline{x}(t) \quad (34)$$

where  $F$ , the feedback gain matrix, is

$$F = -R^{-1} B^T P \quad (35)$$

and where  $P$  is the solution to the steady state Ricatti equation

$$PA + A^T P - PB R^{-1} B^T P + Q = 0 \quad (36)$$

For the discrete-time case, an appropriate performance index for systems described by

$$\underline{x}[(k+1)T] = \Phi \underline{x}(kT) + \Gamma \underline{u}(kT) \quad (37)$$

is given by

$$J = \frac{1}{2} \sum_{k=0}^{\infty} \int_{kT}^{(k+1)T} \underline{x}^T(t) Q \underline{x}(t) + \underline{u}^T(t) R \underline{u}(t) dt \quad (38)$$

But for discrete systems

$$\underline{u}(t) = \underline{u}(kT)$$

$$\underline{x}(t) = e^{A(t-kT)} \underline{x}(kT) + \int_{kT}^t e^{A(t-\tau)} d\tau B \underline{u}(kT) \quad (39)$$

for  $kT \leq t < (k+1)T$ . As shown in the preceding chapter, Eq (39) can be written

$$\underline{x}(t) = \Phi(t-kT) \underline{x}(kT) + \Gamma(t-kT) \underline{u}(kT) \quad (40)$$

After making the transformation  $\tau=t-kT$ , the performance index becomes

$$\begin{aligned}
J &= \frac{1}{2} \sum_{k=1}^{\infty} \int_0^T [\Phi(\tau) \underline{x}(kT) + \Gamma(\tau) \underline{u}(kT)]^T Q [\Phi(\tau) \underline{x}(kT) + \\
&\quad \Gamma(\tau) \underline{u}(kT)] + \underline{u}^T(kT) R \underline{u}(kT) d\tau \\
&= \frac{1}{2} \sum_{k=1}^{\infty} \int_0^T [\underline{x}^T(kT) \Phi^T(\tau)] Q [\Phi(\tau) \underline{x}(kT)] + \\
&\quad [\underline{x}^T(kT) \Phi^T(\tau)] Q [\Gamma(\tau) \underline{u}(kT)] + \\
&\quad [\underline{u}^T(kT) \Gamma^T(\tau)] Q [\Phi(\tau) \underline{x}(kT)] + \\
&\quad [\underline{u}^T(kT) \Gamma^T(\tau)] Q [\Gamma(\tau) \underline{u}(kT)] + \\
&\quad \underline{u}^T(kT) R \underline{u}(kT) d\tau \tag{41}
\end{aligned}$$

Finally, the performance index can be written

$$\begin{aligned}
J &= \frac{1}{2} \sum_{k=1}^{\infty} \underline{x}^T(kT) Q_d \underline{x}(kT) + \underline{x}^T(kT) S_d \underline{u}(kT) + \\
&\quad \underline{u}^T(kT) S_d^T \underline{x}(kT) + \underline{u}^T(kT) R_d \underline{u}(kT) \tag{42}
\end{aligned}$$

where

$$Q_d = \int_0^T \Phi^T(t) Q \Phi(t) dt \tag{43}$$

$$S_d = \int_0^T \Phi^T(t) Q \Gamma(t) dt \tag{44}$$

$$R_d = \int_0^T \Gamma^T(t) Q \Gamma(t) + R dt \tag{45}$$

Equations (43) through (45) can be simplified by the approximation

$$e^{At} = I + At + \frac{A^2 t^2}{2!} + \frac{A^3 t^3}{3!} + \dots \quad (46)$$

It can be shown that, if the product of  $T$  with the largest eigenvalue of  $A$  is very small, that is if

$$|\lambda_{\max} T| \ll 1 \quad (47)$$

where  $\lambda_{\max}$  is the largest eigenvalue of  $A$ , then Eq (46) can be approximated by

$$e^{At} = I \quad (48)$$

With this approximation, Eqs (43) through (45) become

$$Q_d = QT \quad (49)$$

$$S_d = 0 \quad (50)$$

$$R_d = RT \quad (51)$$

and the simplified performance index can be written

$$J = \frac{1}{2} \sum_{k=1}^{\infty} \underline{x}^T(kT) QT \underline{x}(kT) + \underline{u}^T(kT) RT \underline{u}(kT) \quad (52)$$

For a state equation of the form of Eq (37), the solution for this simplified performance index is

$$\underline{u}^*(kT) = F \underline{x}(kT) \quad (53)$$

where

$$F = -[I + (RT)^{-1} P^T P \Gamma]^{-1} (RT)^{-1} P^T P \quad (54)$$

and where  $P$  is the solution to the discrete steady-state Ricatti equation

$$P = \Phi^T P \Phi - \Phi^T P \Gamma (R \Gamma + \Gamma^T P \Gamma)^{-1} \Gamma^T P \Phi + Q \quad (55)$$

#### IV Design I

##### System Design

The first design makes the assumption that the suppressed modes can be ignored. The simplified approximation of the performance index is used. The state equation for the controller is

$$\underline{x}_c[(k+1)T] = \underline{\Phi}_c \underline{x}_c(kT) + \underline{\Gamma}_c \underline{u}(kT) \quad (56)$$

and the output equation is assumed to be

$$\underline{y}(kT) = \underline{C}_c \underline{x}_c(kT) \quad (57)$$

The performance index for this system is

$$J = \frac{1}{2} \sum_{k=1}^{\infty} \underline{x}_c^T(kT) \underline{Q} T \underline{x}_c(kT) + \underline{u}^T(kT) \underline{R} T \underline{u}(kT) \quad (58)$$

From Chapter III, the solution to this problem is

$$\underline{u}^*(kT) = \underline{F} \underline{x}_c(kT) \quad (59)$$

where

$$\underline{F} = - [\underline{I} + (\underline{R}T)^{-1} \underline{\Gamma}_c^T \underline{P} \underline{\Gamma}_c]^{-1} (\underline{R}T)^{-1} \underline{\Gamma}_c^T \underline{P} \underline{\Phi}_c \quad (60)$$

and where  $\underline{P}$  is the solution to the discrete steady-state Ricatti equation



$$P = \Phi_c^T P \Phi_c - \Phi_c^T P \Gamma_c (R T + \Gamma_c^T P \Gamma_c)^{-1} \Gamma_c^T P \Phi_c + Q T \quad (61)$$

Then the state equation can be rewritten

$$\underline{x}_c[(k+1)T] = \Phi_c \underline{x}_c(kT) + \Gamma_c F \underline{x}_c(kT) \quad (62)$$

The states are not directly available to the controller; therefore, an observer is required to provide inputs to the controller. The observer state equation is

$$\hat{\underline{x}}_c[(k+1)T] = \Phi_c \hat{\underline{x}}_c(kT) + \Gamma_c \underline{u}(kT) + K [\underline{y}(kT) - \hat{\underline{y}}(kT)] \quad (63)$$

where  $K$  is the observer feedback gain matrix and the observer output equation is

$$\hat{\underline{y}}(kT) = C_c \hat{\underline{x}}_c(kT) \quad (64)$$

The output,  $\underline{y}(kT)$ , is still assumed to be determined by Eq (57). Thus, Eq (63) can be written

$$\hat{\underline{x}}_c[(k+1)T] = (\Phi_c - K C_c + \Gamma_c F) \hat{\underline{x}}_c(kT) + K C_c \underline{x}_c(kT) \quad (65)$$

To determine  $K$ , a new state vector must first be defined; the error state vector

$$\underline{e}(kT) \equiv \underline{x}_c(kT) - \hat{\underline{x}}_c(kT) \quad (66)$$

Then

$$\begin{aligned}
\underline{e}[(k+1)T] &= \underline{x}_c[(k+1)T] - \hat{\underline{x}}_c[(k+1)T] \\
&= \underline{\Phi}_c \underline{x}_c(kT) + \Gamma_c F \hat{\underline{x}}_c(kT) - [\underline{\Phi}_c - K C_c + \Gamma_c F] \hat{\underline{x}}_c(kT) \\
&\quad - K C_c \underline{x}_c(kT) \\
&= (\underline{\Phi}_c - K C_c) \underline{e}(kT)
\end{aligned} \tag{67}$$

It is desired to design  $K$  such that  $\underline{e}$  is minimized. Eq (67) is not of the form of Eq (37) from Chapter III, for which the optimal solution is known. However, the eigenvalues of a matrix are the same as those of its transpose. Therefore, the following equation will have the same closed-loop eigenvalues as Eq (67).

$$\underline{w}[(k+1)T] = \underline{\Phi}_c^T \underline{w}(kT) - C_c^T \underline{f}(kT) \tag{68}$$

where

$$\underline{f}(kT) = K^T \underline{w}(kT) \tag{69}$$

This equation is of the form of Eq (37) so that the performance index is

$$J = \frac{1}{2} \sum_{k=1}^{\infty} \underline{w}^T(kT) Q_{ob}^T \underline{w}(kT) + \underline{f}^T(kT) R_{ob}^T \underline{f}(kT) \tag{70}$$

The solution is

$$\underline{f}^*(kT) = K^T \underline{w}(kT) \tag{71}$$

where

$$K^T = [I + (R_{OB}T)^{-1} C_c P_{OB} C_c^T]^{-1} (R_{OB}T)^{-1} C_c P_{OB} \Phi_c^T \quad (72)$$

and where  $P_{OB}$  is the solution to the discrete steady-state Ricatti equation

$$P_{OB} = \Phi_c P_{OB} \Phi_c^T - \Phi_c P_{OB} C_c^T (R_{OB}T + C_c P_{OB} C_c^T)^{-1} C_c P_{OB} \Phi_c^T + Q_{OB}T \quad (73)$$

The transpose of  $K^T$  gives the desired observer feedback gain matrix,  $K$ .

Thus the system equations based on the assumption that the suppressed modes can be ignored are

$$\begin{aligned} \underline{x}_c[(k+1)T] &= \Phi_c \underline{x}_c(kT) + \Gamma_c F \hat{x}_c(kT) \\ &= (\Phi_c + \Gamma_c F) \underline{x}_c(kT) - \Gamma_c F \underline{e}(kT) \end{aligned} \quad (74)$$

$$\underline{e}[(k+1)T] = (\Phi_c - KC_c) \underline{e}(kT) \quad (75)$$

In many cases, the suppressed modes cannot be simply ignored. To see their effect, the total closed loop system of equations is derived. The output equation was assumed to be Eq (57); however, with the suppressed modes included, it is actually (ignoring the residual modes)

$$\underline{y}(kT) = C_c \underline{x}_c(kT) + C_s \underline{x}_s(kT) \quad (76)$$

With this output equation, the observer state equation becomes

$$\hat{\underline{x}}_c[(k+1)T] = (\Phi_c - KC_c + \Gamma_c F) \hat{\underline{x}}_c(kT) + KC_c \underline{x}_c(kT) + KC_s \underline{x}_s(kT) \quad (77)$$

The error state equation is thus

$$\underline{e}[(k+1)T] = (\Phi_c - KC_c) \underline{e}(kT) - KC_s \underline{x}_s(kT) \quad (78)$$

and the suppressed state equation is

$$\begin{aligned} \underline{x}_s[(k+1)T] &= \Phi_s \underline{x}_s(kT) + \Gamma_s \underline{u}(kT) \\ &= \Phi_s \underline{x}_s(kT) + \Gamma_s \hat{\underline{x}}_c(kT) \\ &= \Gamma_s F \underline{x}_c(kT) - \Gamma_s F \underline{e}(kT) + \Phi_s \underline{x}_s(kT) \end{aligned} \quad (79)$$

The total system state equation can be written in matrix form as

$$\begin{bmatrix} \underline{x}_c[(k+1)T] \\ \underline{e}[(k+1)T] \\ \underline{x}_s[(k+1)T] \end{bmatrix} = \begin{bmatrix} \Phi_c + \Gamma_c F & -\Gamma_c F & 0 \\ 0 & \Phi_c - KC_c & KC_s \\ \Gamma_s F & -\Gamma_s F & \Phi_s \end{bmatrix} \begin{bmatrix} \underline{x}_c(kT) \\ \underline{e}(kT) \\ \underline{x}_s(kT) \end{bmatrix} \quad (80)$$

The  $\Gamma_s F$  and  $KC_s$  terms are the control and observation spillover terms. The eigenvalues of  $\Phi_c + \Gamma_c F$ ,  $\Phi_c - KC_c$ , and  $\Phi_s$  are the designed eigenvalues. Unfortunately, due to the spillover terms, the total system eigenvalues are altered from the desired eigenvalues. As the gain matrices  $F$  and  $K$  are increased (with increased control of the system), the altered eigenvalues can become unstable.

### System Performance

In the following analysis, the system eigenvalues are plotted in the  $z$ -domain. Before examining the system eigenvalues and time response, it is perhaps best to review the interpretation of eigenvalue placement in the  $z$ -plane. There is a correlation between eigenvalue position in the  $s$ -plane and that in the  $z$ -plane. The  $s$ -plane is mapped into the  $z$ -plane via the transformation  $z = e^{sT} = e^{\sigma T} \pm j\omega_d T$  where  $s = \sigma \pm j\omega_d$ . This transformation maps the entire left-half  $s$ -plane into a unit circle centered at the origin in the  $z$ -plane. In order for a system to be stable, all eigenvalues must lie within the unit circle. The entire real axis in the  $s$ -plane is mapped onto the positive real axis in the  $z$ -plane. Lines of constant damping,  $\sigma$ , in the  $s$ -plane map into concentric circles centered at the origin.  $\sigma=0$  lies on the unit circle and  $\sigma=-\infty$  is at the origin. Lines of constant frequency,  $\omega_d$ , map into radial lines. And lines of constant damping ratio become logarithmic spirals in the  $z$ -plane.

Listed in Table IV are the eigenvalues of the above system design for a sampling time of 0.1 seconds and with the state and control weighting matrices entered as identity matrices. The system eigenvalues are plotted in the  $z$ -plane in Figure 3. The time response to the initial conditions given in Chapter III is shown in Figures 4 and 5.

) As a basis for comparison, the discrete open-loop eigenvalues and time response are presented in Appendix C. It can be seen that the open-loop system is stable but the transient response is unsatisfactory. After twenty seconds, the X and Y displacements of the line of sight are still quite large. For this design and those which follow, it is desired to reduce the X and Y displacements to less than 0.0004 radians and 0.00025 radians respectively, in twenty seconds.

Table IV demonstrates the effects of the spillover terms. The designed eigenvalues are listed in the left-hand column and the resulting system eigenvalues from Eq (80) are listed on the right. Because the weighting matrices  $Q$  and  $Q_{OB}$  are only identity matrices, the gain matrices  $F$  and  $K$  are small and the system eigenvalues are not altered drastically. The system is still stable and Figures 4 and 5 show that the time response has been improved. The desired specifications are still not met, however.

To meet the specifications, more emphasis must be placed on controlling the states. This is done by increasing the state weighting matrices  $Q$  and  $Q_{OB}$  in the performance indices. Table V presents the eigenvalues of the system design for  $Q$  and  $Q_{OB}$  increased to  $10 I$  matrices. For this case, the spillover terms are increased enough to drastically change the designed eigenvalues. In fact, one of the suppressed eigenvalues is now unstable. These

system eigenvalues are also plotted in Figure 3. The time response, shown in Figures 6 and 7, bears out this instability. Further trials of  $Q$  and  $Q_{OB}$  would show that this controller design cannot achieve the desired system performance because the system goes unstable before the desired performance can be reached.

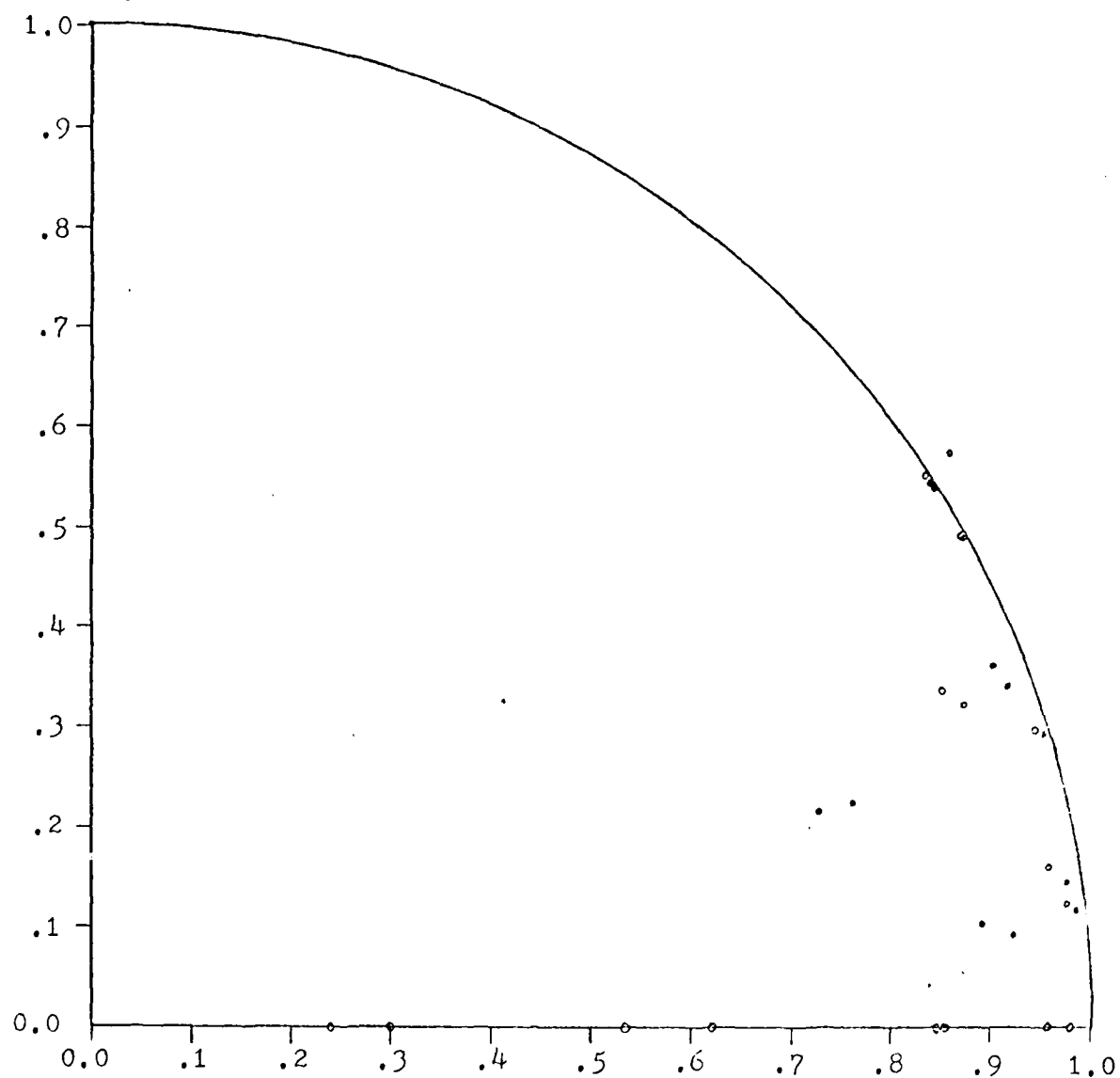
Table IV

## Eigenvalues of Design I

$$Q = 1.0 \text{ I} ; Q_{OB} = 1.0 \text{ I}; T = .1$$

<u>Eigenvalues of <math>\phi_c + \Gamma_c F</math></u>		<u>System Eigenvalues</u>
.98548 $\pm$ .11585i	-C-	.98572 $\pm$ .11690i
.91600 $\pm$ .33968i	-C-	.91587 $\pm$ .33988i
.97811 $\pm$ .14434i	-C-	.97810 $\pm$ .14547i
.90144 $\pm$ .36415i	-C-	.90142 $\pm$ .36416i
<u>Eigenvalues of <math>\phi_c - KC_c</math></u>		
.92264 $\pm$ .10453i	-O-	.92237 $\pm$ .09049i
.76201 $\pm$ .22371i	-O-	.76207 $\pm$ .22300i
.88784 $\pm$ .111419i	-O-	.88937 $\pm$ .10111i
.72520 $\pm$ .21495i	-O-	.72540 $\pm$ .21470i
<u>Eigenvalues of <math>\phi_s</math></u>		
.95496 $\pm$ .29170i	-S-	.95363 $\pm$ .29292i
.84081 $\pm$ .53607i	-S-	.84090 $\pm$ .53862i
.86809 $\pm$ .49121i	-S-	.86809 $\pm$ .49121i
.83892 $\pm$ .53899i	-S-	.83856 $\pm$ .54050i





$\bullet$   $Q = Q_{OB} = I$   
 $\circ$   $Q = Q_{OB} = 10 I$   
 $\times$   $Q = Q_{OB} = 100 I$

Figure 3. Z-Plane Plot of Eigenvalues of Design I

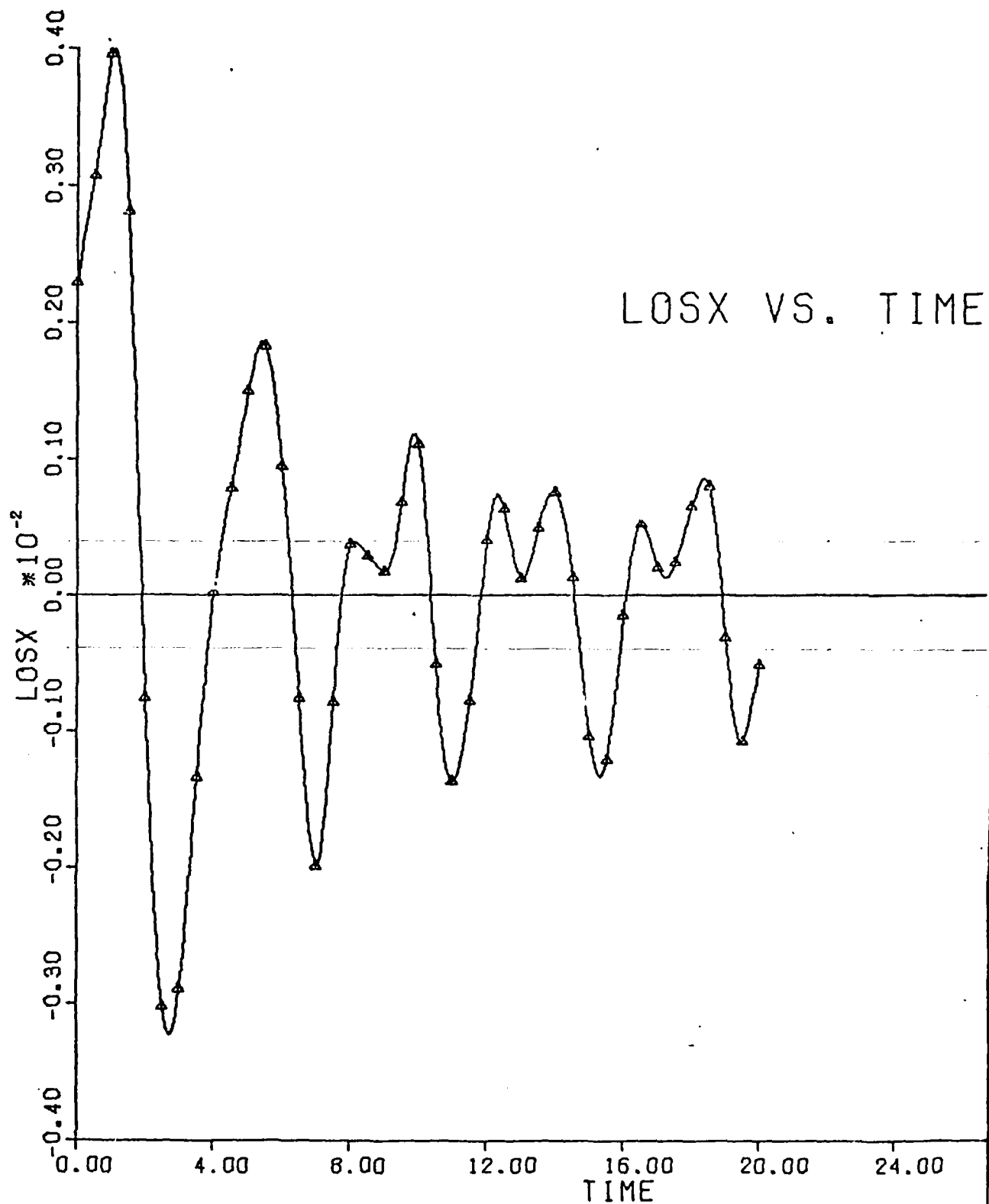


Figure 4. LOSX VS. TIME, Design I,  $Q = Q_{CB} = 1$ ,  $T = .1$

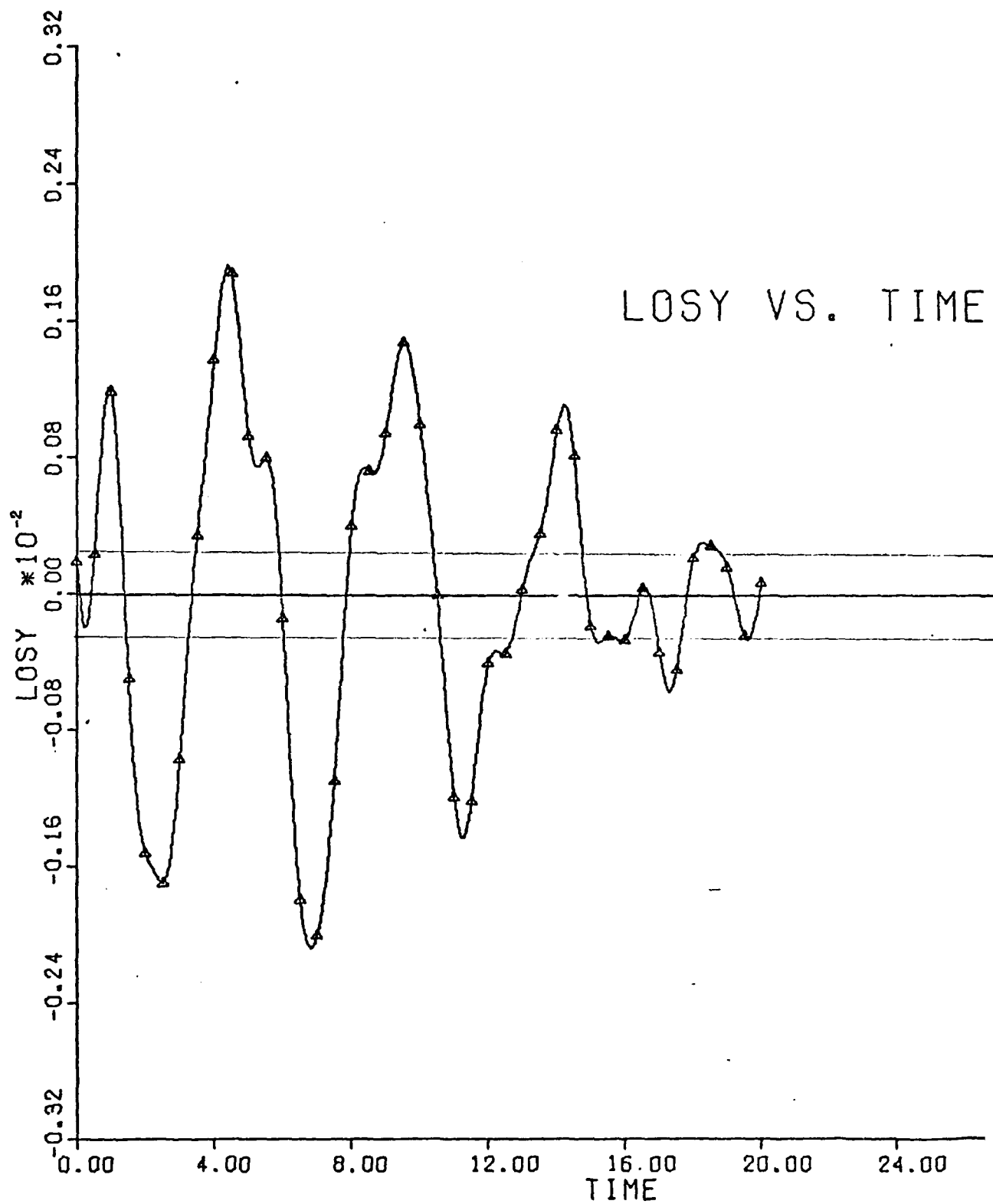


Figure 5. LOS VS. TIME, Design I,  $Q = Q_{OB} = 1$ ,  $T = .1$

Table V

## Eigenvalues of Design I

$$Q = 10.0 \text{ I} ; Q_{OB} = 10.0 \text{ I} ; T = .1$$

<u>Eigenvalues of <math>\phi_c + \Gamma_c F</math></u>		<u>System Eigenvalues</u>
.96930 $\pm$ .11360i	-C-	.97633 $\pm$ .12079i
.87318 $\pm$ .31781i	-C-	.87073 $\pm$ .31938i
.95475 $\pm$ .13946i	-C-	.95827 $\pm$ .15080i
.85127 $\pm$ .33561i	-C-	.85064 $\pm$ .33575i
 <u>Eigenvalues of <math>\phi_c - KC_c</math></u>		
.29844 + 0i	-0-	.29965 + 0i
.87953 + 0i	-0-	.85149 + 0i
.80409 $\pm$ .01949i	-0-	.98221 + 0i
.23649 + 0i	-0-	.23670 + 0i
.58986 + 0i	-0-	.61812 + 0i
.88935 + 0i	-0-	.84875 + 0i
.84675 + 0i	-0-	.53363 + 0i
	-0-	.95642 + 0i
 <u>Eigenvalues of <math>\phi_s</math></u>		
.95496 $\pm$ .29170i	-S-	.94752 $\pm$ .29673i
.84081 $\pm$ .53607i	-S-	.85356 $\pm$ .57269i
.86809 $\pm$ .49121i	-S-	.86809 $\pm$ .49121i
.83892 $\pm$ .53899	-S-	.83686 $\pm$ .55492i

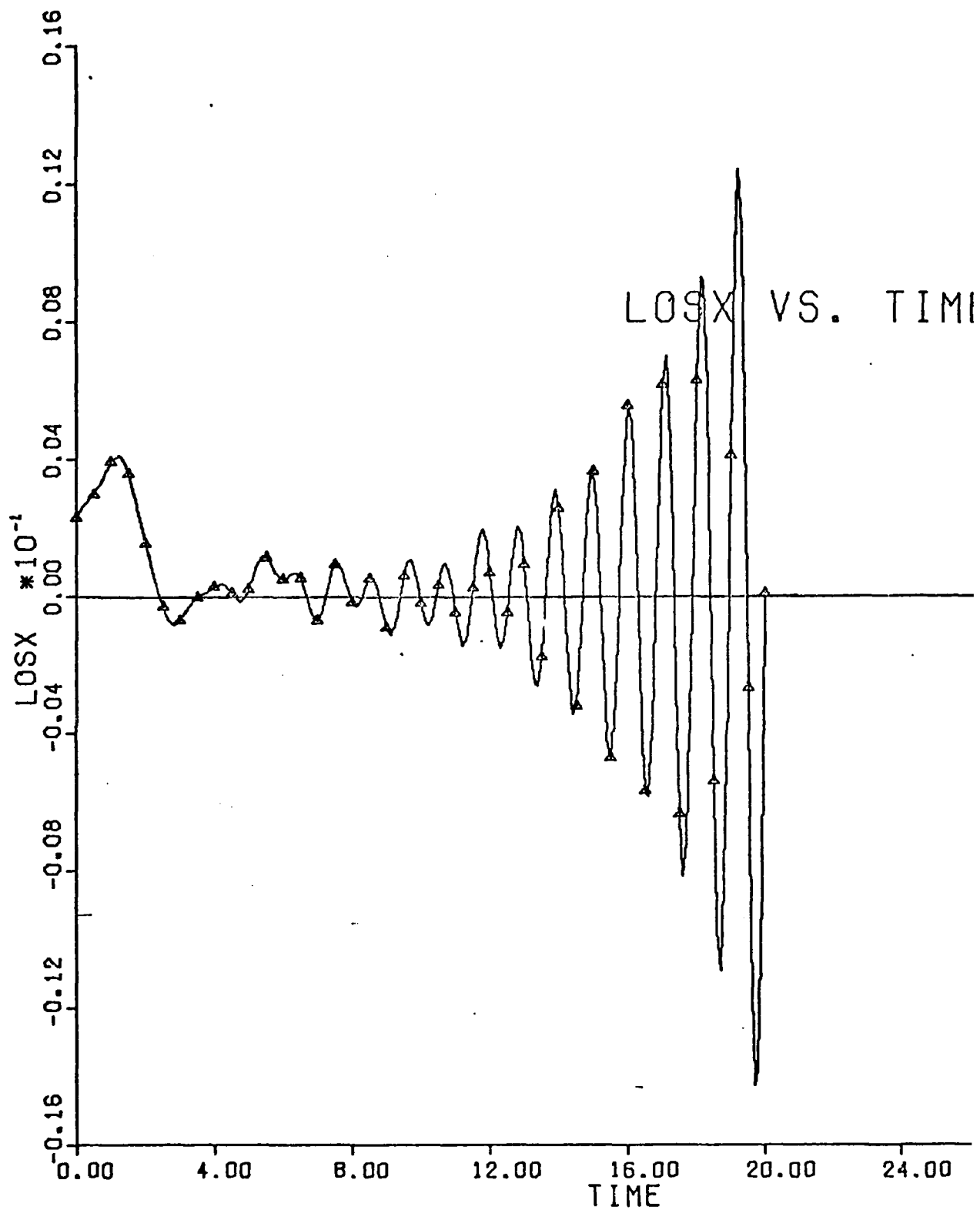


Figure 6. LOSX VS. TIME, Design I,  $Q = Q_{OB} = 10 I$ ,  $T = .1$

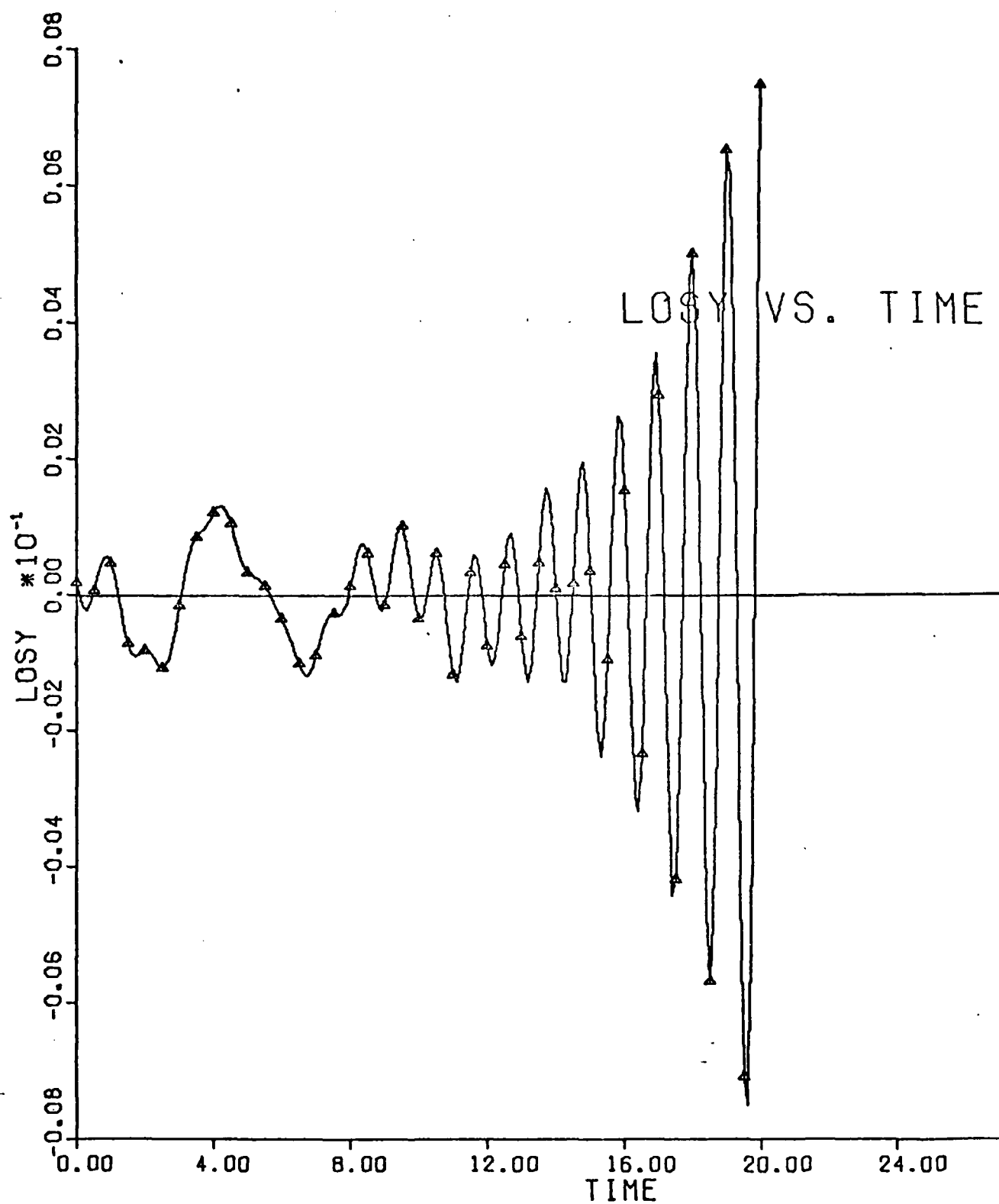


Figure 7. LOS Y VS. TIME, Design I,  $Q = Q_{CB} = 10 I$ ,  $T = .1$

## V Design II

In the second design, the effects of the suppressed modes are accounted for. The system is designed to eliminate their influence, hence their effects are "suppressed". The design begins with the same state equation as the first design

$$\underline{x}_c[(k+1)T] = \underline{F}_c \underline{x}_c(kT) + \underline{G}_c \underline{u}(kT) \quad (81)$$

but this time the output equation is assumed to be

$$\underline{y}(kT) = \underline{C}_c \underline{x}_c(kT) + \underline{C}_s \underline{x}_s(kT) \quad (82)$$

The performance index is the same as before

$$J = \frac{1}{2} \sum_{k=1}^{\infty} \underline{x}_c^T(kT) \underline{Q}^T \underline{x}_c(kT) + \underline{u}^T(kT) \underline{R}^T \underline{u}(kT) \quad (83)$$

The solution is again

$$\underline{u}^*(kT) = \underline{F} \underline{x}_c(kT) \quad (84)$$

This time, however, in order to eliminate the control spillover,  $\underline{F}$  must satisfy the following conditions

$$\underline{G}_c^T \underline{F} \neq 0 \quad (85)$$

$$\underline{G}_s^T \underline{F} = 0 \quad (86)$$

This can be achieved by defining a new control variable,  $\underline{v}$  linearly related to  $\underline{u}$  by

$$\underline{u}(kT) = \underline{M} \underline{v}(kT) \quad (87)$$

where the matrix  $M$  satisfies the relationships

$$\Gamma_c M \neq 0 \quad (88)$$

$$\Gamma_s M = 0 \quad (89)$$

By applying optimal control theory using  $\underline{v}$  as the control vector, a control law of the form

$$\underline{v}(kT) = G \underline{x}_c(kT) \quad (90)$$

can be found. Transforming back to  $\underline{u}$  one finds

$$\underline{u}(kT) = M G \underline{x}_c(kT) = F \underline{x}_c(kT) \quad (91)$$

which satisfies Eqs (85) and (86). Applying the transformation given in Eq (87), the state equation becomes

$$\underline{x}_c[(k+1)T] = \Phi_c \underline{x}_c(kT) + \Gamma_c M \underline{v}(kT) \quad (91)$$

and the performance index becomes

$$J = \frac{1}{2} \sum_{k=1}^{\infty} \underline{x}_c^T(kT) Q T \underline{x}_c(kT) + \underline{v}^T(kT) R_M \underline{v}(kT) \quad (92)$$

where  $R_M = M^T R T M$ . The solution to this problem is

$$\underline{v}^*(kT) = G \underline{x}_c(kT) \quad (93)$$

where

$$G = -[I + R_M^{-1} M^T \Gamma_c^T P \Gamma_c M]^{-1} R_M^{-1} M^T \Gamma_c^T P \Phi_c \quad (94)$$

and  $P$  is the solution to the discrete Ricatti equation



$$P = \bar{I}_c^T P \bar{I}_c - \bar{I}_c^T P \Gamma_c^T M (R_M + M^T \Gamma_c^T P \Gamma_c M)^{-1} M^T \Gamma_c^T P \bar{I}_c + Q T \quad (95)$$

The matrix  $M$ , which satisfies the conditions of Eqs (88) and (89), is found by the method known as Singular Value Decomposition (Ref 4). It is desired to satisfy Eq (88) with a non-zero matrix  $M$ . Since  $\Gamma_s$  is given by Eq (29b), Eq (88) can be written

$$\int_0^{kT} e^{A_s^T \tau} d\tau B_s M = 0 \quad (96)$$

Thus, to satisfy Eq (86) it is only necessary that

$$B_s M = 0 \quad (97)$$

In Chapter II, it was shown that  $B_s$  is

$$B_s = \begin{bmatrix} 0 \\ \underline{B}_s \end{bmatrix} \quad (98)$$

where

$$\underline{B}_s = \phi_s^T D \quad (99)$$

Thus, to satisfy Eq (97), it is only necessary that

$$\underline{B}_s M = 0 \quad (100)$$

Now, using a singular value decomposition of the matrix  $\underline{B}_s$ , the matrix can be written as

$$\underline{B}_s = U \Sigma V \quad (101)$$

where

$U$  is an  $n_s \times n_s$  orthogonal matrix of left singular vectors

$V$  is an  $n_{act} \times n_{act}$  orthogonal matrix of right singular vectors

and

$$\Sigma = \left[ \begin{array}{c|c} N & 0 \\ \hline 0 & 0 \end{array} \right] \quad (102)$$

such that  $N$  is an  $n_o \times n_o$  diagonal matrix of the singular values of  $B_s$ . The dimension  $n_o$  is the number of non-zero singular values. Each singular value is real and must be greater than or equal to zero. The total number of non-zero singular values is equal to the rank of  $B_s$ . If  $B_s$  is full rank, then  $n_o$  is equal to either  $n_s$  or  $n_{act}$ , whichever is least. When the number of actuators is greater than the number of suppressed modes (which is the case for this analysis), then  $n_s < n_{act}$  and  $n_o = n_s$ . In this case, the matrix  $\Sigma$  becomes

$$\Sigma = \left[ \begin{array}{c|c} N & 0 \end{array} \right] \quad (103)$$

Now, the matrix  $V$  can be partitioned into

$$V = \left[ \begin{array}{c|c} V_1 & V_2 \end{array} \right] \quad (104)$$

where  $V_1$  is  $n_{act} \times n_s$  and  $V_2$  is  $n_{act} \times (n_{act} - n_s)$ . Then Eq (100) can be written

$$\underline{B}_s = U \begin{bmatrix} N & | & 0 \end{bmatrix} \begin{bmatrix} V_1^T \\ \hline V_2^T \end{bmatrix} \quad (105)$$

or

$$\underline{B}_s = U N V_1^T \quad (106)$$

If both sides of Eq (106) are multiplied by  $V_2$ , then

$$\begin{aligned} \underline{B}_s V_2 &= U N V_1^T V_2 \\ &= 0 \end{aligned} \quad (107)$$

because  $V$  is an orthogonal matrix. The matrix  $V_2$  meets the condition of Eq (99), thus

$$M = V_2 \quad (108)$$

is a possible choice.

The state equation can now be written

$$\underline{x}_c[(k+1)T] = \Phi_c \underline{x}_c(kT) + \Gamma_c F \hat{\underline{x}}_c(kT) \quad (109)$$

where  $F$  is given by Eqs (90b), (94), and (108). The observer state vector in the above equation is given by the observer state equation

$$\hat{\underline{x}}_c[(k+1)T] = \Phi_c \hat{\underline{x}}_c(kT) + \Gamma_c \underline{u}(kT) + K[\underline{y}(kT) - \hat{\underline{y}}(kT)] \quad (110)$$

where  $K$  is the observer feedback gain matrix and the observer output equation is

$$\hat{\underline{y}}(kT) = C_c \hat{\underline{x}}_c(kT) \quad (111)$$

Substituting Eqs (82) and (111) into Eq (110), the observer state equation can be written

$$\hat{\underline{x}}_c[(k+1)T] = (\Phi_c - KC_c + \Gamma_c F) \hat{\underline{x}}_c(kT) + KC_c \underline{x}_c(kT) + KC_s \underline{x}_s(kT) \quad (112)$$

To determine K, the error state vector is defined

$$\underline{e}(kT) = \underline{x}_c(kT) - \hat{\underline{x}}_c(kT)$$

Then

$$\begin{aligned} \underline{e}[(k+1)T] &= \underline{x}_c[(k+1)T] - \hat{\underline{x}}_c[(k+1)T] \\ &= \Phi_c \underline{x}_c(kT) + \Gamma_c F \hat{\underline{x}}_c(kT) - (\Phi_c - KC_c + \Gamma_c F) \hat{\underline{x}}_c(kT) \\ &\quad - KC_c \underline{x}_c(kT) - KC_s \underline{x}_s(kT) \\ &= (\Phi_c - KC_c) \underline{e}(kT) - KC_s \hat{\underline{x}}_s(kT) \end{aligned} \quad (113)$$

In order to eliminate the observation spillover, the gain matrix, K, must satisfy the conditions

$$KC_c \neq 0 \quad (114)$$

$$KC_s = 0 \quad (115)$$

As with F, the observer gain matrix can be defined as the product of two matrices

$$K = LM_{OB} \quad (116)$$

where

$$M_{0B} C_c \neq 0 \quad (117)$$

$$M_{0B} C_s = 0 \quad (118)$$

Then the error state equation becomes

$$\underline{e}[(k+1)T] = (\Phi_c - KC_c) \underline{e}(kT) \quad (119)$$

As in Design I, this equation will have the same closed-loop eigenvalues as the equation

$$\underline{w}[(k+1)T] = \Phi_c^T \underline{w}(kT) - C_c^T \underline{g}(kT) \quad (120)$$

where

$$\underline{g}(kT) = K^T \underline{w}(kT) \quad (121)$$

With K defined as in Eq (116), this equation can be transformed into

$$\underline{w}[(k+1)T] = \Phi_c^T \underline{w}(kT) - C_c^T M_{0B}^T \underline{h}(kT) \quad (122)$$

where

$$\underline{h}(kT) = L^T \underline{w}(kT) \quad (123)$$

The performance index for this state equation is

$$J = \frac{1}{2} \sum_{k=1}^{\infty} \underline{w}^T(kT) Q_{0B}^T \underline{w}(kT) + \underline{h}^T(kT) R_{0B_M} \underline{h}(kT) \quad (124)$$

where

$$R_{0B_M} = M_{0B} R_{0B}^T M_{0B}^T \quad (125)$$

The solution is

$$\underline{h}^*(kT) = L^T \underline{w}(kT) \quad (126)$$

where

$$L^T = [I + R_{OB_M}^{-1} M_{OB} C_c P_{OB} C_c^T M_{OB}^T]^{-1} R_{OB_M}^{-1} M_{OB} C_c P_{OB} \Phi_c^T \quad (127)$$

and where  $P_{OB}$  is the solution to the discrete steady-state Ricatti equation

$$P_{OB} = \Phi_c P_{OB} \Phi_c^T - \Phi_c P_{OB} C_c^T M_{OB}^T (R_{OB_M} + M_{OB} C_c P_{OB} C_c^T M_{OB}^T)^{-1} M_{OB} C_c P_{OB} \Phi_c^T + Q_{OB}^T \quad (128)$$

The transpose of  $L^T$  given in Eq (127) is the desired matrix  $L$  in Eq (116).  $M_{OB}$  must be determined by another singular value decomposition. This time it is desired to satisfy Eqs (117) and (118). In Chapter II, it was shown that  $C_s$  is

$$C_s = [\underline{c}_s \mid 0] \quad (129)$$

where

$$\underline{c}_s = C_p \phi_s \quad (130)$$

To satisfy Eq (118), it is only necessary that

$$M_{OB} \underline{c}_s = 0 \quad (131)$$

A singular value decomposition of the matrix  $\underline{c}_s$  gives

$$\underline{c}_s = U_{OB} \sum_{OB} V_{OB} \quad (132)$$

where

$U_{OB}$  is an  $n_{sen} \times n_{sen}$  orthogonal matrix of left singular vectors

$V_{OB}$  is an  $n_s \times n_s$  orthogonal matrix of right singular vectors

and

$$\Sigma_{OB} = \begin{bmatrix} N_{OB} & 0 \\ 0 & 0 \end{bmatrix} \quad (133)$$

such that  $N_{OB}$  is an  $n_\sigma \times n_\sigma$  diagonal matrix of non-zero singular values of  $C_s$ . The dimension  $n_\sigma$ , the number of non-zero singular values, is equal to the rank of  $C_s$ . If  $C_s$  is full rank, then  $n_\sigma$  is equal to either  $n_s$  or  $n_{sen}$ , whichever is least. When the number of sensors is greater than the number of suppressed modes (which is the case for this analysis), then  $n_s < n_{sen}$  and  $n_\sigma = n_s$ . In this case, the matrix becomes

$$C_s = U_{O2} \begin{bmatrix} N_{OB} \\ 0 \end{bmatrix} V_{OB} \quad (134)$$

Now, the matrix  $U_{OB}$  can be partitioned into

$$U_{OB} = \begin{bmatrix} U_{OB1} & U_{OB2} \end{bmatrix} \quad (135)$$

where  $U_{OB1}$  is  $n_{sen} \times n_s$  and  $U_{OB2}$  is  $n_{sen} \times (n_{sen} - n_s)$ . Then

Eq (132) can be written

$$C_s = \begin{bmatrix} U_{OB1} & U_{OB2} \end{bmatrix} \begin{bmatrix} N_{OB} \\ 0 \end{bmatrix} V \quad (136)$$

Since the matrix  $U_{OB2}$  is multiplied by zero, this equation becomes

$$\underline{C}_s = U_{OB1} N_{OB} V_{OB} \quad (137)$$

If both sides of Eq (137) are multiplied by  $U_{OB2}^T$ , then

$$\begin{aligned} U_{OB2}^T \underline{C}_s &= U_{OB2}^T U_{OB1} N_{OB} V_{OB} \\ &= 0 \end{aligned} \quad (138)$$

because  $U_{OB}$  is an orthogonal matrix. The matrix  $U_{OB2}^T$  meets the condition of Eq (131), thus

$$M_{OB} = U_{OB2}^T \quad (139)$$

The error state equation is now as given in Eq (119) with the observer gain matrix,  $K$ , as given by Eqs (116), (127), and (139).

The suppressed state equation is

$$\begin{aligned} \underline{x}_s[(k+1)T] &= \bar{\Phi}_s \underline{x}_s(kT) + \Gamma_s \underline{u}(kT) \\ &= \bar{\Phi}_s \underline{x}_s(kT) + \Gamma_s F \hat{\underline{x}}_c(kT) \\ &= \bar{\Phi}_s \underline{x}_s(kT) \end{aligned}$$

The total system state equation can be written in matrix form as

$$\begin{bmatrix} \underline{x}_c[(k+1)T] \\ \underline{e}[(k+1)T] \\ \underline{x}_s[(k+1)T] \end{bmatrix} = \begin{bmatrix} \bar{\Phi}_c + \Gamma_c F & -\Gamma_c F & 0 \\ 0 & \bar{\Phi}_c - K C_c & 0 \\ 0 & 0 & 0 \end{bmatrix} \begin{bmatrix} \underline{x}_c(kT) \\ \underline{e}(kT) \\ \underline{x}_s(kT) \end{bmatrix} \quad (141)$$



### System Performance

Table VI presents the closed-loop system eigenvalues for Design II. With the spillover terms eliminated, the system eigenvalues are identical to the desired eigenvalues (to at least eight decimal places). The eigenvalues for  $Q = 1.0 I$  and  $Q_{OB} = 1.0 I$  are shown in the left-hand column. These eigenvalues are plotted in Figure 8. They are all stable and the controlled state eigenvalues (those of  $\Phi_c + \Gamma_c F$ ) are slightly closer to the origin than the open-loop eigenvalues in Appendix C. This implies that the time response should be slightly improved, which, as seen in Figures 9 and 10, is the case. In comparison with the corresponding system response of Design I, it can be seen that the eigenvalues of Design II are slightly farther from the origin than those in Design I. The time response is actually somewhat poorer for Design II. Thus, there seems to be some loss of control (for the same  $Q$  and  $Q_{OB}$ ) in return for suppression of the spillover. This is due to the transformation of Eq (87), because the new control vector,  $\underline{v}$ , is of lower dimension than  $\underline{u}$ .

To improve the performance, the state weighting matrices  $Q$  and  $Q_{OB}$  are increased by a factor of 10. The resulting eigenvalues are shown in the center column of Table VI and are plotted in Figure 8. These have remained stable (unlike those of Design I) and have moved closer to

the origin. The time response, shown in Figures 11 and 12, is markedly improved but the specifications have still not been met.

For the eigenvalues of the right-hand column of Table VI, the state weighting matrices have been increased by 10 again. The eigenvalues are all stable and have moved even closer to the origin. They are again plotted in Figure 8. The time response for this system is presented in Figures 13 and 14 and shows that the specifications have been approximately met.

Table VI  
Eigenvalues of Design II

$Q = 1.0 \text{ I}$	$Q = 10.0 \text{ I}$	$Q = 100.0 \text{ I}$
$Q_{OB} = 1.0 \text{ I}$	$Q_{OB} = 10.0 \text{ I}$	$Q_{OB} = 100.0 \text{ I}$

Eigenvalues of  $\phi_c + \Gamma_c F$

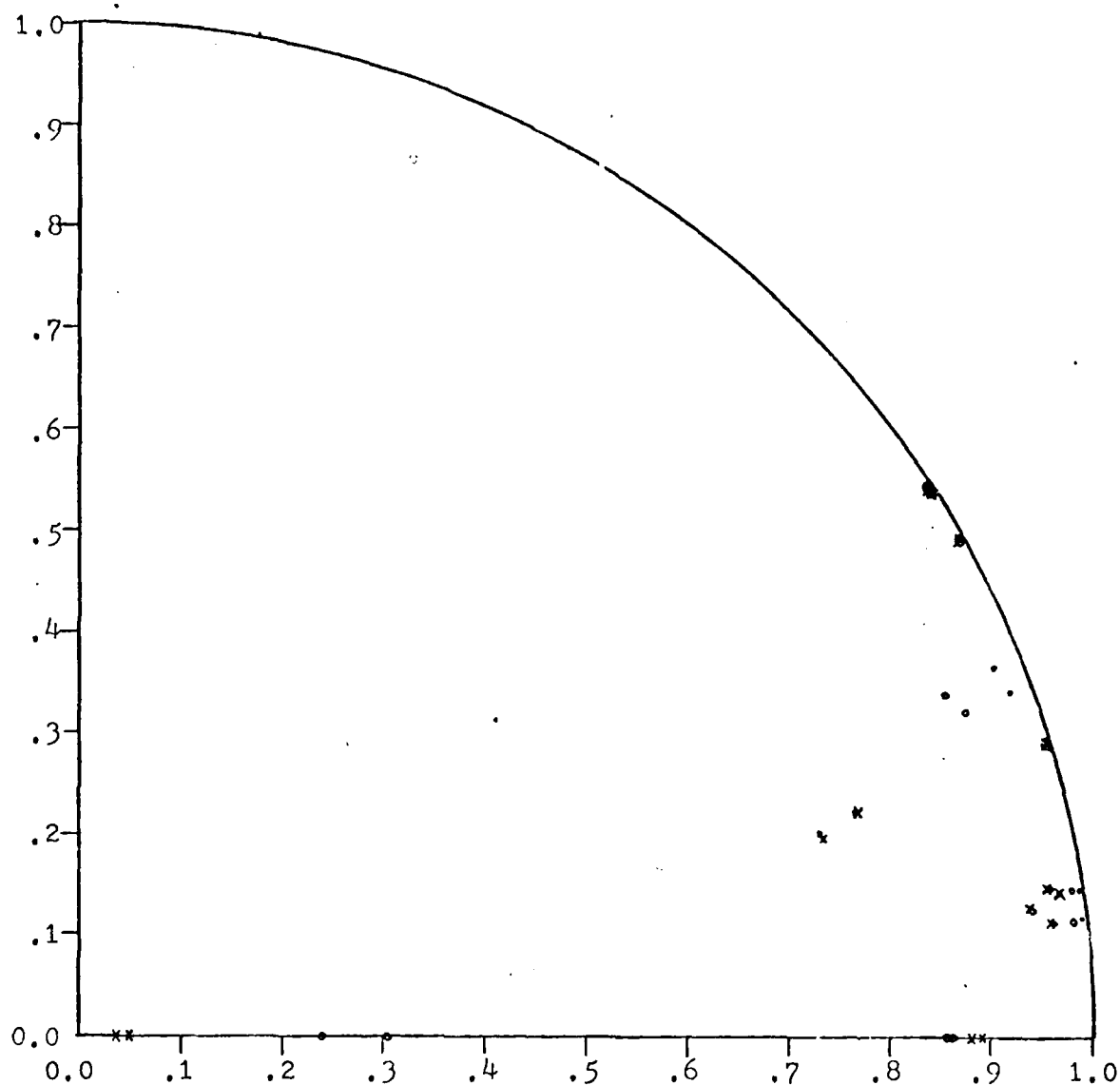
.98892 ± .11629i	.98014 ± .11519i	.95726    .11396i
.91629 ± .33980i	.87409 ± .31830i	.76732    .22188i
.98613 ± .14568i	.97988 ± .14468i	.96482    .14330i
.90177 ± .36430i	.85225 ± .33620i	.73133    .21138i

Eigenvalues of  $\phi_c - KC_c$

.76513 ± .22486i	.30172 + 0i	.04862 + 0i
.95803 ± .11399i	.93797 ± .12381i	.93596 ± .12776i
.72822 ± .21638i	.86204 + 0i	.88921 + 0i
.96553 ± .14334i	.95463 ± .14609i	.95291 ± .14725i
	.23944 + 0i	.03449 + 0i
	.85228 + 0i	.87946 + 0i

Eigenvalues of  $\phi_s$

.95496 ± .29170i	.95496 ± .29170i	.95496 ± .29170i
.84081 ± .53607i	.84081 ± .53607i	.84081 ± .53607i
.86809 ± .49121i	.86809 ± .49121i	.86809 ± .49121i
.83892 ± .53899i	.83892 ± .53899i	.83892 ± .53899i



$\bullet$   $Q = Q_{OB} = I$   
 $\circ$   $Q = Q_{OB} = 10 I$   
 $\times$   $Q = Q_{OB} = 100 I$

Figure 8. Z-Plane Plot of Eigenvalues of Design II

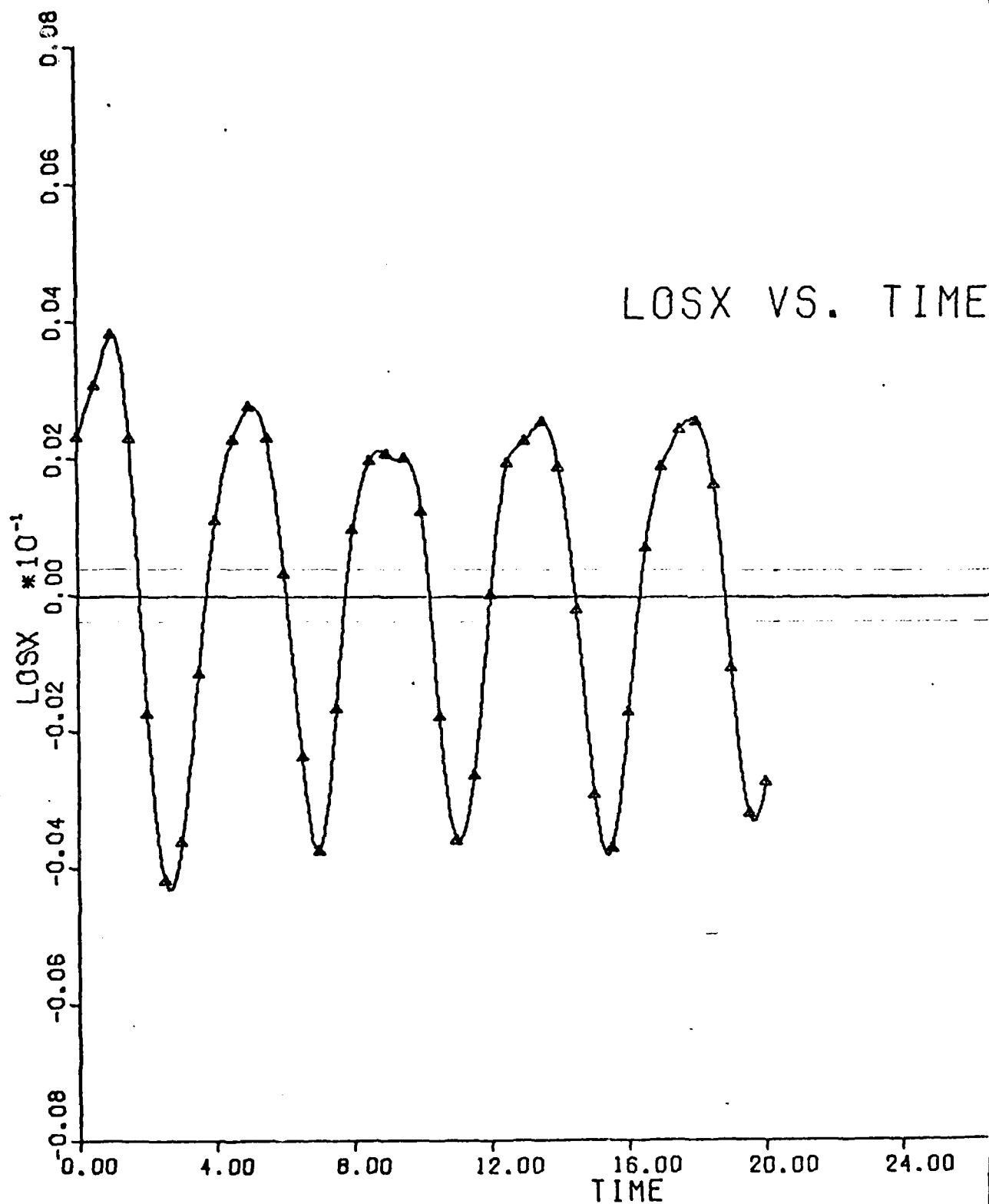


Figure 9. LOSX VS TIME, Design II,  $Q = Q_{OB} = 1$ ,  $T = .1$

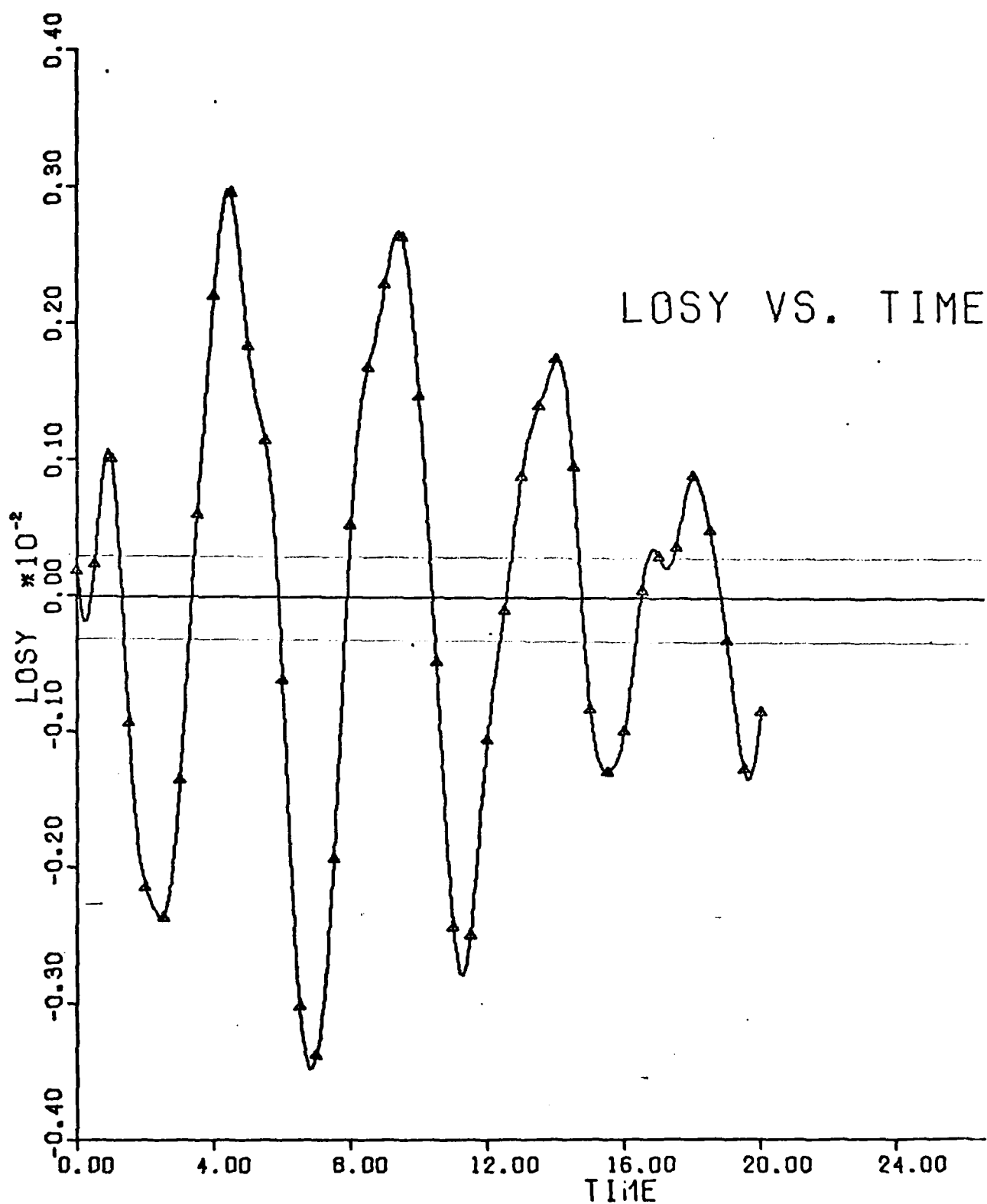


Figure 10. LOS Y VS. TIME, Design II,  $Q = Q_{OB} = 1$ ,  $T = .1$

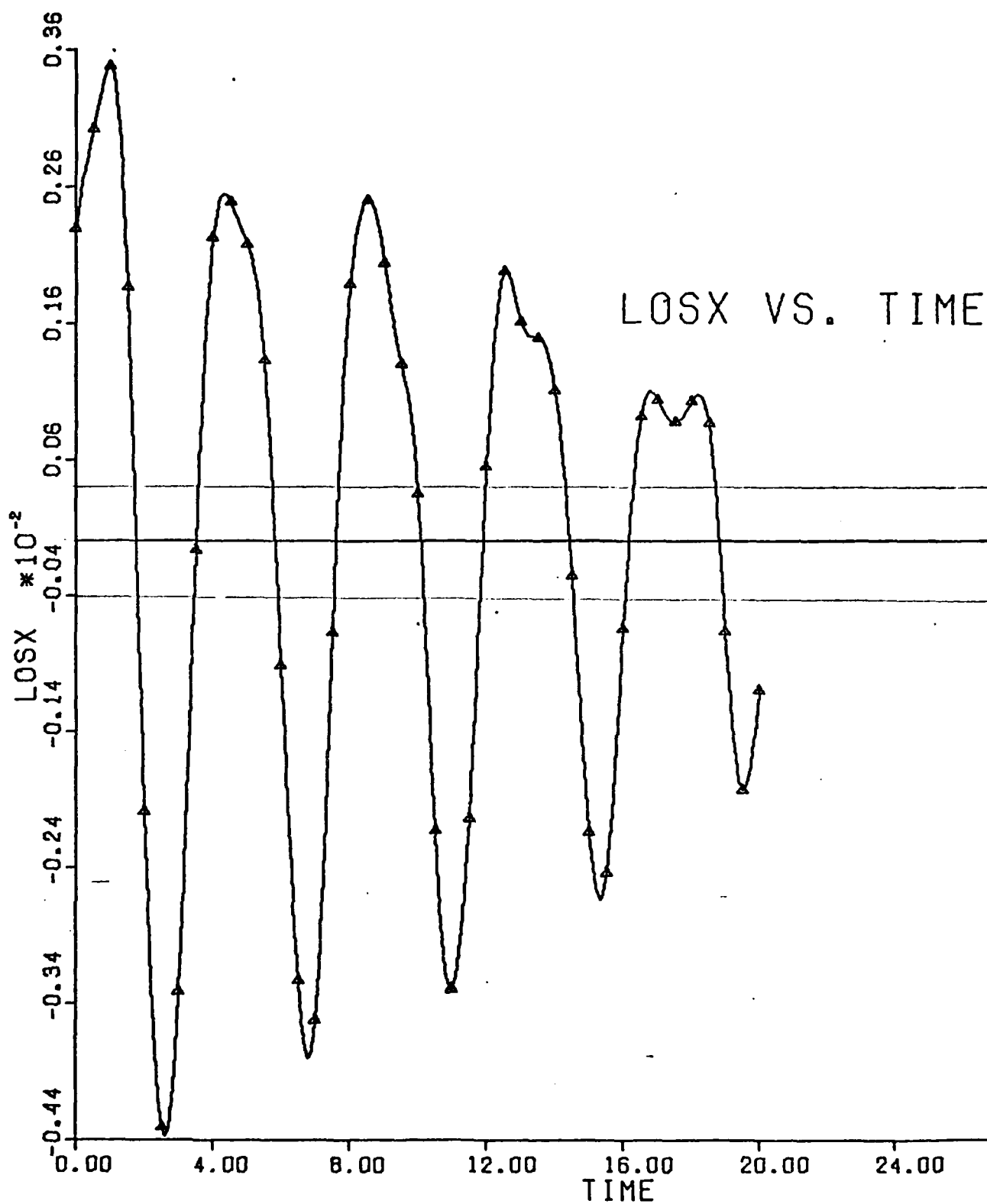


Figure 11. LOSX VS. TIME, Design II,  $Q = Q_{OB} = 10 I$ ,  $T = .1$

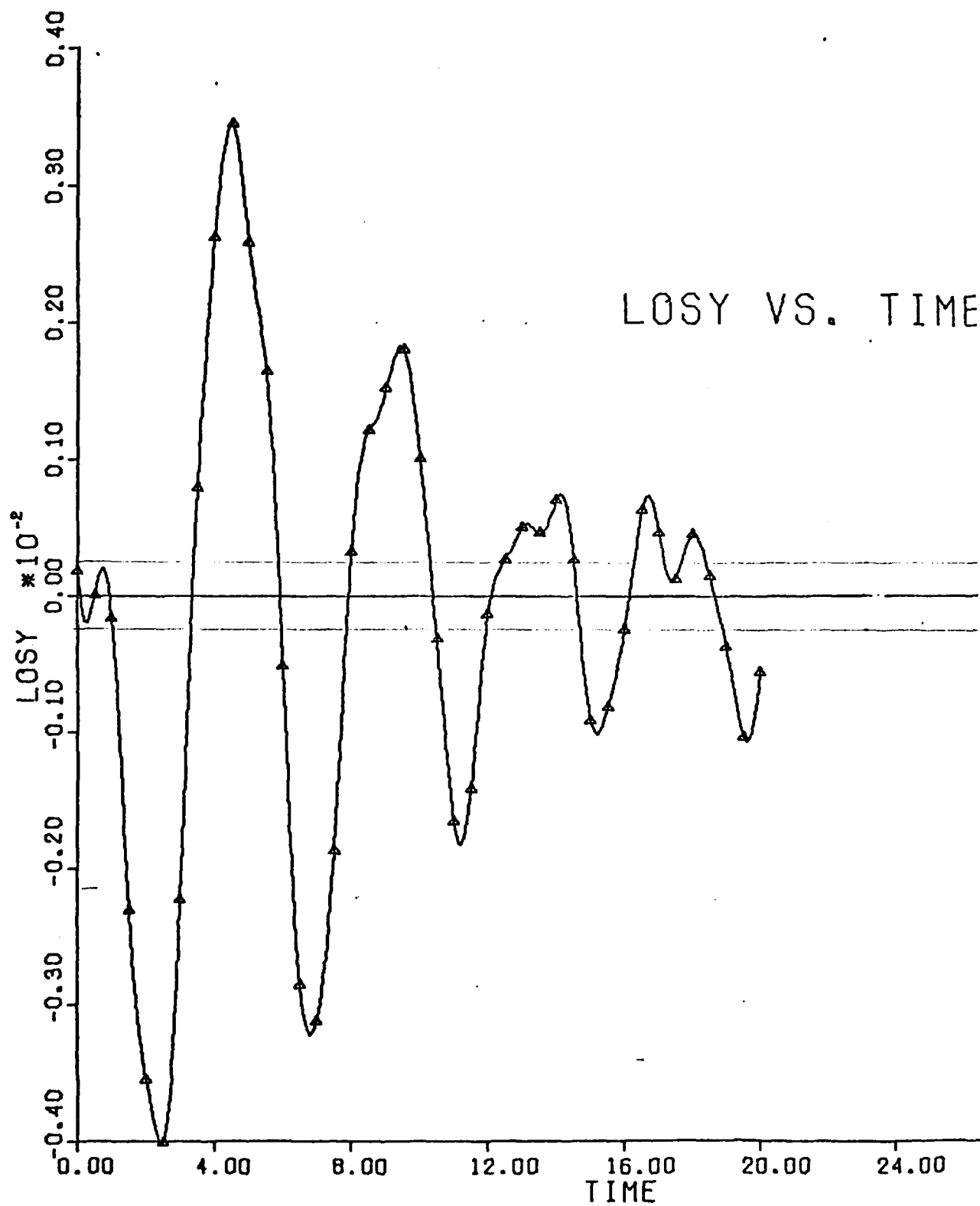


Figure 12. LOS Y VS. TIME, Design II,  $Q = Q_{OB} = 10 I$ ,  $T = .1$



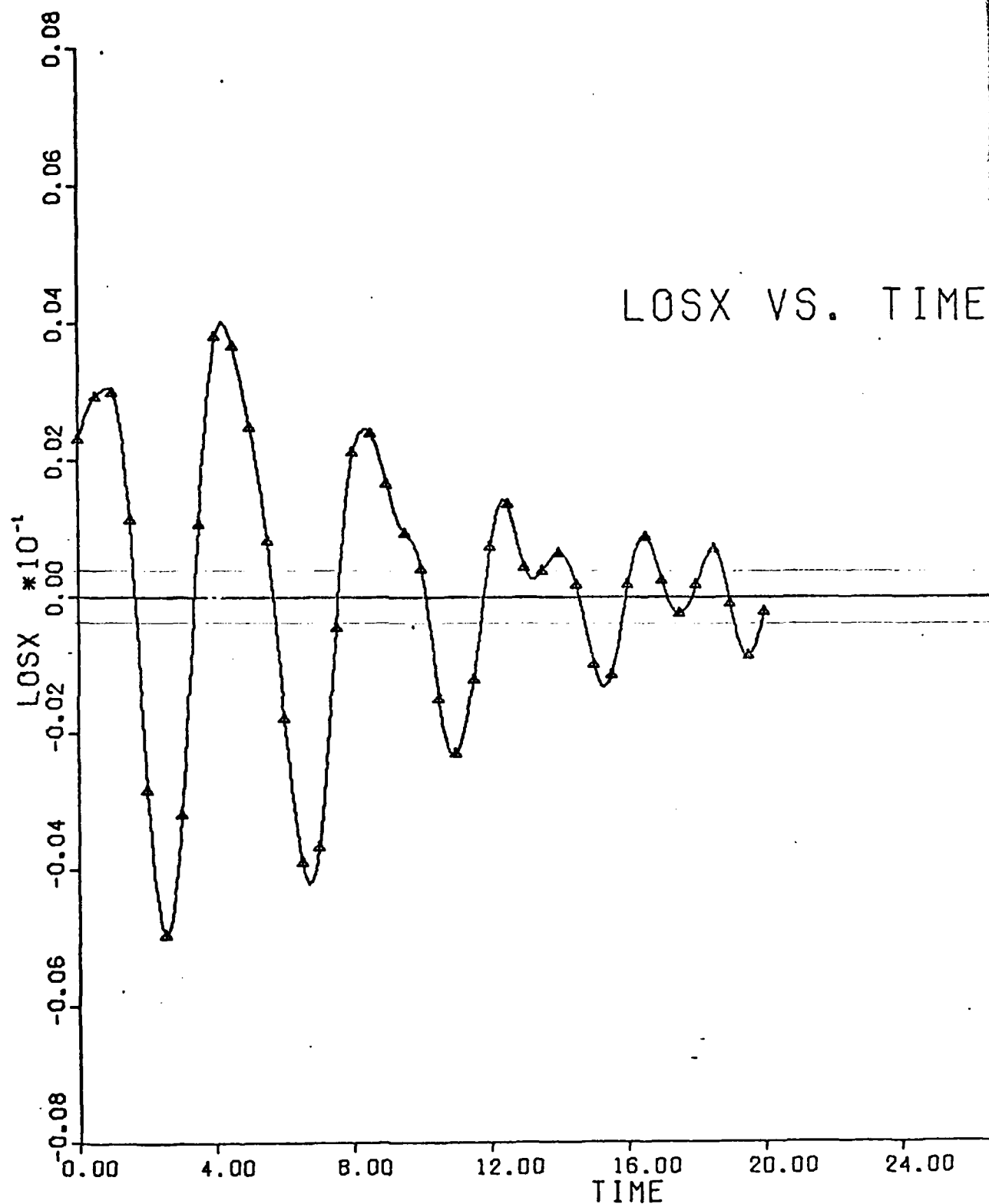


Figure 13, LOSX VS. TIME, Design II,  $Q = Q_{CB} = 100 I$ ,  $T = .1$

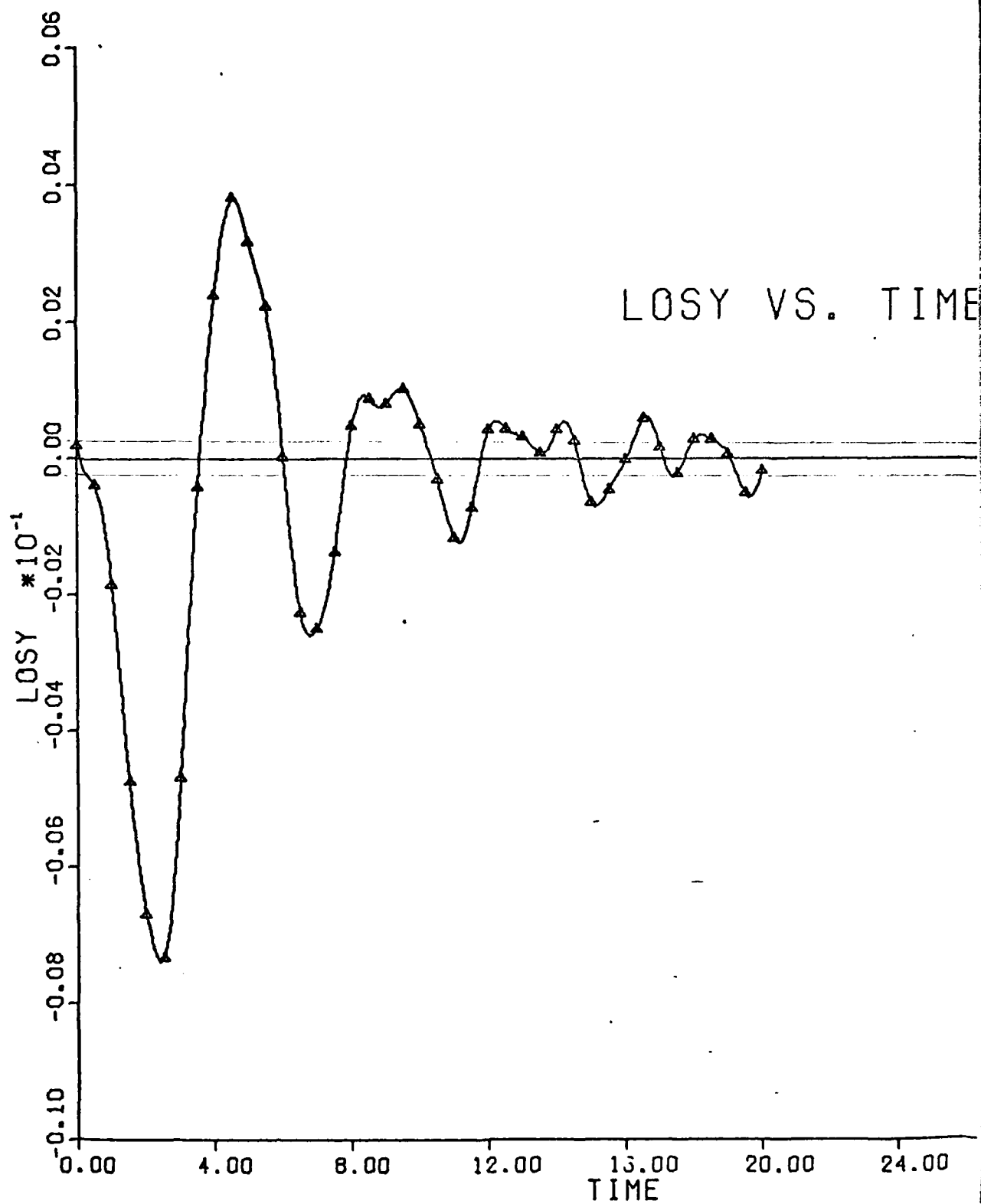


Figure 14. LOS Y VS. TIME, Design II,  $Q = Q_{CB} = 100 I$ ,  $T = .1$

## VI Design III

In the previous two designs the discrete performance indices have been of the form of the simplified performance index of Chapter III, Eq (52). This approximation's validity depends on the accuracy of the assumption in Eq (47). To see the effect of this approximation, Design III makes use of a much more accurate performance index.

The form of the discrete performance index was shown in Chapter III to be

$$J = \frac{1}{2} \sum_{k=1}^{\infty} \underline{x}^T(kT) Q_d \underline{x}(kT) + \underline{x}^T(kT) S_d \underline{u}(kT) + \underline{u}^T(kT) S_d^T \underline{x}(kT) + \underline{u}^T(kT) R_d \underline{u}(kT) \quad (142)$$

where

$$Q_d = \int_0^T \Phi^T(t) Q \Phi(t) dt \quad (143)$$

$$S_d = \int_0^T \Phi^T(t) Q \Gamma(t) dt \quad (144)$$

$$R_d = \int_0^T \Gamma^T(t) Q \Gamma(t) + R dt \quad (145)$$

Equations (143), (144), and (145) can be approximated by numerical integration equations

$$Q_d \approx \frac{T}{10} \left\{ \Phi^T(0) Q \Phi(0) + \Phi^T\left(\frac{T}{10}\right) Q \Phi\left(\frac{T}{10}\right) + \dots + \Phi^T\left(\frac{9T}{10}\right) Q \Phi\left(\frac{9T}{10}\right) \right\} \quad (146)$$

$$S_d \approx \frac{T}{10} \{ \bar{x}^T(0) Q \Gamma(0) + \bar{x}^T(\frac{T}{10}) Q \Gamma(\frac{T}{10}) + \dots + \bar{x}^T(\frac{9T}{10}) Q \Gamma(\frac{9T}{10}) \} \quad (147)$$

$$R_d \approx \frac{T}{10} \{ \Gamma^T(0) Q \Gamma(0) + \bar{x}^T(\frac{T}{10}) Q \Gamma(\frac{T}{10}) + \dots + \Gamma^T(\frac{9T}{10}) Q \Gamma(\frac{9T}{10}) \} + RT \quad (148)$$

This performance index is not of the form of Eq (52) for which the solution is known. However, by defining a matrix  $W$  as

$$W^T = S_d R_d^{-1} \quad (149)$$

$$W^T R_d = S_d \quad (150)$$

then, to complete the square in Eq (142)

$$\begin{aligned} [W \underline{x}(kT) + \underline{u}(kT)]^T R_d [W \underline{x}(kT) + \underline{u}(kT)] &= \underline{x}(kT) W^T R_d W \underline{x}(kT) \\ &+ \underline{u}^T(kT) R_d W \underline{x}(kT) + \underline{x}(kT) W^T R_d \underline{u}(kT) + \underline{u}^T(kT) R_d \underline{u}(kT) \end{aligned} \quad (151)$$

Now the performance index of Eq (142) can be written

$$\begin{aligned} J &= \frac{1}{2} \sum_{k=1}^{\infty} \underline{x}^T(kT) [Q_d - W^T R_d W] \underline{x}(kT) + \\ &\quad [W \underline{x}(kT) + \underline{u}(kT)]^T R_d [W \underline{x}(kT) + \underline{u}(kT)] \end{aligned} \quad (152)$$

By defining a new control variable

$$\underline{z}(kT) = W \underline{x}(kT) + \underline{u}(kT) \quad (153)$$

the performance index can be put into the form of Eq (52)

$$J = \frac{1}{2} \sum_{k=1}^{\infty} \underline{x}^T(kT) Q' \underline{x}(kT) + \underline{z}^T(kT) R_d \underline{z}(kT) \quad (154)$$

where

$$Q' = Q_d - W^T R_d W \quad (155)$$

This performance index is of the form of Eq (52). The solution for a state equation of the form of Eq (37) is given by

$$\underline{z}^*(kT) = F \underline{x}(kT) \quad (156)$$

$$\underline{u}^*(kT) = (F - W) \underline{x}(kT) \quad (157)$$

where

$$F = -[I + R_d^{-1} \Gamma^T P \Gamma]^{-1} R_d^{-1} \Gamma^T P [\bar{x} - \Gamma W] \quad (158)$$

and where P is the solution to the discrete steady-state Ricatti equation

$$P = [\bar{x} - \Gamma W]^T P [\bar{x} - \Gamma W] - [\bar{x} - \Gamma W]^T P \Gamma (R_d + \Gamma^T P \Gamma)^{-1} \Gamma^T P [\bar{x} - \Gamma W] + Q' \quad (159)$$

Design III begins with the same state equation as the previous two designs

$$\underline{x}_c[(k+1)T] = \bar{F}_c \underline{x}_c(kT) + \Gamma_c \underline{u}(kT) \quad (160)$$

The output equation is the same as for Design II

$$\underline{y}(kT) = C_c \underline{x}_c(kT) + C_s \underline{x}_s(kT) \quad (161)$$

In order to eliminate the control spillover the same transformation as in Design II is made to the control vector,  $\underline{u}$

$$\underline{u}(kT) = M \underline{v}(kT) \quad (162)$$

The state equation becomes

$$\underline{x}_c[(k+1)T] = \Phi_c \underline{x}_c(kT) + \Gamma_c^T M \underline{v}(kT) \quad (163)$$

and the performance index for this state equation is

$$\begin{aligned} J = \frac{1}{2} \sum_{k=1}^{\infty} \underline{x}_c^T(kT) Q_d \underline{x}_c(kT) + \underline{x}_c(kT) S_M \underline{v}(kT) \\ + \underline{v}^T(kT) S_M^T \underline{x}_c(kT) + \underline{v}^T(kT) R_M \underline{v}(kT) \end{aligned} \quad (164)$$

where

$$S_M = S_d M \quad (165)$$

$$R_M = M^T R_d M \quad (166)$$

As shown earlier in this chapter, this performance index can be written

$$J = \frac{1}{2} \sum_{k=1}^{\infty} \underline{z}^T(kT) Q' \underline{z}(kT) + \underline{z}^T(kT) R_M \underline{z}(kT) \quad (167)$$

where

$$W^T = S_M R_M^{-1} \quad (168)$$

$$\underline{z}(kT) = W \underline{x}_c(kT) + \underline{v}(kT) \quad (169)$$

and the state equation is now

$$Q' = Q_d - W^T R_M W \quad (170)$$

The solution is

$$\underline{z}^*(kT) = F \hat{\underline{x}}_c(kT) \quad (172)$$

$$\underline{v}^*(kT) = (F-W) \hat{\underline{x}}_c(kT) \quad (173)$$

$$\underline{u}^*(kT) = M(F-W) \hat{\underline{x}}_c(kT) \quad (174)$$

where

$$F = -[I + R_M^{-1} M^T \Gamma_c^T P \Gamma_c M]^{-1} R_M^{-1} M^T \Gamma_c^T P [\Phi_c - \Gamma_c M W] \quad (175)$$

and where P is the solution to the discrete steady-state Ricatti equation

$$P = [\Phi_c - \Gamma_c M W]^T P [\Phi_c - \Gamma_c M W] - [\Phi_c - \Gamma_c M W]^T P \Gamma_c M (R_M + M^T \Gamma_c^T P \Gamma_c M)^{-1} M^T \Gamma_c^T P [\Phi_c - \Gamma_c M W] + Q' \quad (176)$$

The state equation can now be written

$$\underline{x}_c[(k+1)T] = \Phi_c \underline{x}_c(kT) + \Gamma_c M (F-W) \hat{\underline{x}}_c(kT) \quad (177)$$

where F is given by Eq (173), W is given by Eq (168), and M is given by Eq (108) from Chapter V. The observer state vector in the above equation is given by the observer state equation

$$\hat{\underline{x}}_c[(k+1)T] = \Phi_c \underline{x}_c(kT) + \Gamma_c \underline{u}(kT) \quad (178)$$

and the observer output equation is

$$\hat{\underline{y}}(kT) = C_c \hat{\underline{x}}_c(kT) \quad (179)$$

Substituting Eqs (161) and (179) into Eq (178), the observer state equation can be written

$$\hat{\underline{x}}_c[(k+1)T] = (\Phi_c - KC_c - \Gamma_c MW + \Gamma_c MF) \hat{\underline{x}}_c(kT) + KC_c \underline{x}_c(kT) + KC_s \underline{x}_s(kT) \quad (180)$$

The error state vector is again defined as

$$\underline{e}(kT) = \underline{x}_c(kT) - \hat{\underline{x}}_c(kT) \quad (181)$$

Then

$$\begin{aligned} \underline{e}[(k+1)T] &= \underline{x}_c[(k+1)T] - \hat{\underline{x}}_c[(k+1)T] \\ &= \Phi_c \underline{x}_c(kT) + \Gamma_c M(F-W) \hat{\underline{x}}_c(kT) \\ &\quad - [\Phi_c - KC_c + \Gamma_c M(F-W)] \hat{\underline{x}}_c(kT) - KC_c \underline{x}_c(kT) - KC_s \underline{x}_s(kT) \\ &= (\Phi_c - KC_c) \underline{e}(kT) - KC_s \underline{x}_s(kT) \end{aligned} \quad (182)$$

In order to eliminate the observation spillover, the gain matrix,  $K$ , is again defined as the product of two matrices

$$K = LM_{OB} \quad (183)$$

where  $M_{OB}$  is as given in Eq (139) in Chapter V. Then the error state equation becomes

$$\underline{e}[(k+1)T] = (\Phi_c - KC_c) \underline{e}(kT) \quad (184)$$

As in the previous chapters, this equation will have the same closed-loop eigenvalues as the equation

$$\underline{w}[(k+1)T] = \Phi_c^T - C_c^T \underline{g}(kT) \quad (185)$$



where

$$\underline{q}(kT) = K^T \underline{w}(kT) \quad (186)$$

With  $K$  defined as in Eq (183), this equation can be transformed into

$$\underline{w}[(k+1)T] = \underline{I}_c^T \underline{w}(kT) - \underline{C}_c^T M_{oB}^T \underline{h}(kT) \quad (187)$$

where

$$\underline{h}(kT) = L^T \underline{w}(kT) \quad (188)$$

The performance index for this state equation is

$$\begin{aligned} J = \frac{1}{2} \sum_{k=1}^{\infty} \underline{w}^T(kT) Q_{d_{oB}} \underline{w}(kT) + \underline{w}^T(kT) S_{M_{oB}} \underline{h}(kT) \\ + \underline{h}^T(kT) S_{M_{oB}}^T \underline{w}(kT) + \underline{h}^T(kT) R_{M_{oB}} \underline{h}(kT) \end{aligned} \quad (189)$$

where

$$S_{M_{oB}} = S_{d_{oB}} M_{oB} \quad (190)$$

$$R_{M_{oB}} = M_{oB}^T R_{oB} M_{oB} \quad (191)$$

As shown earlier, this performance index can be written

$$J = \frac{1}{2} \sum_{k=1}^{\infty} \underline{w}^T(kT) Q'_{oB} \underline{w}(kT) + \underline{z}_{oB}^T(kT) R_{M_{oB}} \underline{z}_{oB}(kT) \quad (192)$$

where

$$\underline{w}_{oB}^T = S_{M_{oB}} R_{M_{oB}}^{-1} \quad (193)$$

$$\underline{z}_{oB}(kT) = \underline{w}_{oB} \underline{x}_c(kT) + \underline{h}(kT) \quad (194)$$

$$Q'_{oB} = Q_{d_{oB}} - \underline{w}_{oB}^T R_{M_{oB}} \underline{w}_{oB} \quad (195)$$

and the state equation can now be written as

$$\underline{w}[(k+1)T] = [\underline{F}_c^T + C_c^T M_{OB}^T W_{OB}^T] \underline{w}(kT) - C_c^T M_{OB}^T \underline{z}_{OB}(kT) \quad (196)$$

The solution is

$$\underline{z}_{OB}^*(kT) = \underline{K}^T \underline{w}(kT) \quad (197)$$

$$\underline{h}^*(kT) = (\underline{K}^T - W_{OB}) \underline{w}(kT) \quad (198)$$

$$\underline{g}^*(kT) = M_{OB}^T (\underline{K}^T - W_{OB}) \underline{w}(kT) \quad (199)$$

where

$$\underline{K}^T = [I + R_{OB}^{-1} M_{OB} C_c P C_c^T M_{OB}^T]^{-1} R_{OB}^{-1} M_{OB} C_c P [\underline{F}_c^T + C_c^T M_{OB}^T W_{OB}] \quad (200)$$

and where  $P_{OB}$  is the solution to the discrete steady-state Ricatti equation

$$P_{OB} = [\underline{F}_c^T + C_c^T M_{OB}^T (W_{OB} - \underline{K}^T)]^T P [\underline{F}_c^T + C_c^T M_{OB}^T (W_{OB} - \underline{K}^T)] + K R_{OB} K^T + Q'_{OB} \quad (201)$$

The matrix  $L$  of Eq (183) is thus given by

$$L = (\underline{K}^T - W_{OB})^T \quad (202)$$

The error state equation is now as given in Eq (184) with the  $K$  matrix as given in Eq (183). The suppressed state equation is now

$$\begin{aligned} \underline{x}_s[(k+1)T] &= \underline{\Phi}_s \underline{x}_s(kT) + \Gamma_s \underline{u}(kT) \\ &= \underline{\Phi}_s \underline{x}_s(kT) + \Gamma_s M(F-W) \underline{u}(kT) \\ &= \underline{\Phi}_s \underline{x}_s(kT) \end{aligned} \quad (203)$$

The total system state equation can now be written in matrix form as

$$\begin{bmatrix} \underline{x}_c[(k+1)T] \\ \underline{e}[(k+1)T] \\ \underline{x}_s[(k+1)T] \end{bmatrix} = \begin{bmatrix} \Phi_c + \Gamma_c M(F-W) & -\Gamma_c M(F-W) & 0 \\ 0 & \Phi_c - KC_c & 0 \\ 0 & 0 & \Phi_s \end{bmatrix} \begin{bmatrix} \underline{x}_c(kT) \\ \underline{e}(kT) \\ \underline{x}_s(kT) \end{bmatrix}$$

### System Performance

In Chapter III it was stated that the simplified performance index was a good approximation so long as the assumption in Eq (47) was valid. To test the accuracy of the simplified performance index of Design II, Design III was run at the same sampling rate and with the same state weighting matrices as those of Design II in the preceding chapter.

The largest eigenvalue of  $A_c$  is  $-.01924 \pm 3.84834i$ . With a sampling time of 0.1 seconds, the magnitude of the product of eigenvalue and sampling time is equal to .38484.

The eigenvalues of Design III for the different weighting matrices are shown in Table VII and plotted in Figure 15. Comparison with the corresponding eigenvalues of Design II in Table VI shows very good agreement between the two designs for all weighting matrices. Figures 16 through 21 show the time response of Design III for each different  $Q$  and  $Q_{OB}$ . In each case, the corresponding

time response of Design II is almost identical. Thus, for T equal to .1 seconds, at least, the assumption in Eq (47) is valid and the simplified performance index is a good approximation of the optimal performance index.

Table VII  
Eigenvalues of Design III

$Q = 1.0 \text{ I}$	$Q = 10.0 \text{ I}$	$Q = 100.0 \text{ I}$
$Q_{OB} = 1.0 \text{ I}$	$Q_{OB} = 10.0 \text{ I}$	$Q_{OB} = 100.0 \text{ I}$

Eigenvalues of  $\phi_c + \Gamma_c F$

.98892 ± .11629i	.98014 ± .11519i	.95730 ± .11401i
.91628 ± .33983i	.87392 ± .31848i	.76457 ± .22166i
.98613 ± .14568i	.97988 ± .14469i	.96488 ± .14333i
.90175 ± .36434i	.85196 ± .33647i	.72697 ± .21018i

Eigenvalues of  $\phi_c - KC_c$

.76125 ± .23961i	.33956 + 0i	.07775 + 0i
.96046 ± .11408i	.94487 ± .11869i	.94238 ± .12067i
.72265 ± .23957i	.80540 + 0i	.83848 + 0i
.96762 ± .14348i	.96003 ± .14442i	.95882 ± .14480i
	.28392 + 0i	.06949 + 0i
	.78030 + 0i	.80943 + 0i

Eigenvalues of  $\phi_s$

.95496 ± .29170i	.95496 ± .29170i	.95496 ± .29170i
.84081 ± .53607i	.84081 ± .53607i	.84081 ± .53607i
.86809 ± .49121i	.86809 ± .49121i	.86809 ± .49121i
.83892 ± .53899i	.83892 ± .53899i	.83892 ± .53899i

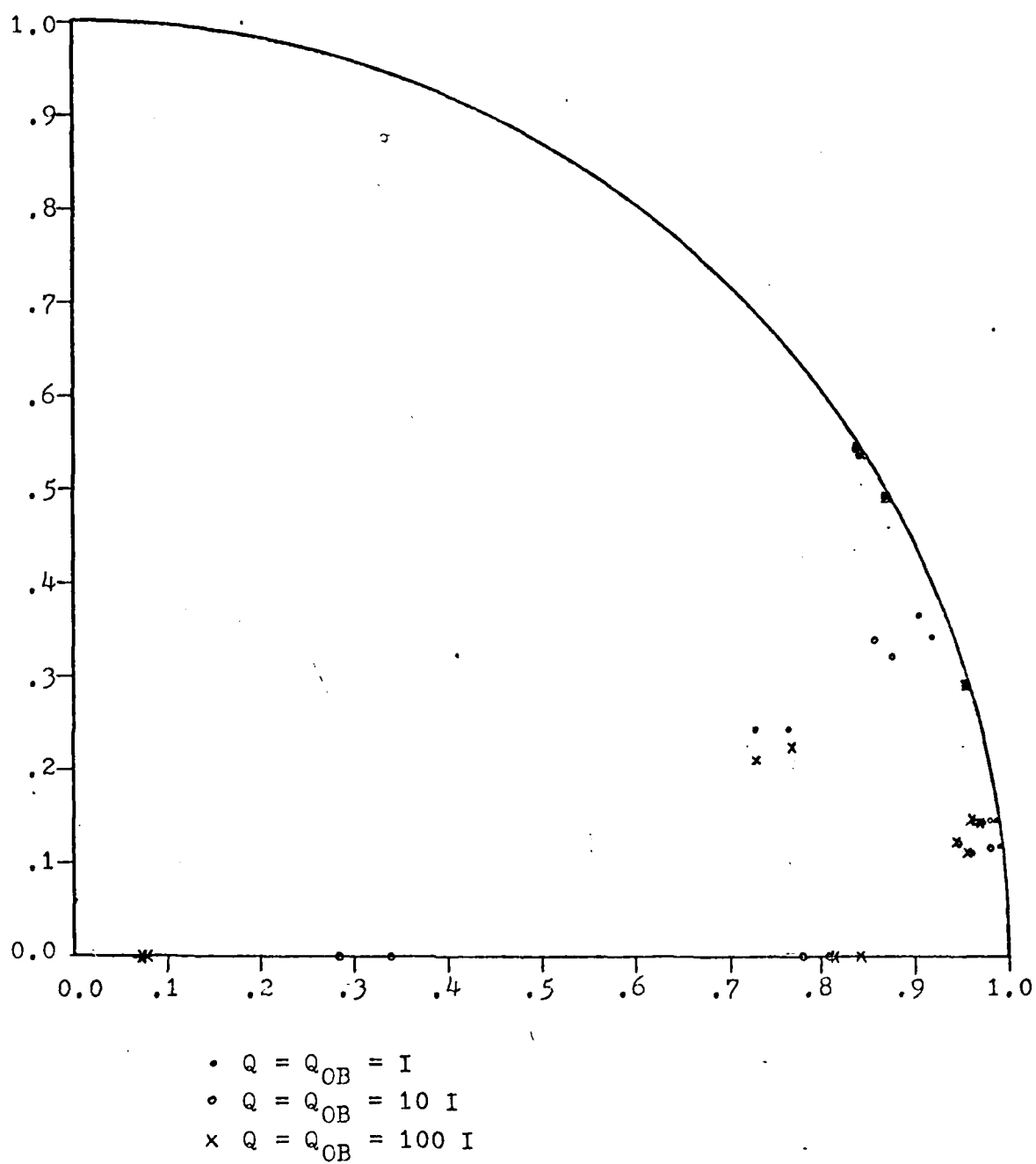


Figure 15. Z-Plane Plot of Eigenvalues of Design III

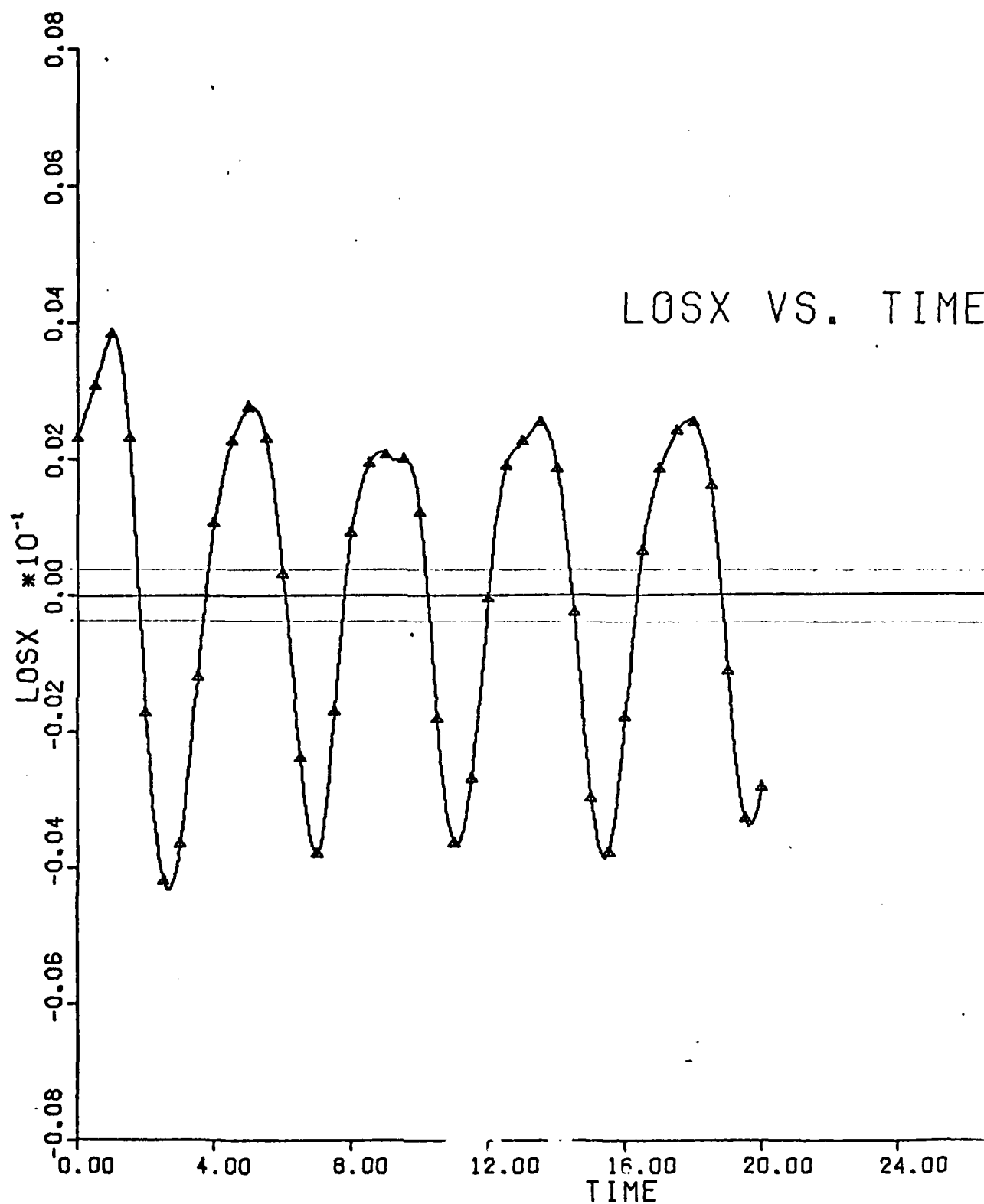


Figure 16.. LOSX VS. TIME, Design III,  $Q = Q_{OB} = 1$ ,  $T = .1$

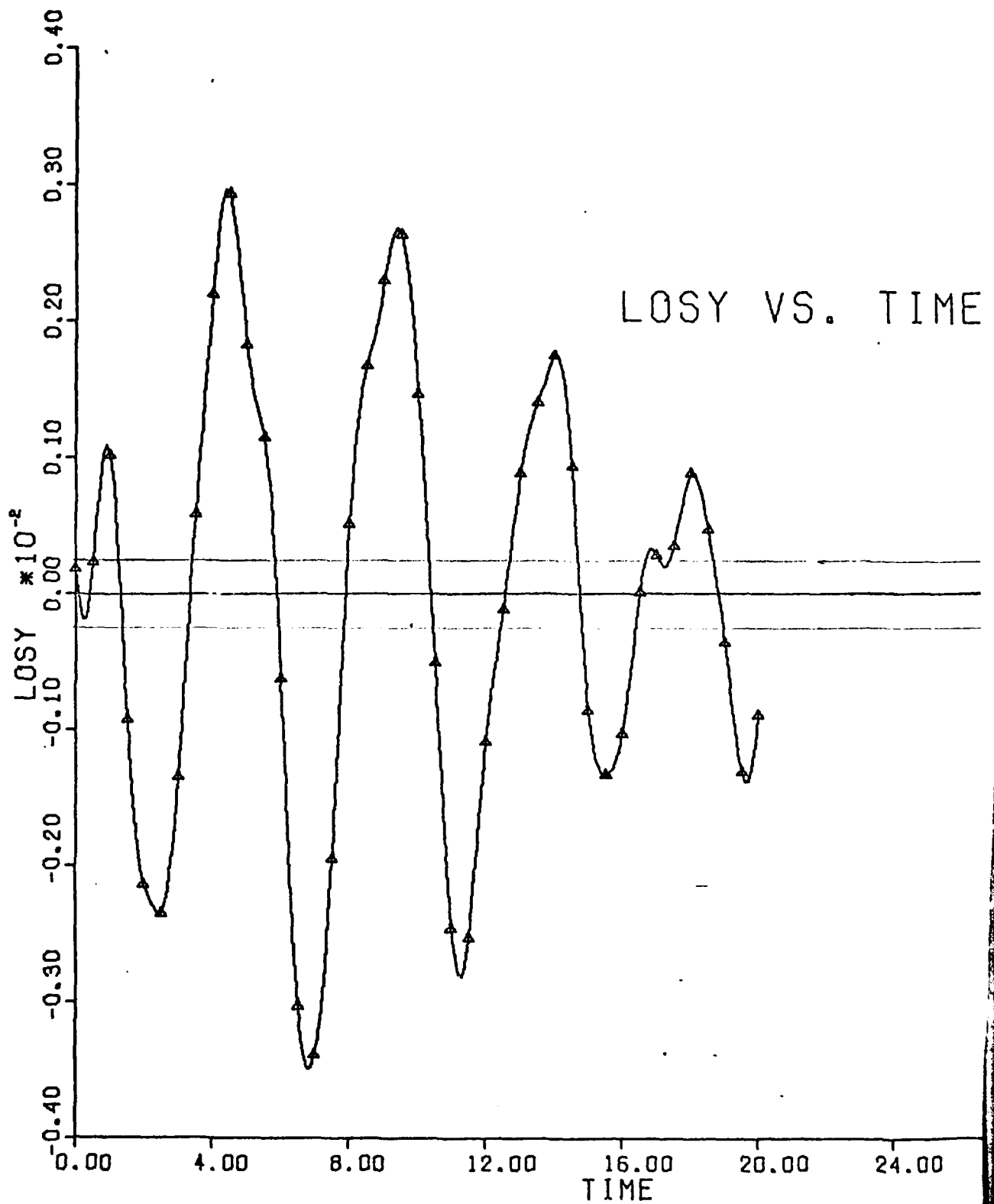


Figure 17. LOS Y VS. TIME, Design III,  $Q = Q_{CB} = 1$ ,  $T = .1$



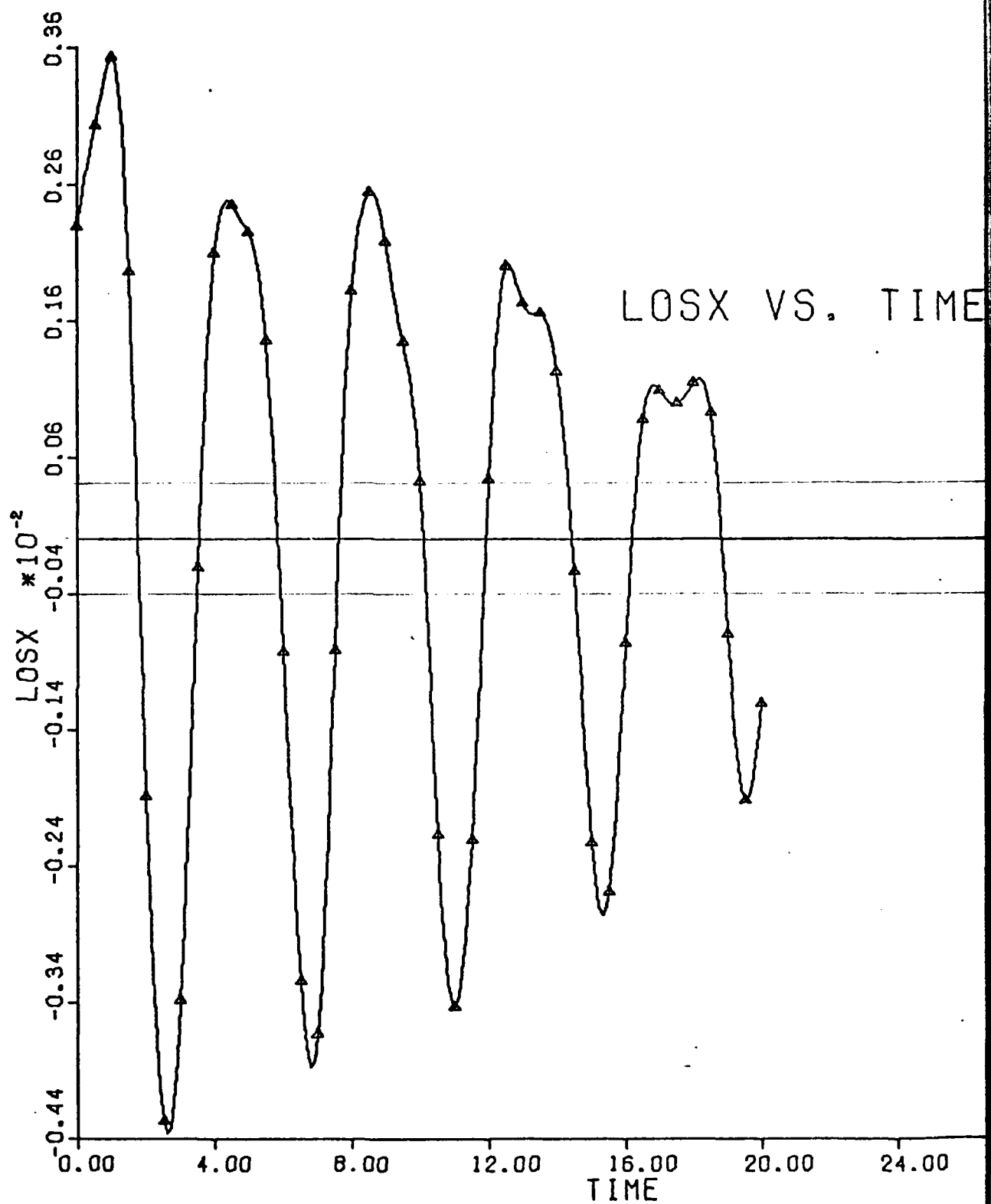


Figure 18. LOSX VS. TIME, Design III,  $Q = Q_{OB} = 10$  I,  $T = .1$

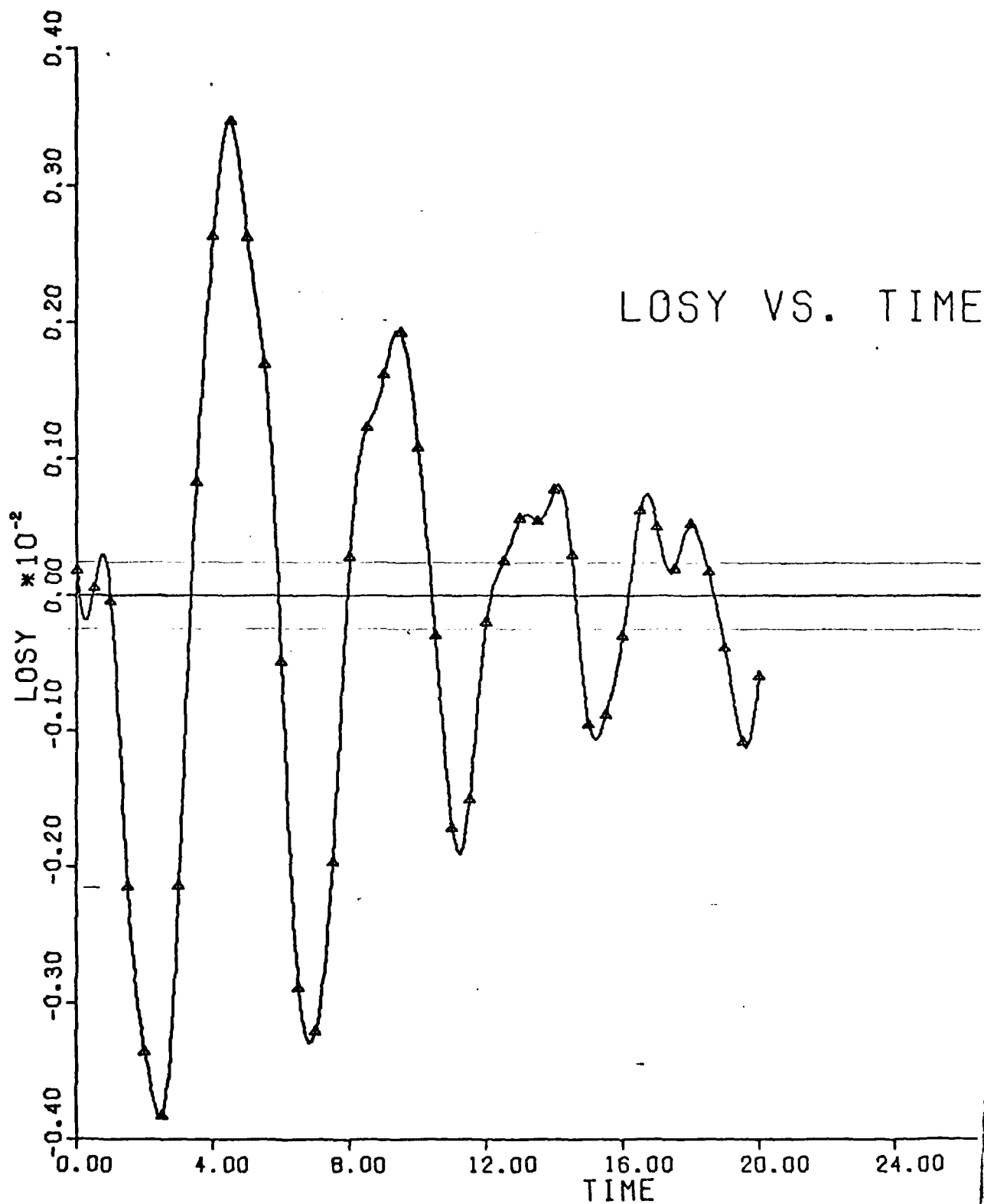


Figure 19, LOS Y VS. TIME, Design III,  $Q = Q_{OB} = 10 I$ ,  $T = .1$

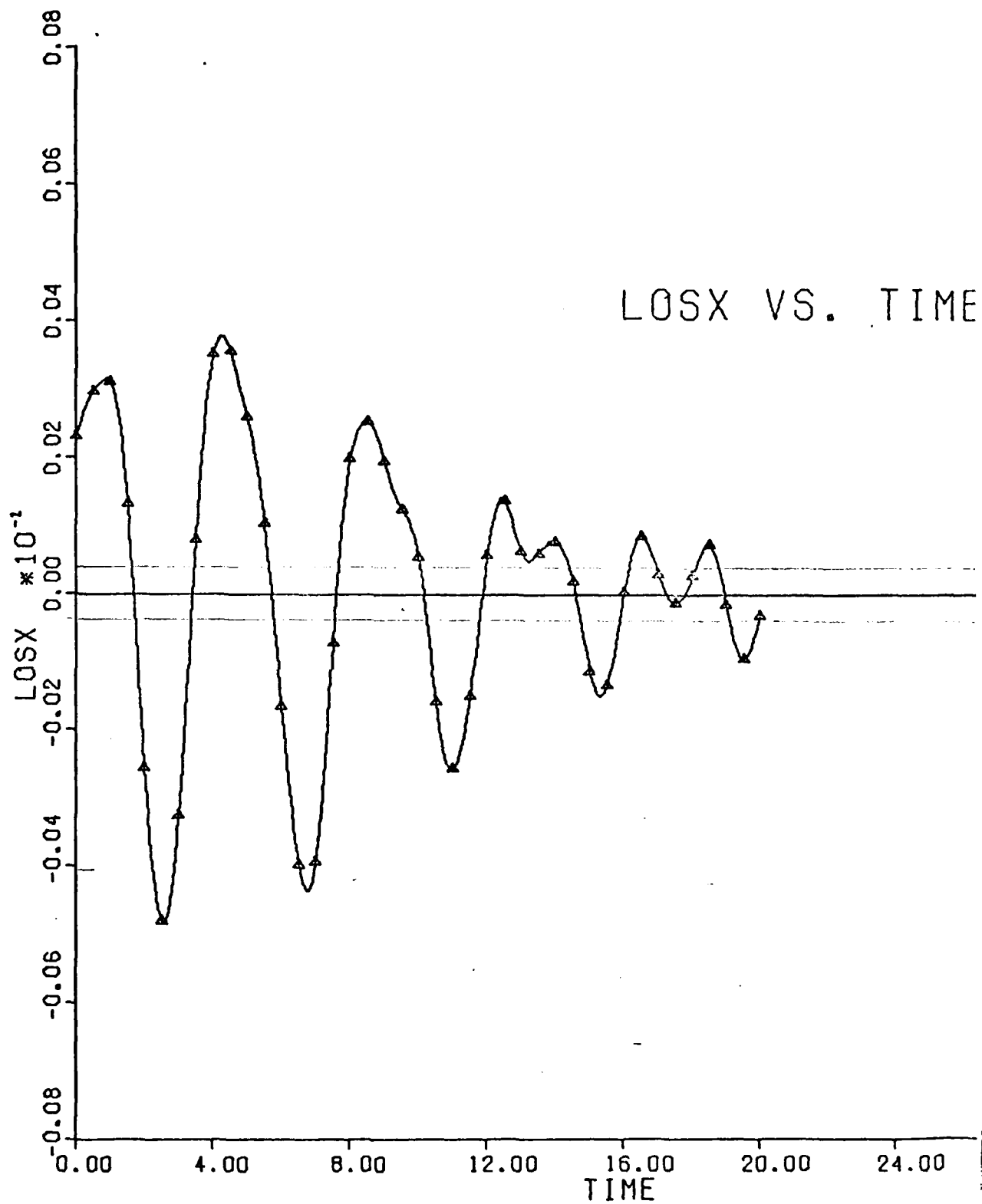


Figure 20. LOSX VS. TIME, Design III,  $Q = Q_{GB} = 100 I$ ,  $T = .1$

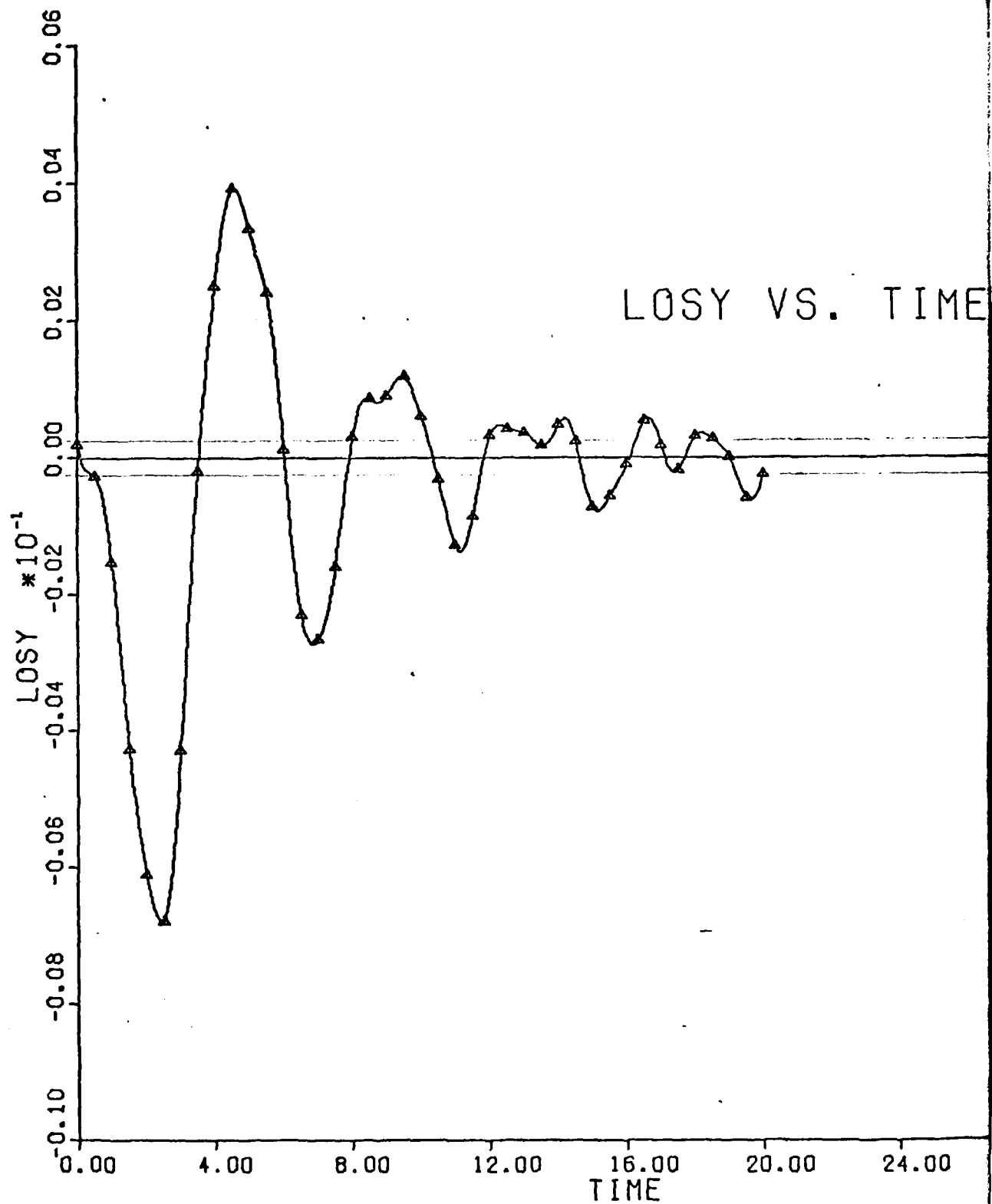


Figure 21. LOS Y VS. TIME, Design III,  $Q = Q_{CB} = 100$  l,  $T = .1$

## VII Effects of Sampling Time

### Aliasing

The size of the sampling time plays a critical role in determining system response. Theoretically, the lower limit on desired sampling time is  $T = 0$ , for which the controller becomes a continuous-time system. The upper limit on desired sampling time depends on the natural frequencies of the system to be controlled. To illustrate this dependency consider a continuous-time system with a time response given by

$$X_1(t) = \sin(\omega_1 t + \theta) \quad (205)$$

If this system were discretized at a sampling frequency,  $\omega_s = \frac{2\pi}{T}$ , such that  $0 \leq \omega_1 \leq \frac{\omega_s}{2}$ , the discrete time response would be

$$X_1(kT) = \sin(k\omega_1 T + \theta) \quad (206)$$

Next, consider a continuous-time system given by

$$X_2(t) = \sin\left[\left(\omega_1 + \frac{2\pi j}{T}\right)t + \theta\right]; j=1,2,3,\dots \quad (207)$$

If this system were discretized at the same sampling rate, the discrete-time response would be

$$\begin{aligned} X_2(kT) &= \sin\left[\left(\omega_1 + \frac{2\pi j}{T}\right)kT + \theta\right] \\ &= \sin[kT\omega_1 + \theta + 2\pi kj] \end{aligned}$$

$$x_2(kT) = \sin(kT\omega_1 + \theta) \quad (208)$$

Note that Eqs (206) and (208) are identical. As far as a digital controller with the same sampling rate is concerned, these two systems are the same. But actually they are quite different. This effect is known as aliasing. For an open-loop system which is stable, this effect will degrade the closed-loop response as  $T$  is increased. But for an unstable open-loop system, this effect will cause the closed-loop response to be unstable. Thus, the upper limit on the desired sampling time is set by what is known as the Shannon Sampling Theorem. Basically, it is desired to always choose a sampling frequency,  $\omega_s$ , such that

$$\omega_s \geq 2\omega_c \quad (209)$$

where  $\omega_c$  is the highest natural frequency in the open-loop system. Therefore, the desired sampling time must be

$$T \leq \frac{\pi}{\omega_c} \quad (210)$$

In the following analysis, the system response is examined for Designs II and III for sampling times of .1, .3, .5, and .7 seconds. In all cases, the state weighting matrices are  $Q = Q_{OB} = 100 I$ . For this model, the sampling time of .7 seconds exceeds the condition of Eq (210) for modes 7, 8, and 9.

### System Performance

Presented in Table VIII are the eigenvalues of Design II for sampling times of .3, .5, and .7 seconds. The plot of these eigenvalues, together with the eigenvalues in the right-hand column of Table VI, shows the general trend of eigenvalue movement as  $T$  increases. Those eigenvalues that start to the right of the origin, move to the left and away from the real axis as  $T$  increases. This would imply that the system performance is being degraded. On the left of the origin the eigenvalues continue to move to the left but begin to move toward the real axis again. For eigenvalues on this side of the origin, this also implies poorer response. However, note that for  $T = .7$  seconds, three of the eigenvalues of  $\phi_s$  are to the left of the origin but have begun to move to the right and away from the real axis indicating improving system response. The time responses, shown in Figures 13, 14, and 23 through 28, reflect these results. As shown in Chapter V, the time response for  $T = .1$  meets the desired specifications. For  $T = .3$  and  $T = .5$ , the time response is progressively worse. However, for  $T = .7$ , the time response is progressively worse. However, for  $T = .7$ , the time response is actually slightly better than for  $T = .3$ .

In Table IX are the corresponding eigenvalues of Design III. Figure 29 plots these eigenvalues and shows the same trends as those of Design II. Figures 20 and 21

from Chapter VI and Figures 30 through 35 show the time responses of Design III for the above sampling times. Again these figures show the same trends as Design II.

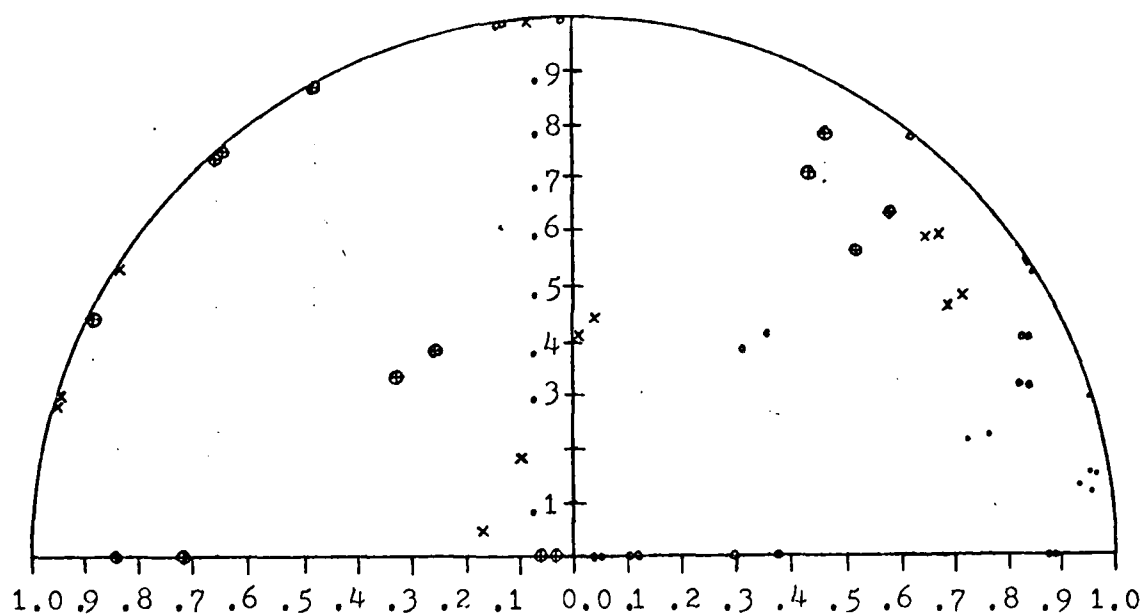
#### Effects of Performance Index Approximation

In Chapter III it was shown that if the conditions of Eq (47) are met, then the discrete weighting matrices  $Q_d$ ,  $S_d$ , and  $R_d$ , can be approximated by Eqs (49) through (51). As  $T$  increases, these approximations become worse. To examine the effect of the increasing disparity between the approximations and the optimal weighting matrices, compare the results of Design II and Design III. Recall from Chapter VI that for  $T = .1$ , the results of Design II and Design III were almost identical. Now compare the two time responses for  $T = .3$ . For  $T = .3$ , the product of the largest eigenvalue with the sampling time is equal to 1.1545 which violates the condition of Eq (47). Thus, the approximations of the weighting matrices can no longer be considered very accurate. However, in examining the time responses it can be seen that they are still quite similar. They have the same general form and differ only slightly in amplitude. Thus, although the approximations of the weighting matrices have declined in accuracy, they are still adequate to provide system performance approximately equal to optimal performance index.



Table VIII  
Eigenvalues of Design II

T = .3		T = .5		T = .7	
<u>Eigenvalues of <math>\phi_c + \Gamma_c F</math></u>					
.83954 ± .31080i		.69058 ± .46021i		.52615 ± .56060i	
.35627 ± .41297i		.04233 ± .43947i		-.25409 ± .37689i	
.31332 ± .37699i		.00962 ± .40257i		.43217 ± .70772i	
.83790 ± .39627i		.65179 ± .58802i		-.32576 ± .32880i	
<u>Eigenvalues of <math>\phi_c - KC_c</math></u>					
.11587 + 0i		.71273 ± .47869i		.58061 ± .62675i	
.81828 ± .31328i		-.09740 ± .18358i		-.05999 + 0i	
.37675 + 0i		.67699 ± .61238i		-.71708 + 0i	
.83436 ± .39749i		-.16727 ± .04321i		.47035 ± .78033i	
.10188 + 0i				-.03550 ± 0i	
.29535 + 0i				-.84339 + 0i	
<u>Eigenvalues of <math>\phi_s</math></u>					
.62710 ± .77323i		.08774 ± .98873i		-.47830 ± .86642i	
-.13046 ± .98290i		-.94080 ± .29482i		-.66052 ± .72440i	
.02579 ± .99197i		-.83277 ± .53016i		-.87876 ± .43862i	
-.14073 ± .98143i		-.94572 ± .27833i		-.64255 ± .74023i	



• T = .1  
◦ T = .3  
x T = .5  
⊕ T = .7

Figure 22. Eigenvalue Movement as T Increases, Design II

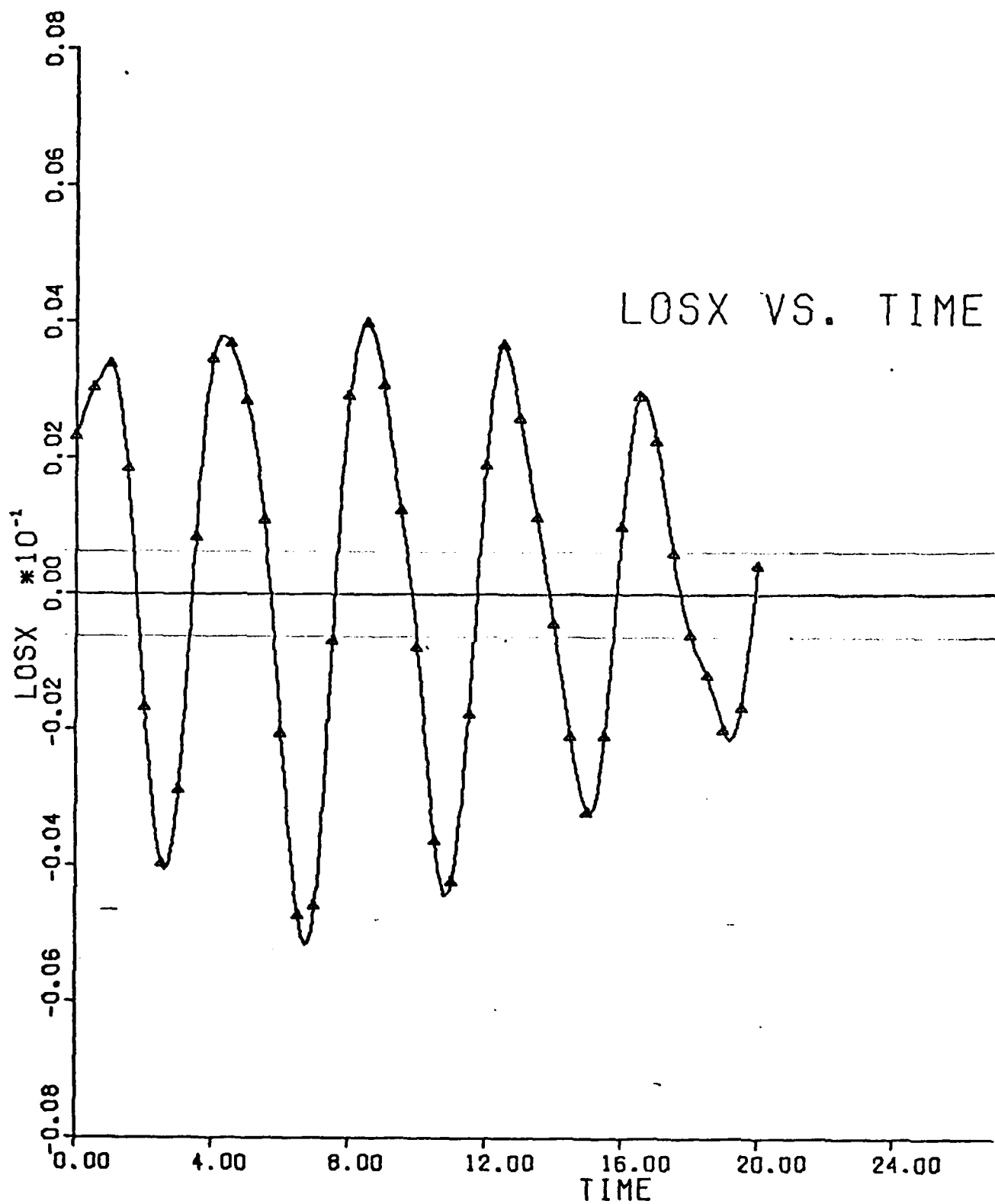


Figure 23. LOSX VS. TIME, Design II,  $Q = Q_{OB} = 100 I$ ,  $T = .3$

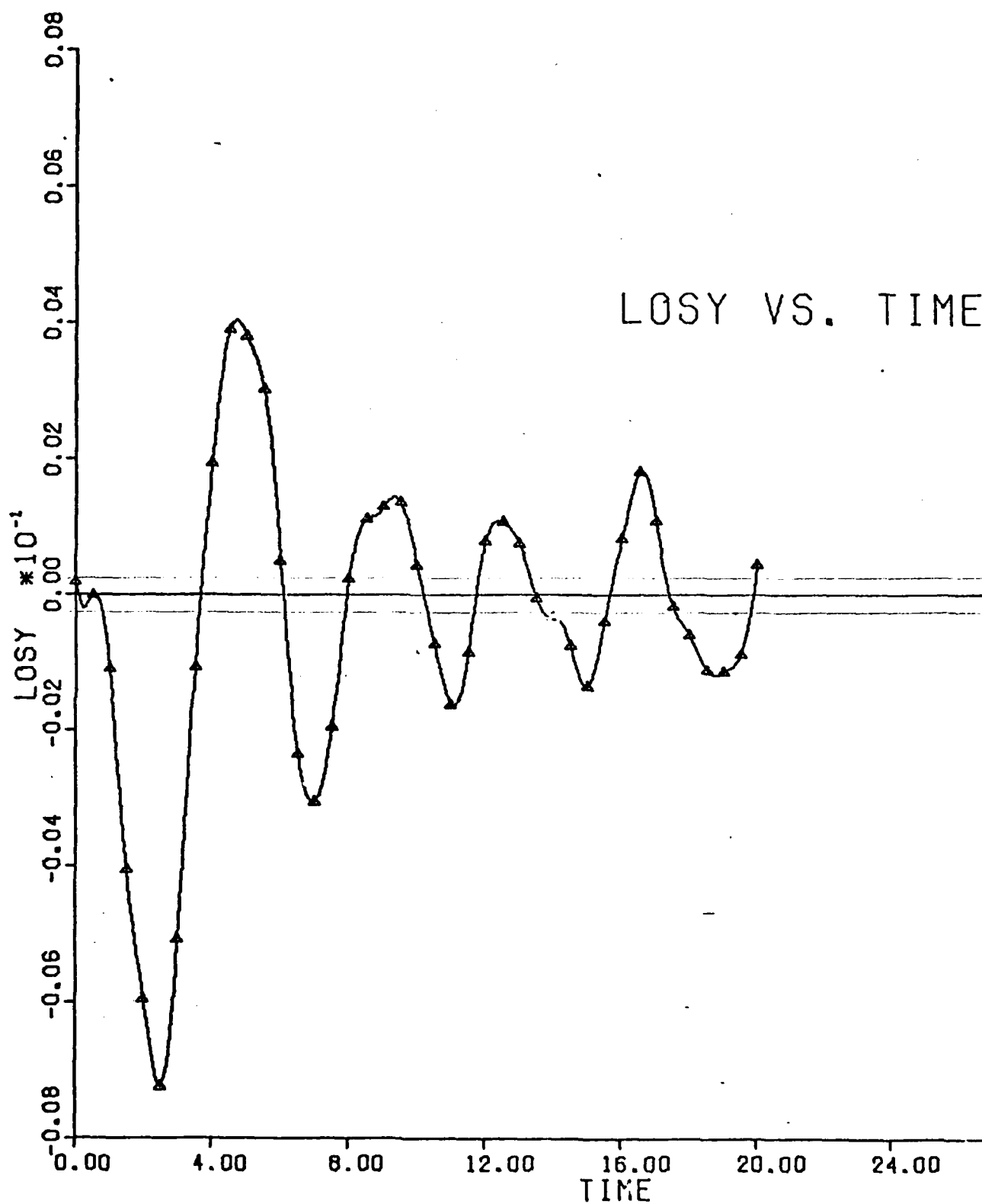


Figure 24. LOS Y VS. TIME, Design II,  $Q = Q_{CB} = 100 I$ ,  $T = .3$

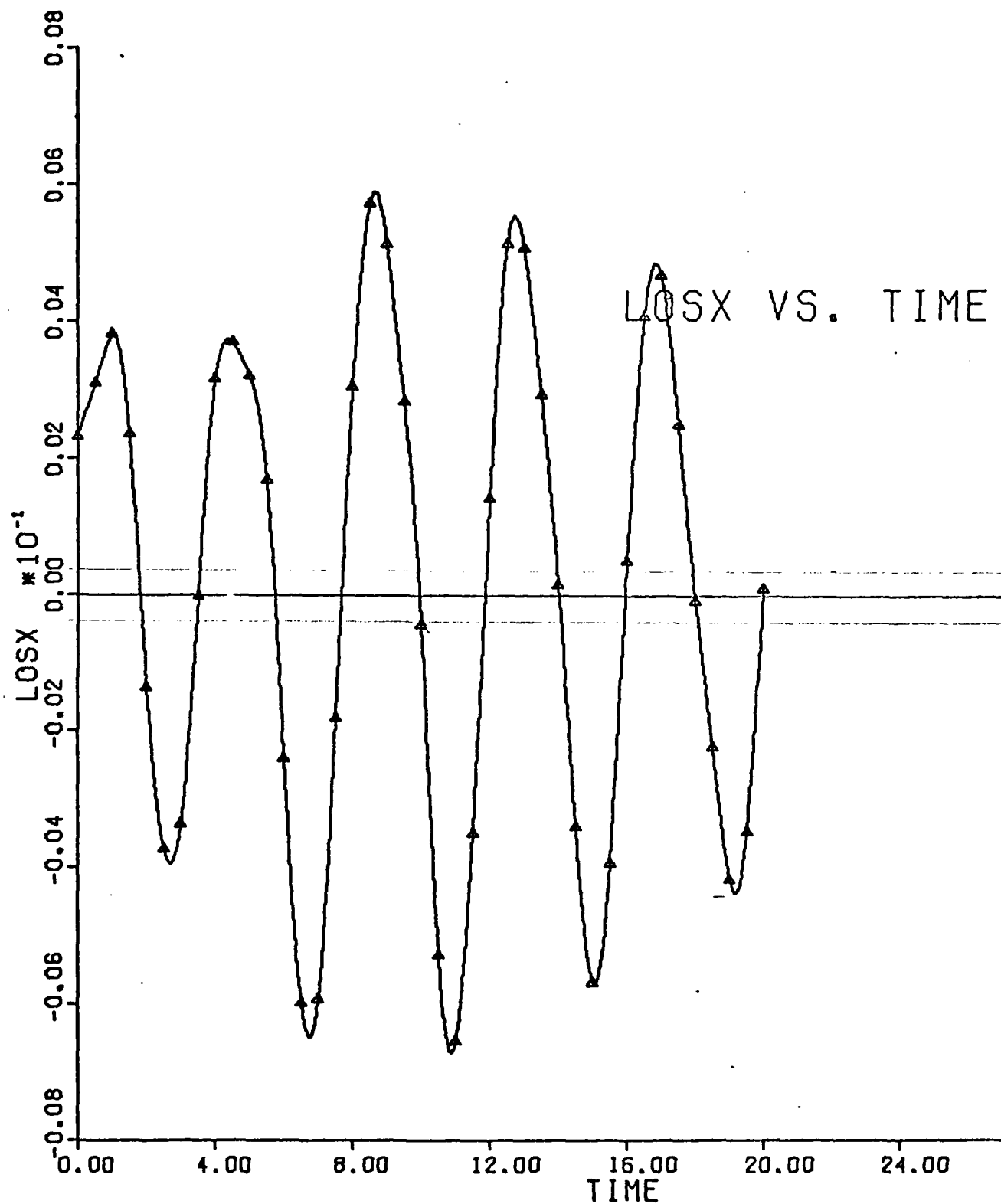


Figure 25. LOSX VS. TIME, Design II,  $Q = Q_{OB} = 100$  I,  $T = .5$

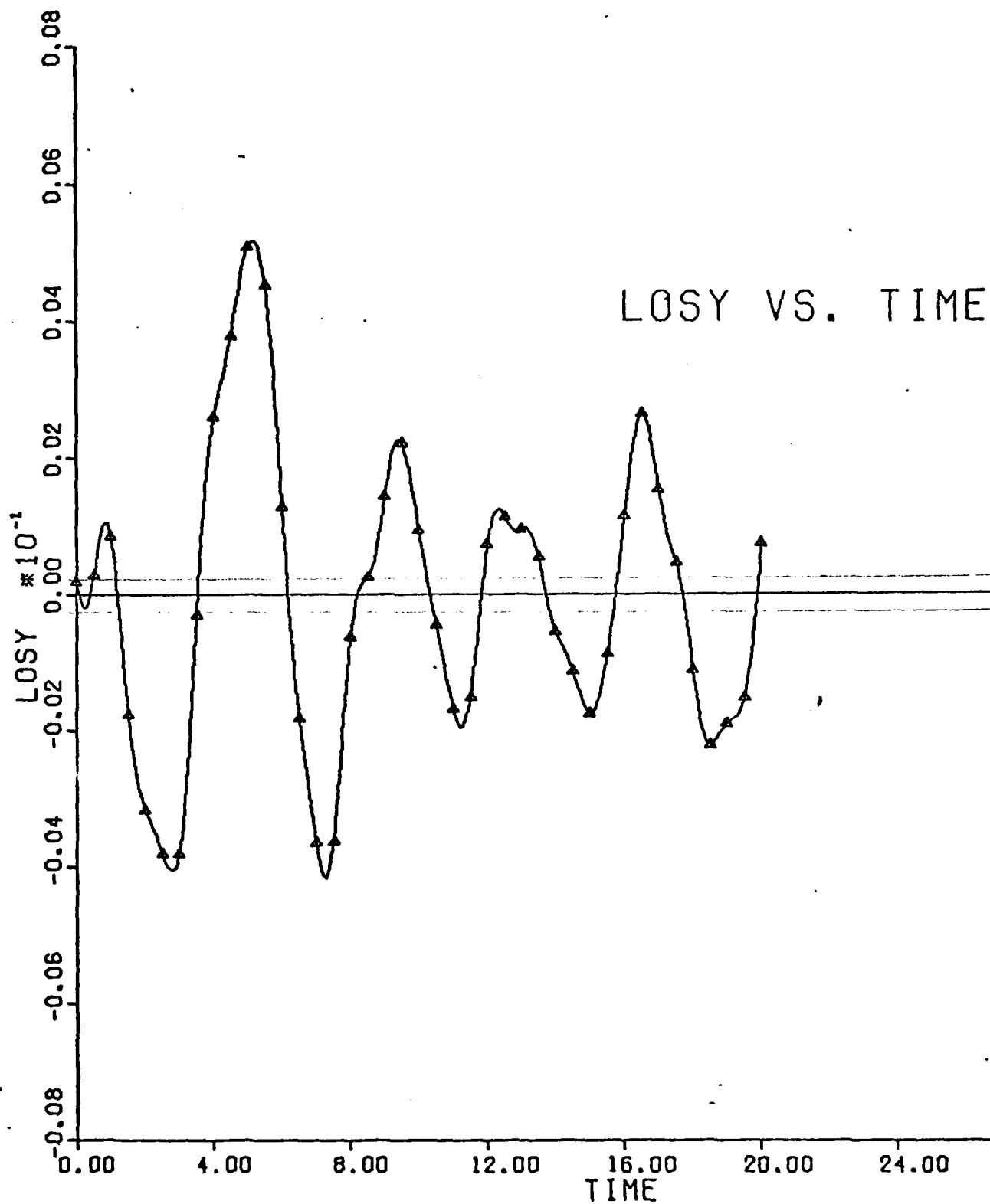


Figure 26. LOS Y VS. TIME, Design II,  $Q = Q_{OB} = 100$  I,  $T = .5$

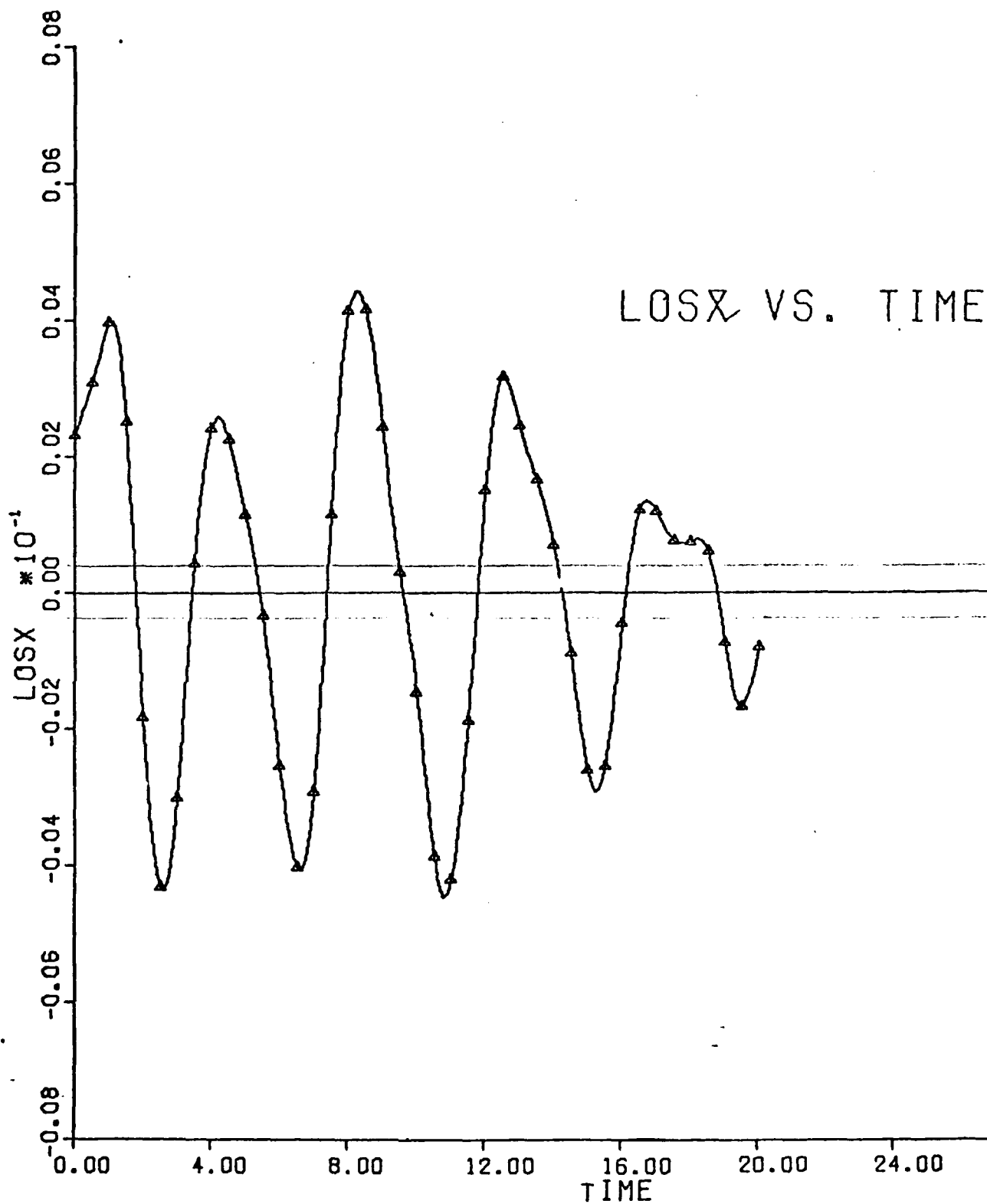


Figure 27. LOSX VS. TIME, Design II,  $Q = Q_{OB} = 100 I$ ,  $T = .7$

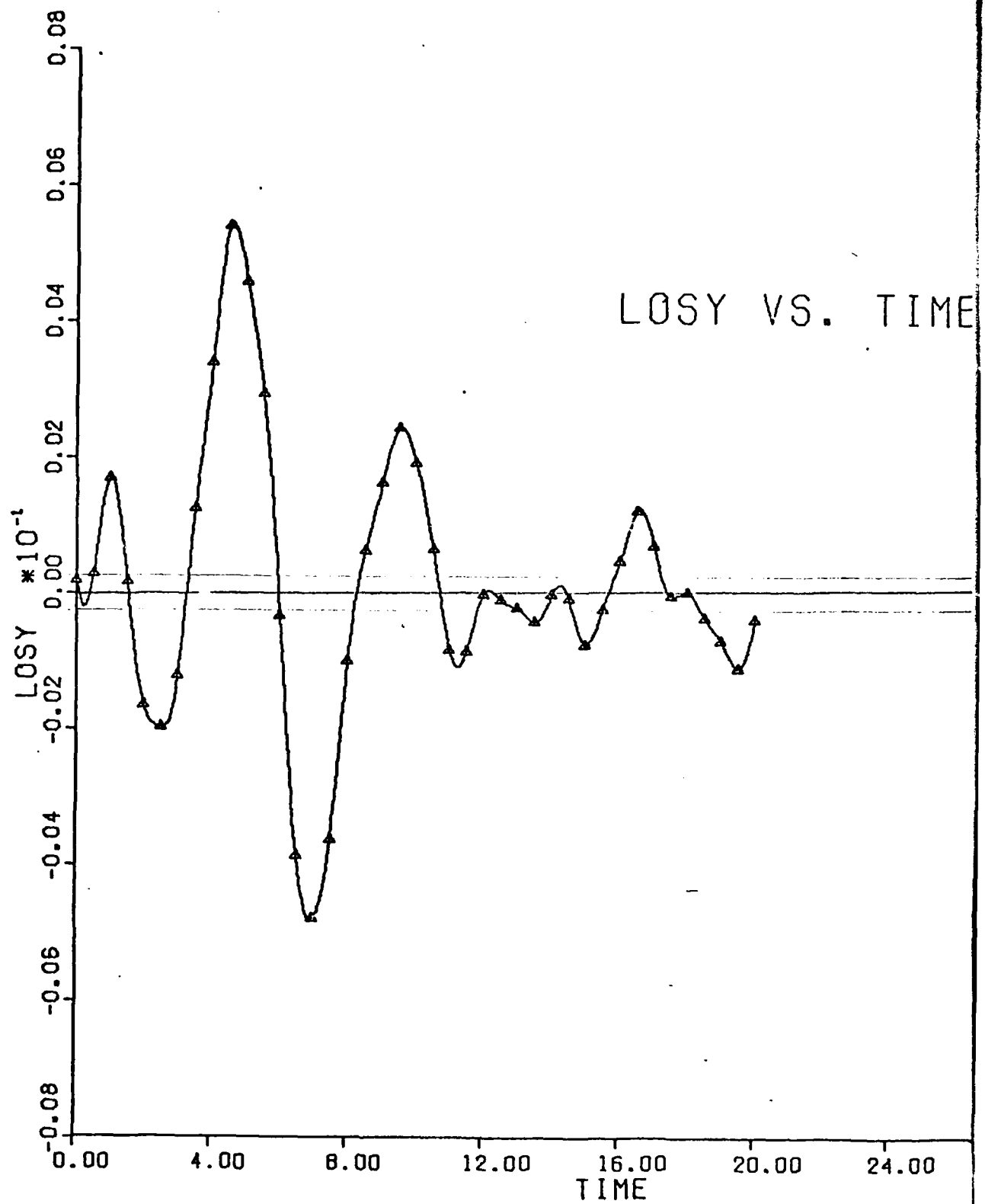


Figure 28. LOS Y VS. TIME, Design II,  $Q = Q_{OB} = 100 I$ ,  $T = .7$



Table IX  
Eigenvalues of Design III

T = .3	T = .5	T = .7
<u>Eigenvalues of <math>\phi_c + \Gamma_c F</math></u>		
.83972 ± .31154i	.68960 ± .46089i	.52487 ± .56463i
.33978 ± .40202i	.04274 ± .43852i	-.25801 ± .31201i
.29519 ± .36135i	.00963 ± .40266i	.43282 ± .71685i
.83826 ± .39684i	.65120 ± .58845i	-.31988 ± .06738i
<u>Eigenvalues of <math>\phi_c - KC_c</math></u>		
.07285 ± .45029i	.76801 ± .51209i	.62671 ± .67532i
.86933 ± .32156i	-.42047 ± .44190i	-.52613 + 0i
-.00061 ± .47548i	.70747 ± .63890i	-.71005 + 0i
.86448 ± .40809i	-.51000 ± .36803i	.49143 ± .81507i
		-.46452 + 0i
		-.78964 + 0i
<u>Eigenvalues of <math>\phi_s</math></u>		
.62710 ± .77323i	.08774 ± .98873i	-.47830 ± .86642i
-.13046 ± .98290i	-.94080 ± .29482i	-.66052 ± .72440i
.02579 ± .99197i	-.83277 ± .53016i	-.87876 ± .43862i
-.14073 ± .98143i	-.94572 ± .27833i	-.64255 ± .74023i

AD-A111 170

AIR FORCE INST OF TECH WRIGHT-PATTERSON AFB OH SCHOO--ETC F/O 22/2  
DESIGN OF A DIGITAL CONTROLLER FOR A LARGE FLEXIBLE SPACE STRUC--ETC(U)

DEC 81 D S LEGGETT

UNCLASSIFIED

AFIT/DAE/AA/81D-18

NL

2 of 2  
AD-A111 170

END  
DATE  
FILMED  
1983  
DTIC

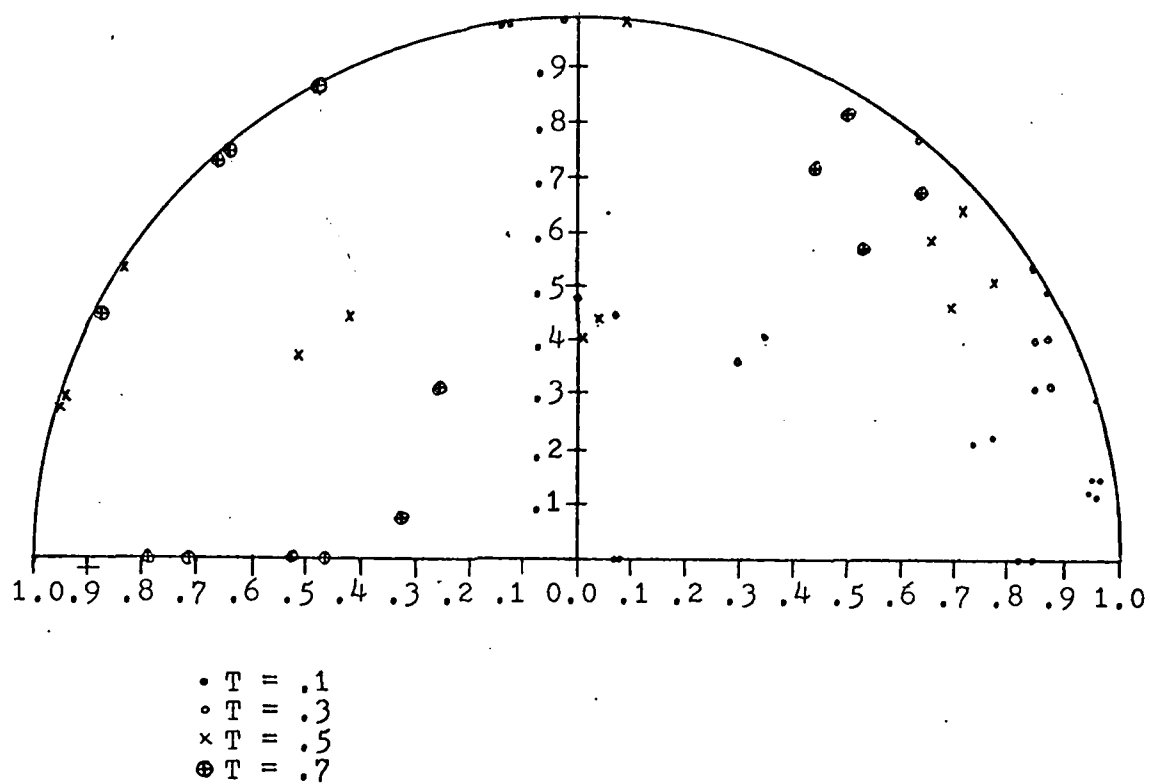


Figure 29. Eigenvalue Movement as  $T$  Increases, Design III

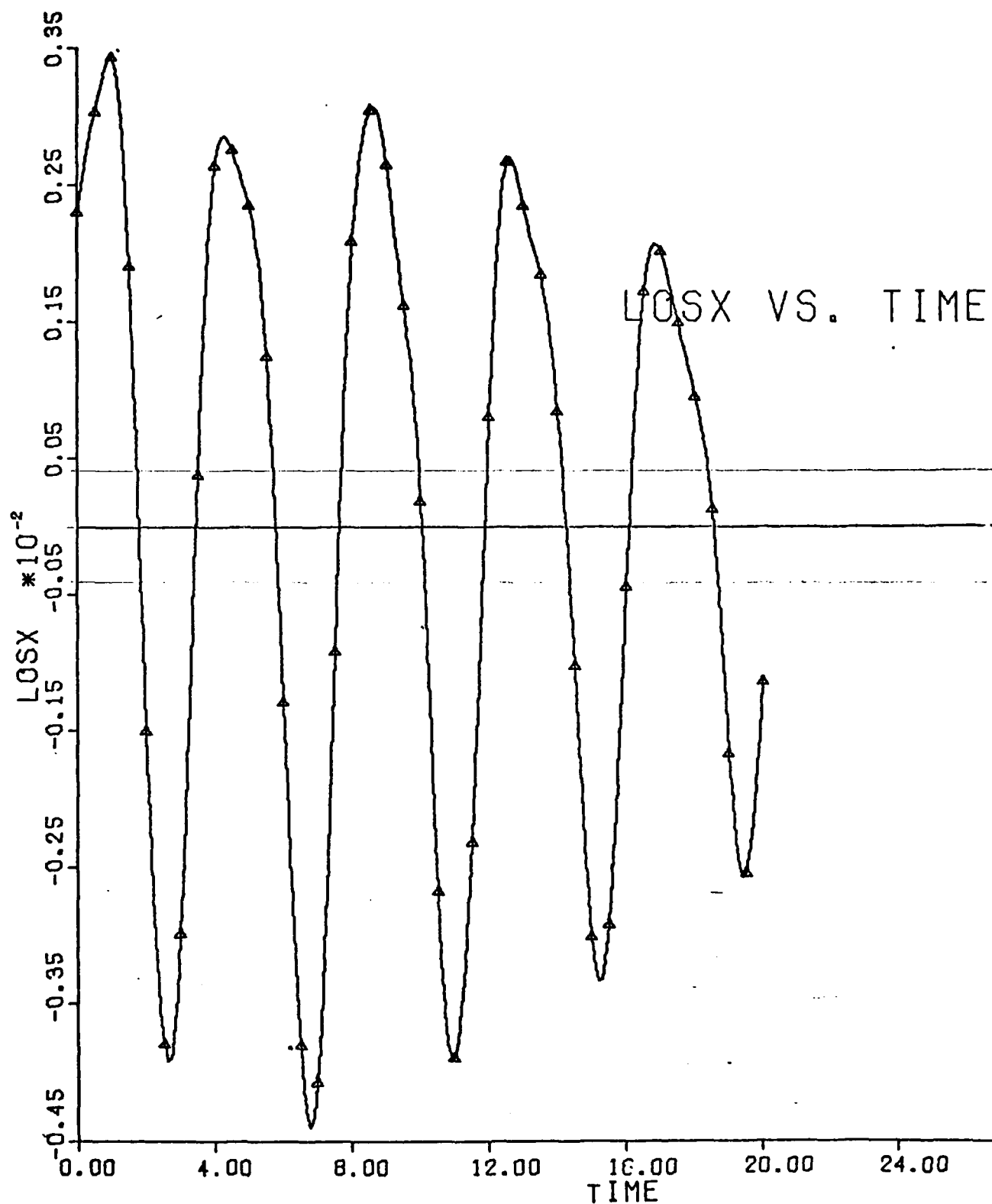


Figure 30. LOSX VS. TIME, Design III,  $Q = Q_{OB} = 100 I$ ,  $T = .3$

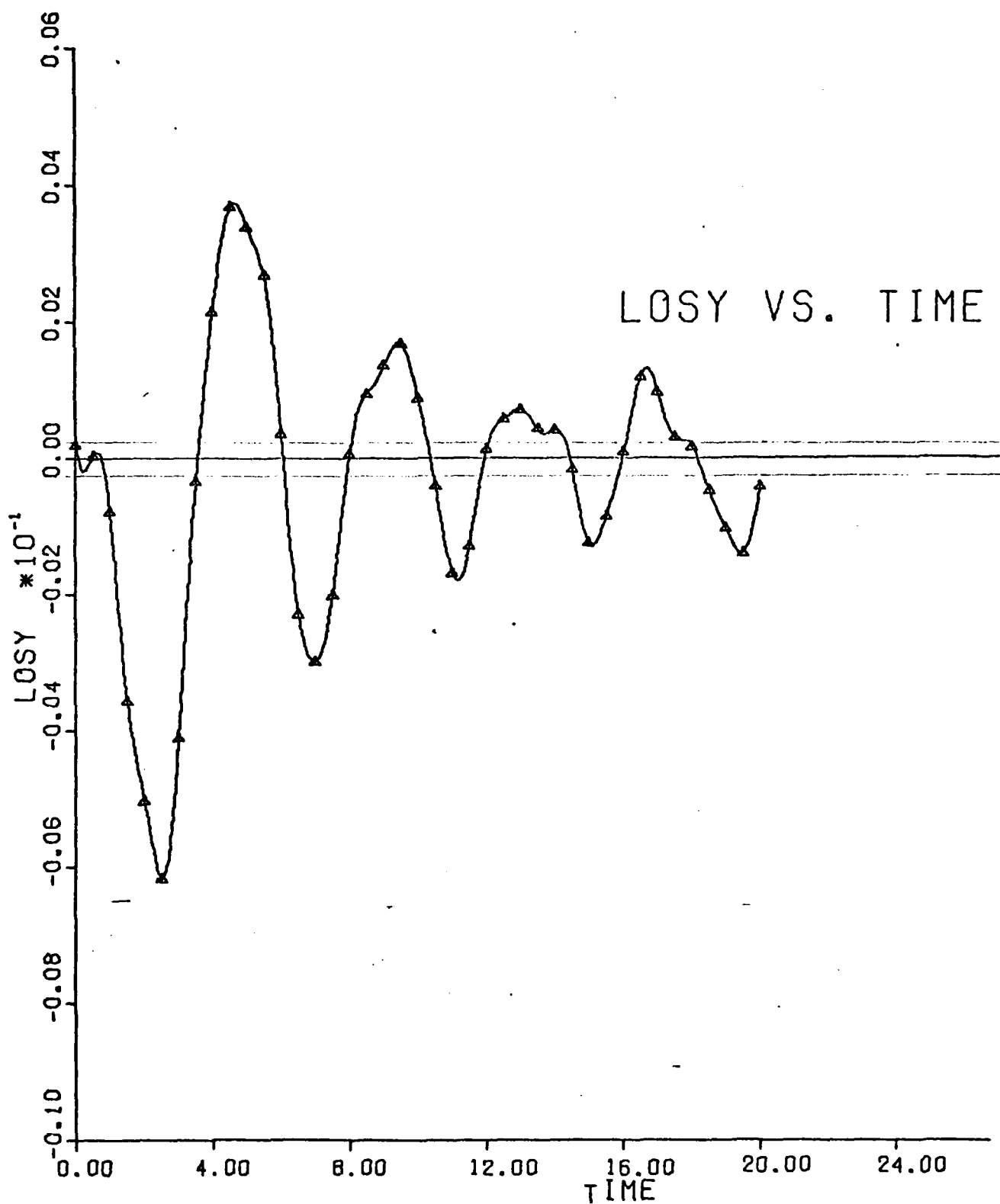


Figure 31. LOS Y VS. TIME, Design III,  $Q = Q_{OB} = 100$  I,  $T = .3$

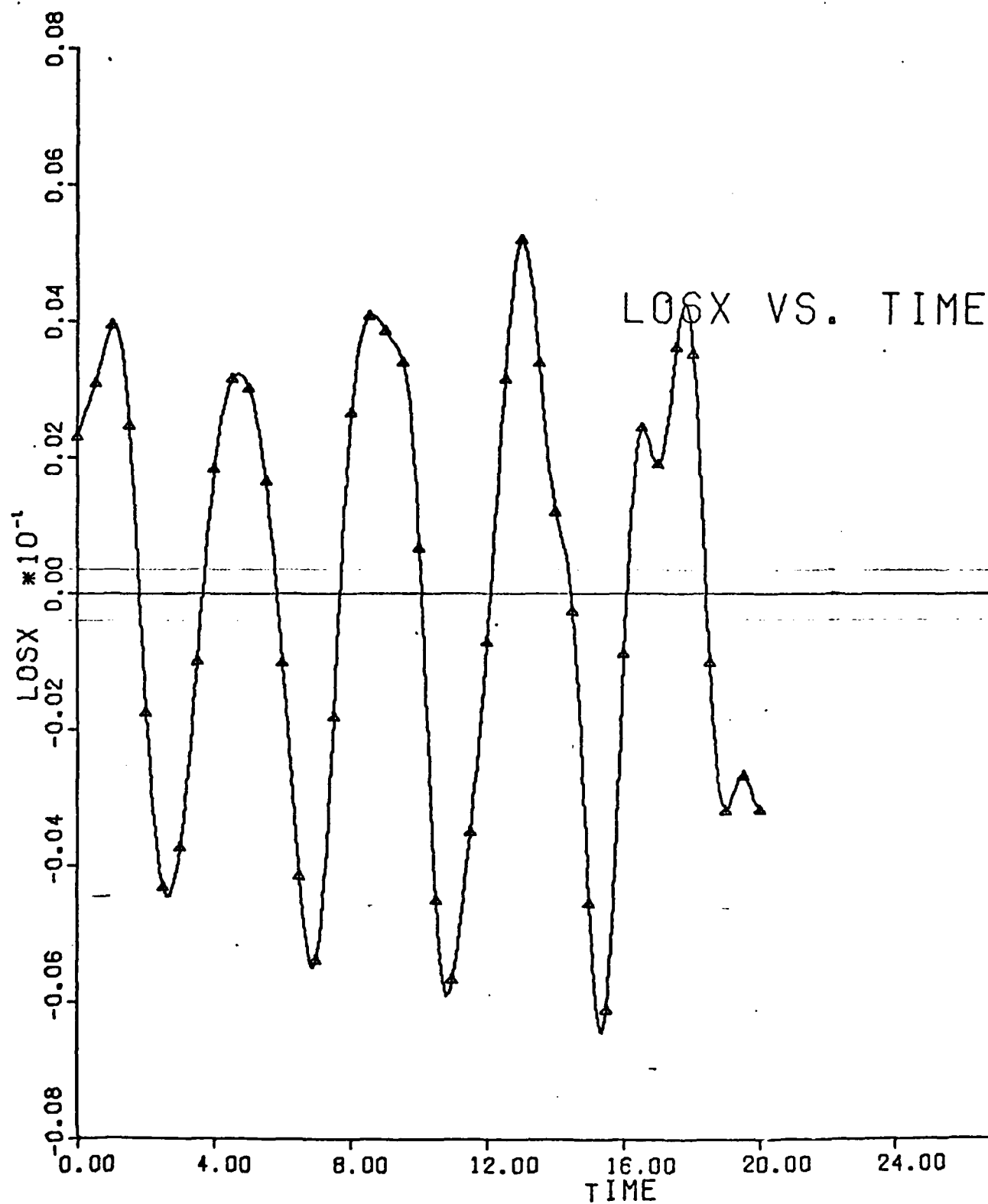


Figure 32. LOGX VS. TIME, Design III,  $Q = Q_{OB} = 100 I$ ,  $T = .5$

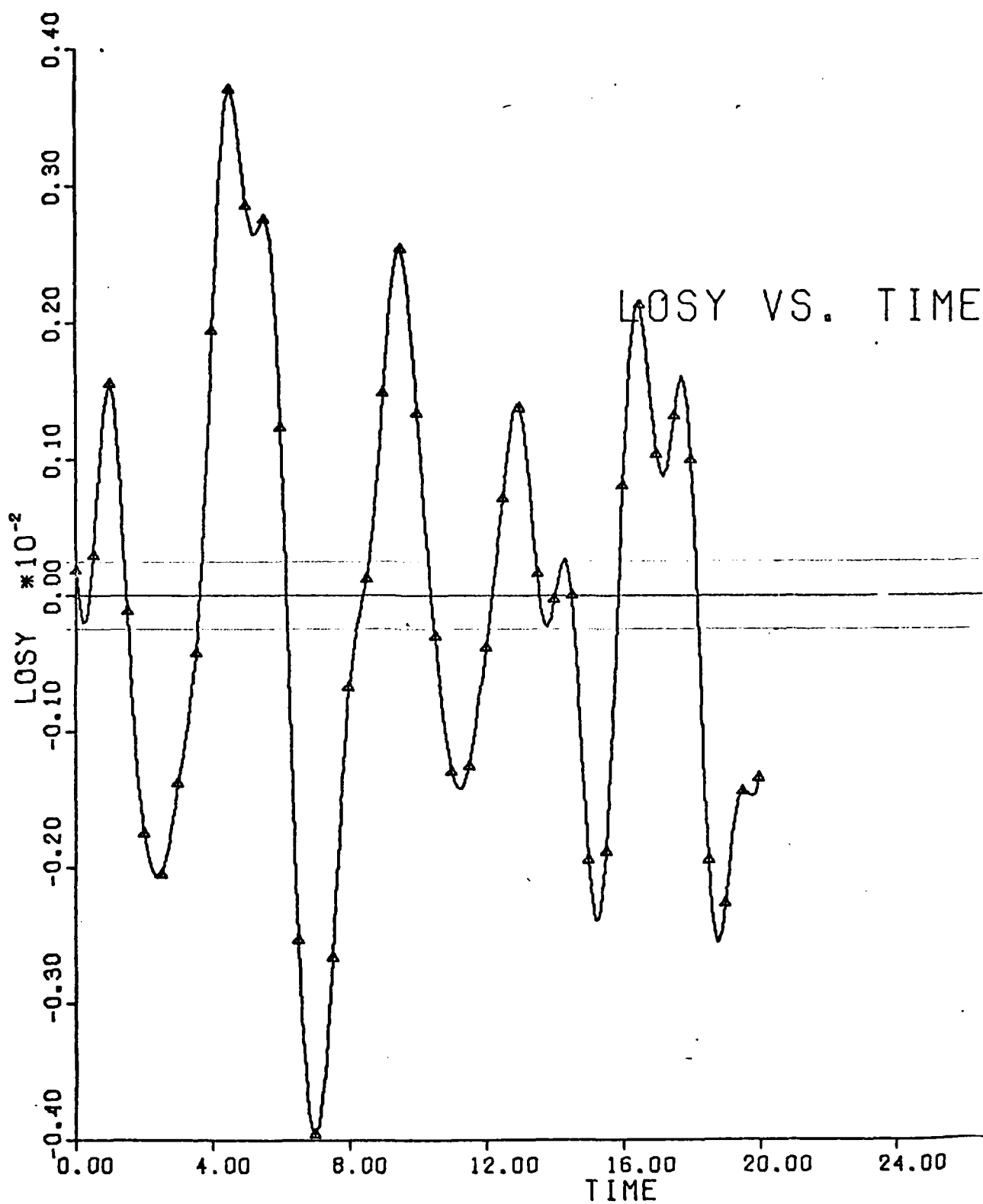


Figure 33, LOS Y VS. TIME, Design III,  $Q = Q_{OB} = 100$  I,  $T = .5$

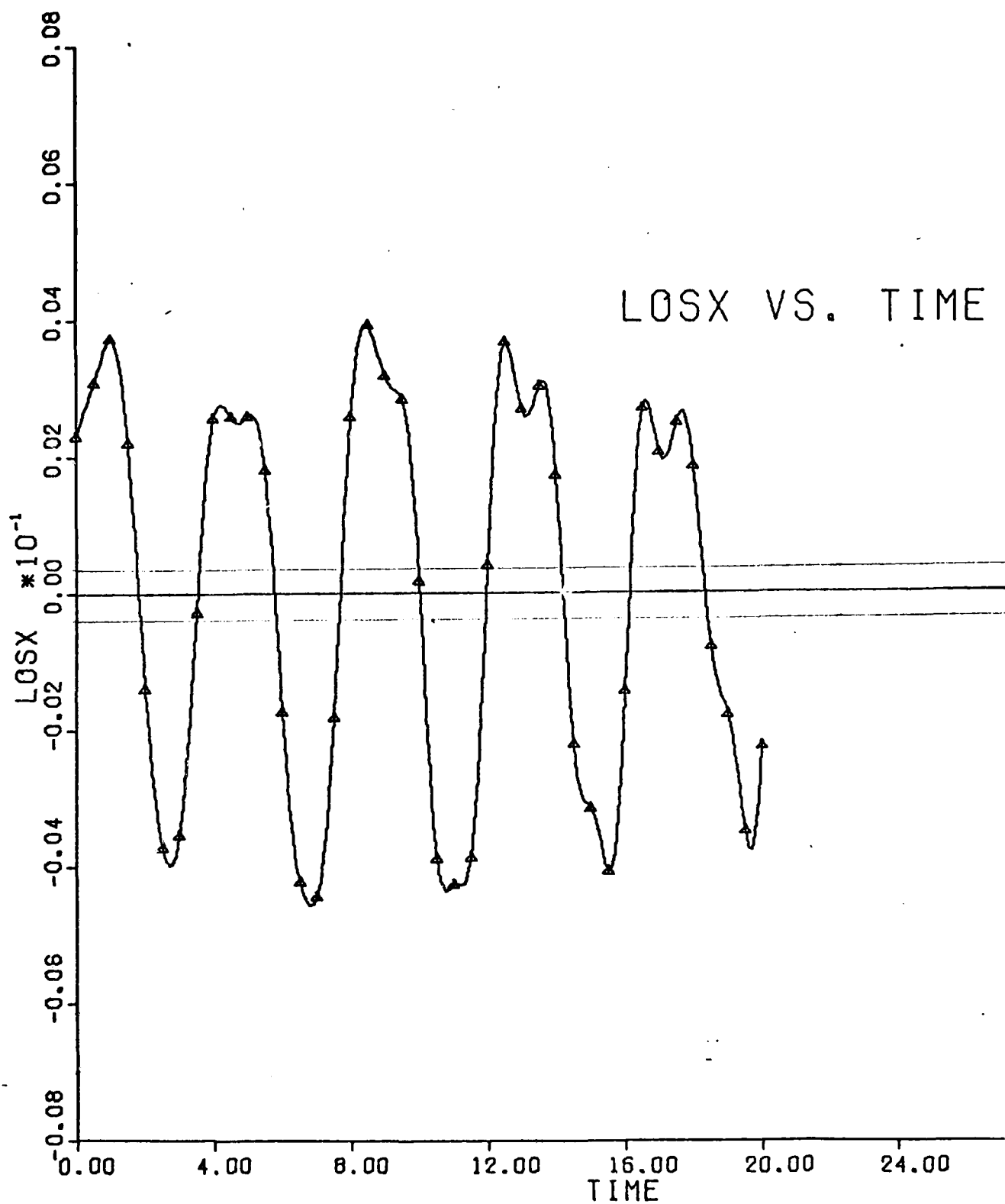


Figure 34. LOSX VS. TIME, Design III,  $Q = Q_{CB} = 100 I$ ,  $T = .7$



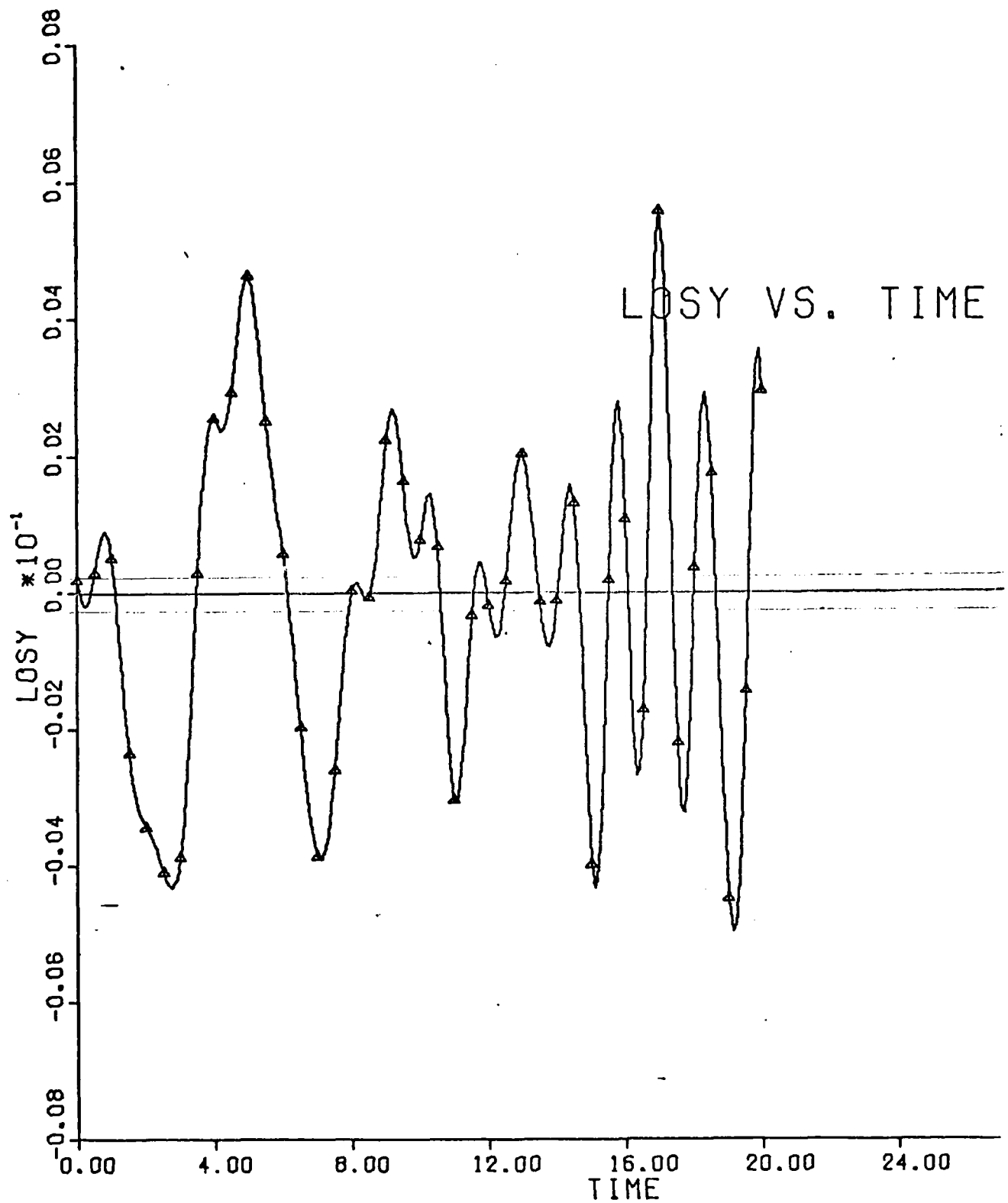


Figure 35. LOS Y VS. TIME, Design III,  $Q = Q_{OB} = 100 I$ ,  $T = .7$

Comparing the time responses of  $T = .5$  shows that for this sampling time some differences begin to appear in the two design performances. For  $T = .5$ , the eigenvalue-sampling time product is 1.9242. Finally, for  $T = .7$ , the two time responses show significant differences. The eigenvalue-sampling time product for this case is 2.6939. From these results it would seem that, though the weighting matrix approximations become poor as  $\Lambda_{\max} T$  approaches 1, they are still good enough, even slightly above 1, to give system performance that is similar to that of a design using more optimal weighting matrices.

## VIII Conclusions

Several conclusions can be drawn from the preceding analysis. First, as was the case in continuous-time, the effects of control and observation spillover are destabilizing. For a fixed number of sensors and actuators with fixed orientation, the singular value decomposition transformation can completely eliminate these effects provided the system is fully controllable. Elimination of the spillover terms guarantees closed-loop stability of a system which has open-loop stability.

For an unstable open-loop system, the spillover terms are not the only destabilizing factors. A large sampling time may drive the closed-loop system unstable even if the spillover terms are eliminated. Even for stable open-loop systems, a large sampling time will have a degrading effect on closed-loop performance. To avoid this, a sampling time must be chosen which, at the very least, obeys the Shannon Sampling Theorem. Preferably, a sampling time well within this criterion should be used to give the best system performance possible.

Finally, the simplified discrete performance index proved to be very accurate for the case where the sample time is small compared to the characteristic times of the system. Even for cases where this condition was slightly exceeded, the approximation yielded performance very close

to optimal. In general, the performance was accurate for  $\Lambda_{\max} T \approx 1$ . Therefore, if the product of the largest eigenvalue and the sampling time is less than one, the simplified performance index may be used without appreciable loss of performance.

## Bibliography

1. Janiszewski, A. M. "Modern Optimal Control Methods Applied in Active Control of a Tetrahedron." Unpublished MS thesis. School of Engineering, Air Force Institute of Technology, Wright-Patterson AFB OH, December 1980.
2. Balas, M. J. "Active Control of Flexible Systems," AIAA Symposium on Dynamics and Control of Large Flexible Spacecraft. Blacksburg, Virginia, June 14, 1977.
3. Oz, H., L. Meirovitch, and C. R. Johnson, Jr. "Some Problems Associated with Digital Control of Dynamical Systems," Journal of Guidance and Control, 3: 523-528 (November-December 1980).
4. Calico, R. A., and A. M. Janiszewski. "Control of a Flexible Satellite Via Elimination of Control Spillover," Proceeds Third VPI/AIAA Symposium on Large Space Structures, Blacksburg, Virginia, June 1981.
5. Kirk, D. E. Optimal Control Theory. Englewood Cliffs NJ: Prentice-Hall, Inc., 1970.
6. Kleinman, D. L. "A Description of Computer Programs For Use in Linear Systems Studies." TR-77-2. University of Connecticut, School of Engineering, July 1977.
7. ----- "Stabilizing a Discrete, Constant, Linear System with Applications to Iterative Methods for Solving the Ricatti Equation," IEEE Transactions Automatic Control, AC-19: 252-254 (June 1974).

APPENDIX A  
Eigenvector Results of NASTRAN Analysis

### Eigenvalues and Eigenvectors

Eigenvalue 1 = 1.370E+00

Eigenvector 1 =  $\begin{bmatrix} -2.471E-01 \\ 4.279E-02 \\ 1.452E-06 \\ -1.963E-02 \\ 3.398E-02 \\ -7.213E-02 \\ -3.696E-02 \\ 4.347E-02 \\ 4.397E-02 \\ -1.962E-02 \\ 5.296E-02 \\ 4.397E-02 \end{bmatrix}$

Eigenvalue 2 = 2.151E+00

Eigenvector 2 =  $\begin{bmatrix} 3.999E-01 \\ 2.309E-01 \\ -1.489E-01 \\ 8.329E-02 \\ 4.808E-02 \\ 6.813E-02 \\ 7.000E-02 \\ 2.253E-02 \\ -4.721E-02 \\ 5.451E-02 \\ 4.936E-02 \\ -4.722E-02 \end{bmatrix}$

Eigenvalue 3 = 8.789E+00

Eigenvector 3 =  $\begin{bmatrix} 6.368E-02 \\ 3.678E-02 \\ 4.000E-01 \\ 1.984E-01 \\ 1.145E-01 \\ 2.010E-01 \\ 1.548E-01 \\ 6.804E-02 \\ 9.782E-02 \\ 1.363E-01 \\ 1.000E-01 \\ 9.784E-02 \end{bmatrix}$

Eigenvalue 4 = 1.266E+00

Eigenvector 4 =  $\begin{bmatrix} 2.746E-02 \\ -4.758E-02 \\ -2.249E-05 \\ -1.718E-01 \\ 2.977E-01 \\ -6.817E-05 \\ -2.512E-01 \\ 3.436E-01 \\ -8.190E-02 \\ -1.718E-01 \\ 3.894E-01 \\ 8.192E-02 \end{bmatrix}$

Eigenvalue 5 = 1.481E+01

Eigenvector 5 =  $\begin{bmatrix} -8.783E-02 \\ -5.070E-02 \\ -1.299E-01 \\ 3.095E-01 \\ 1.786E-01 \\ -3.514E-01 \\ 2.866E-01 \\ 1.224E-01 \\ 1.139E-02 \\ 2.494E-01 \\ 1.868E-01 \\ 1.140E-02 \end{bmatrix}$

Eigenvalue 6 = 2.652E+01

Eigenvector 6 =  $\begin{bmatrix} 1.353E-05 \\ 1.218E-11 \\ 3.402E-11 \\ -2.041E-01 \\ 3.535E-01 \\ -6.057E-06 \\ -2.041E-01 \\ -3.535E-01 \\ 1.086E-04 \\ 4.082E-01 \\ 6.802E-10 \\ 5.065E-10 \end{bmatrix}$

Eigenvalue 7 = 3.222E+01

Eigenvector 7 =  $\begin{bmatrix} -2.661E-02 \\ 4.607E-02 \\ 3.302E-05 \\ 3.374E-02 \\ -5.844E-02 \\ 3.231E-05 \\ 2.733E-02 \\ -5.481E-02 \\ -4.913E-01 \\ 3.382E-02 \\ -5.108E-02 \\ 4.909E-01 \end{bmatrix}$

Eigenvalue 8 = 3.261E+01

Eigenvector 8 =  $\begin{bmatrix} -2.994E-02 \\ -1.731E-02 \\ 8.784E-02 \\ 4.071E-02 \\ 2.360E-02 \\ 3.554E-02 \\ 2.742E-02 \\ 2.798E-02 \\ -4.875E-01 \\ 3.799E-02 \\ 9.810E-03 \\ -4.879E-01 \end{bmatrix}$

Eigenvalue 9 = 7.992E+01

Eigenvector 9 =  $\begin{bmatrix} 9.907E-02 \\ 5.720E-02 \\ 1.729E-01 \\ 1.076E-01 \\ 6.213E-02 \\ -4.953E-01 \\ -1.679E-01 \\ -2.198E-01 \\ -1.110E-02 \\ -2.743E-01 \\ -3.554E-02 \\ -1.109E-02 \end{bmatrix}$

Eigenvalue 10 = 1.062E+02

Eigenvector 10 =  $\begin{bmatrix} -3.390E-03 \\ 5.850E-03 \\ -1.605E-05 \\ -2.286E-01 \\ 3.960E-01 \\ 4.964E-05 \\ 3.783E-01 \\ 4.554E-02 \\ -1.471E-02 \\ -2.286E-01 \\ -3.049E-01 \\ 1.472E-02 \end{bmatrix}$

Eigenvalue 11 = 1.193E+02

Eigenvector 11 =  $\begin{bmatrix} 6.370E-02 \\ 3.678E-02 \\ 9.588E-02 \\ -2.401E-01 \\ -1.386E-01 \\ -2.605E-01 \\ -8.606E-02 \\ 3.944E-01 \\ 6.970E-03 \\ 2.984E-01 \\ -2.719E-01 \\ 6.971E-03 \end{bmatrix}$

Eigenvalue 12 = 1.951E+02

$\begin{bmatrix} 3.206E-02 \\ 1.851E-02 \\ 6.438E-02 \\ -4.026E-01 \\ -2.324E-01 \\ -1.305E-01 \\ 3.204E-01 \\ -1.587E-01 \\ -9.278E-03 \\ 2.272E-02 \\ 3.568E-01 \\ -9.282E-03 \end{bmatrix}$



APPENDIX B

Matrices  $B_c$  ,  $B_s$  ,  $B_r$



## APPENDIX C

### Open-loop Eigenvalues and Time Response

# Discrete Coen-Loop Eigenvalues

<u>Eigenvalues of <math>\underline{\Phi}_c</math></u>	<u>Eigenvalues of <math>\underline{\Phi}_s</math></u>
T = .1	
.99257 ± .11673i	.95496 ± .29170i
.93571 ± .34769i	.84081 ± .53607i
.98854 ± .14604i	.86809 ± .49121i
.92508 ± .37468i	.83892 ± .53899i
T = .3	
.93732 ± .34341i	.62710 ± .77323i
.47991 ± .87124i	-.13046 ± .98290i
.90275 ± .42503i	.02579 ± .99197i
.40205 ± .90933i	-.14073 ± .98143i
T = .5	
.83110 ± .55085i	.08774 ± .98873i
-.20473 ± .96977i	-.94080 ± .29482i
.74020 ± .66694i	-.83277 ± .53016i
-.34275 ± .92923i	-.94572 ± .27833i
T = .7	
.67984 ± .72778i	-.47830 ± .86642i
-.78551 ± .59864i	-.66052 ± .72440i
.51497 ± .85123i	-.87876 ± .43862i
-.88936 ± .42715i	-.64255 ± .74023i

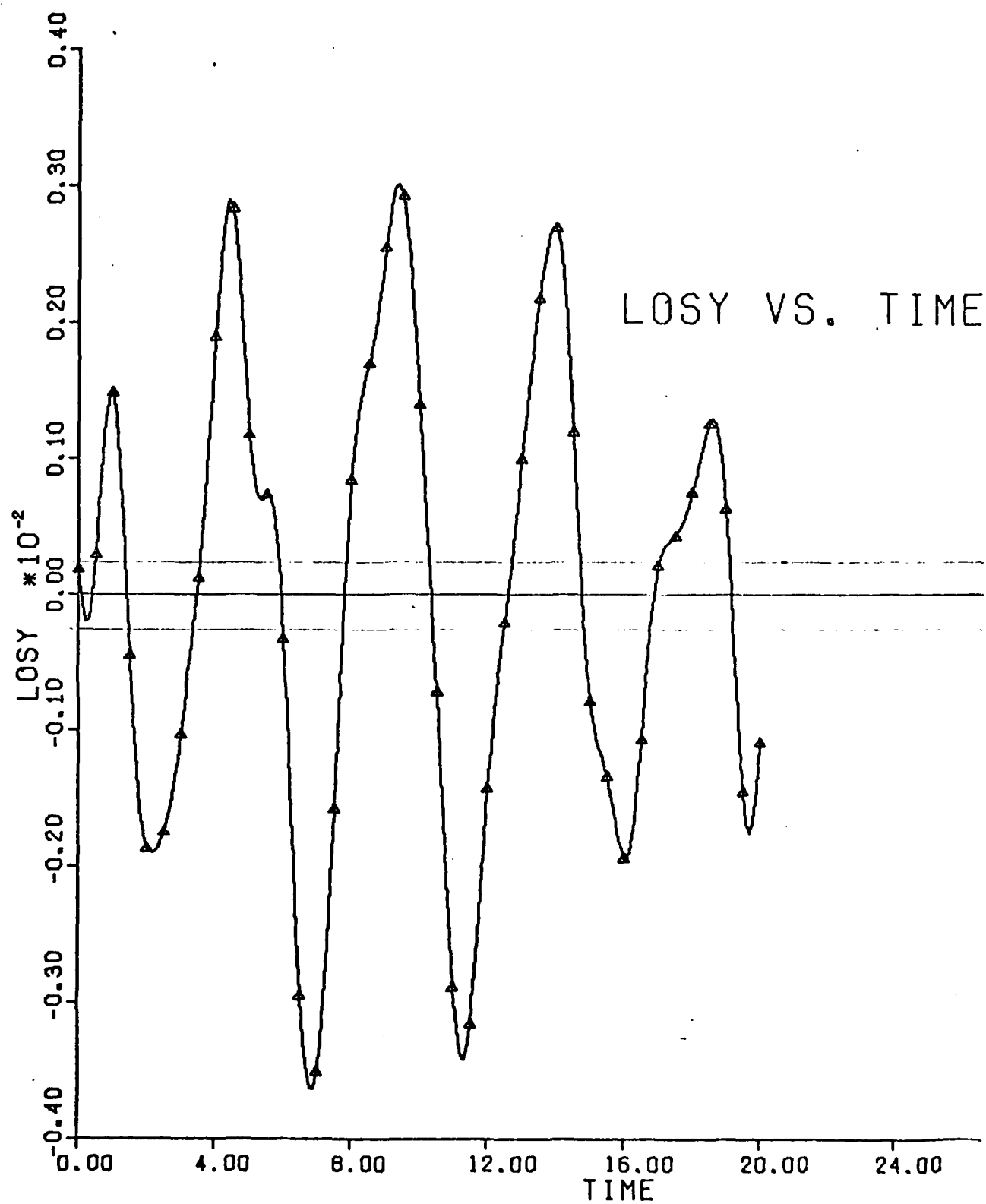


Figure B-2. LOS Y VS. TIME, Open-loop

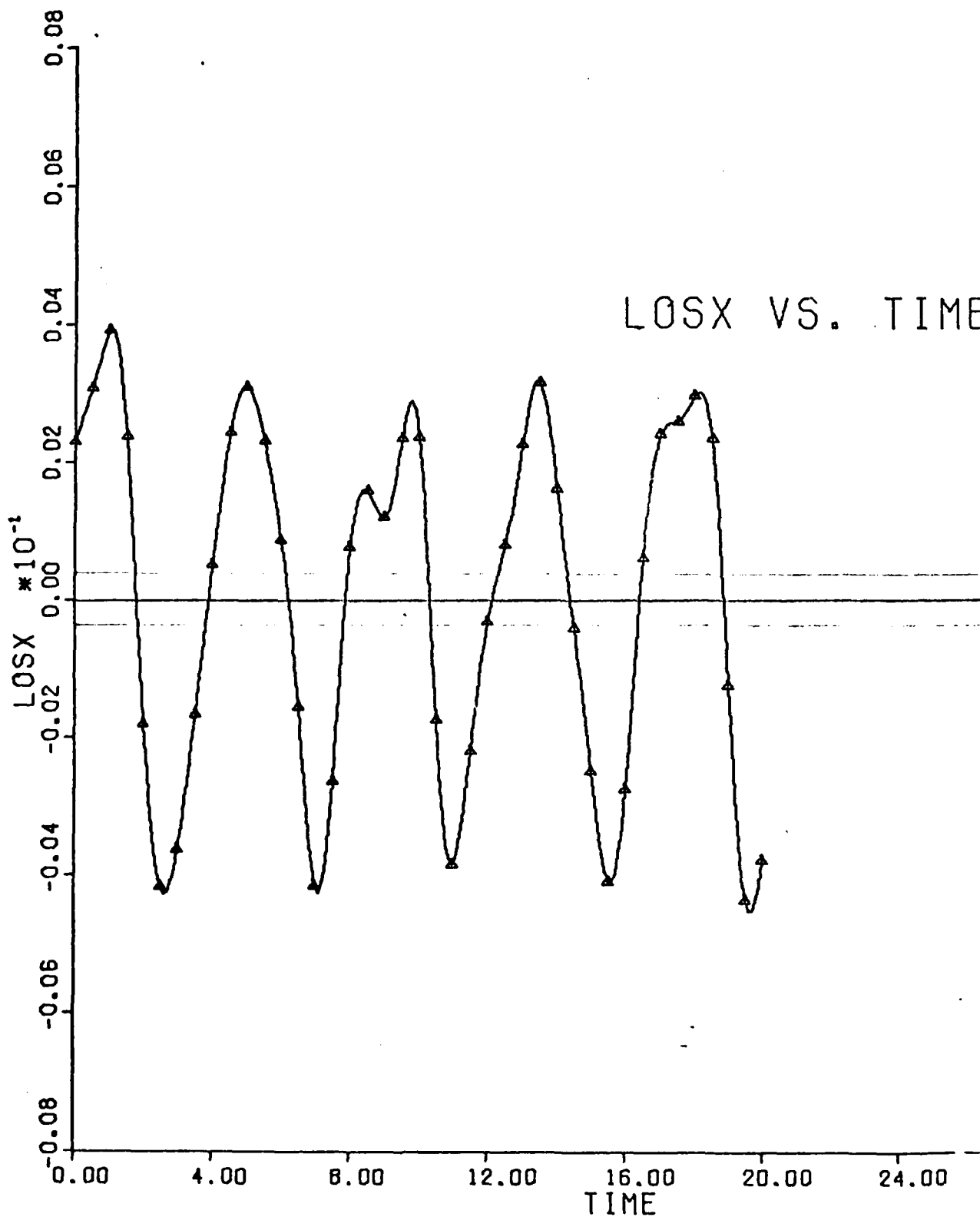


Figure B-1. LOSX VS. TIME, Open-loop

## VITA

David B. Leggett was born on 29 April 1958 in Sherman, Texas. He graduated salutatorian from Lowndes High School, Valdosta, Georgia, in June 1976. He received the degree of Bachelor of Aerospace Engineering from the Georgia Institute of Technology in June, 1980. He was a distinguished graduate of ROTC and received a commission in the United States Air Force. He entered the School of Engineering, Air Force Institute of Technology in June, 1980.

Permanent Address: 646 Mourning Dove Dr.  
Sarasota FL 33577

REPORT DOCUMENTATION PAGE		READ INSTRUCTIONS BEFORE COMPLETING FORM
1. REPORT NUMBER AFIT/GAE/AA/81D-18	2. GOVT ACCESSION NO. AD-A111 170	3. RECIPIENT'S CATALOG NUMBER
4. TITLE (and Subtitle) DESIGN OF A DIGITAL CONTROLLER FOR A LARGE FLEXIBLE SPACE STRUCTURE		5. TYPE OF REPORT & PERIOD COVERED M S Thesis
		6. PERFORMING ORG. REPORT NUMBER
7. AUTHOR(s) David B. Leggett 2nd Lt USAF		8. CONTRACT OR GRANT NUMBER(s)
9. PERFORMING ORGANIZATION NAME AND ADDRESS Air Force Institute of Technology (AFIT-EN) Wright-Patterson AFB, Ohio 45433		10. PROGRAM ELEMENT, PROJECT, TASK AREA & WORK UNIT NUMBERS
11. CONTROLLING OFFICE NAME AND ADDRESS		12. REPORT DATE Dec 1981
		13. NUMBER OF PAGES 116
14. MONITORING AGENCY NAME & ADDRESS (if different from Controlling Office)		15. SECURITY CLASS. (of this report) unclassified
		15a. DECLASSIFICATION DOWNGRADING SCHEDULE
16. DISTRIBUTION STATEMENT (of this Report)  Approved for public release; distribution unlimited		
17. DISTRIBUTION STATEMENT (of the abstract entered in Block 20, if different from Report)  28 JAN 1982		
18. SUPPLEMENTARY NOTES Approved for public release; IAW-190-17 FREDRICK C. LYNCH, Major, USAF Director of Public Affairs		
19. KEY WORDS (Continue on reverse side if necessary and identify by block number) Linear Optimal Regulator theory      Observation Spillover State Space Control Singular Value Decomposition Control Spillover		
20. ABSTRACT (Continue on reverse side if necessary and identify by block number)  Modern optimal control techniques are used to design a digital controller for a large flexible space structure. The structure is modeled as a tetrahedron formed by four lumped masses connected by massless truss members. A NASTRAN analysis is used to generate the twelve mode shapes and frequencies of oscillation. The controller is designed in discrete-time using linear		



optimal regulator theory. An observer is used to estimate the states. Active control is achieved using six collocated sensor actuator pairs. The effectiveness of the controller is determined using pointing accuracy as a figure of merit.

Three controller designs are compared. The first demonstrates the effects of "control" and "observation spillover". The second uses a singular value decomposition to eliminate the spillover terms. The third design uses a more accurate optimal performance index than the first two.

The first design proved inadequate to achieve the desired performance. The second and third designs were able to achieve the desired performance for small sampling times. For small sampling times the simplified performance index used in Design II proved to provide a very accurate approximation to the optimal.

END

DATE  
FILMED

3-82

DTIC